



**Data Rate Change Algorithms for
HF Band Efficient Communications
Using the E/R GRC-525 Radio**

Vasco Ferreira Sequeira

Thesis to obtain the Master of Science Degree in
Electrical and Computer Engineering

Supervisors

Prof. Maria Paula dos Santos Queluz Rodrigues

Prof. António José Castelo Branco Rodrigues

Prof. José Eduardo Charters Ribeiro da Cunha Sanguino

Maj Tm (Eng) Pedro Miguel Martins Grifo

Examination Committee

Chairperson: Prof. António Manuel Raminhos Cordeiro Grilo

Supervisor: Prof. Maria Paula dos Santos Queluz Rodrigues

Members of the Committee: Prof. Francisco António Bucho Cercas

TCor Tm (Eng) José Jaime Soares Pereira

Acknowledgements

First, I would like to thank my family, they gave me all the values as a person and taught me to fight for my goals, regardless of the obstacles that cross my path. To my father José Sequeira and my mother Maria Teresa Sequeira, all my professional and personal successes are yours too. I would like to thank also my girlfriend Verónica Rodriguez, who recently became an architect, for all the support, love and patient she gave me, she motivated me to continue this stage successfully. All the words in the world are few to describe how important you are to me.

A huge thank to the professors Paula Queluz, António Rodrigues and José Sanguino for accepting since the first hour to supervise my thesis, with all the enthusiasm for this subject. All the support, availability and transfer of knowledge resulted in a facilitated work. I expect that this partnership will be an example for future researches, between the *Instituto de Telecomunicações* (IT) and the Portuguese Armed Forces. Once again, I am very grateful for all the patient and dedication that the professors had to help and guide my work.

Special thanks to *Sistemas de Informação e Comunicação - Táctico* (SIC-T) team project, led by Major Pedro Grifo, who proposed the subject and gave me technical support to develop my master dissertation with success, and all the knowledge about military communications equipment that I used to achieve the goals. I also want to thank the Sergeant 1st Class (OR-7) Francisco Pereira and the Staff Sergeant (OR-6) Telmo Patrício, who gave me technical support to assembly and configure the equipment. A huge thank to the remaining team Captain Tiago Guedes, Lieutenant Frederic Mota, Sergeant 1st Class (OR-7) Mário Arede and Staff Sergeant (OR-6) Christopher Monteiro, who welcomed me and provided a good environment to work.

I want to thank to the Signals Regiment of Oporto, in special to the Signals Company from the Intervention Brigade, led by Captain João Monteiro. Special thanks to the Staff Sergeant (OR-6) Luis Pinto who gave me technical support to the field propagation tests and he coordinated the assembly of the equipment in Oporto. These HF long distance communications proved that the Portuguese Army, in special the Signals weapon, is an organization with competent staff interested in the communications research and development; therefore, I want to pay tribute to all the officers, sergeants and soldiers who collaborated in this master thesis research.

I want to thank my course of Military Academy, the *Brigadeiro General D. Carlos Mascarenhas* course. It fills me with pride having shared with you all the difficulties and moments of comradeship that taught me to value the little things of life. Special thanks for my comrades of the general course of engineering who shared with me the same difficulties and helped me to get through it.

Lastly, I want to thank my Karaté-Do Portugal Shotokan family, which I have belonged for 20 years, in special to my masters José Chagas and Cristina Amaral Mendes, who gave me all the moral and behavioural formation, which is identified by the 5 karate maxims (*Dojo Kun*): character, sincerity, effort, etiquette and self-control. To all my karate friends Joana Mendes, Monica Mendes, Diogo Cardoso and João Fernandes thank you for sharing the good and the difficult moments, such as the friendship we developed along these years.

Resumo

Desde os anos 80 que as comunicações na banda das altas frequências (HF) têm evoluído tecnologicamente, sendo esta evolução motivada pela potencial robustez desta forma de comunicação a situações de catástrofe e de emergência, e pelo custo de manutenção e implementação das comunicações via satélite. Para o Exército Português, as comunicações em HF são também muito importantes em Teatros de Operações com regiões montanhosas, como é o caso do Kosovo e do Afeganistão, onde esta força representa Portugal em missões das Nações Unidas (ONU) ou da Organização do Tratado do Atlântico Norte (NATO – *North Atlantic Treaty Organization*). Neste contexto, são particularmente interessantes as comunicações em HF que utilizam ondas de rádio com ângulos de incidência (na Ionosfera) próximos de zero graus, e designadas na literatura Inglesa por *Near Vertical Incidence Sky waves* (NVIS). Apesar do renascimento no interesse das comunicações em HF, existem vários desafios envolvidos, como a operação rádio com relações sinal-ruido (SNR) tipicamente muito baixas, desvanecimento (*fading*), variação do sinal devido a mudanças na camada da Ionosfera, e capacidade limitada do canal. Para lidar com as mudanças do canal em HF, surgiram várias tecnologias como a análise automática da qualidade da ligação (LQA), o estabelecimento automático da ligação (ALE) e a mudança automática do débito binário (DRC), eliminando a necessidade de procedimentos operacionais complexos e manuais.

Motivado pelas soluções desenvolvidas ao longo dos anos, esta Dissertação começa com a visão geral do estado-de-arte disponível na área dos algoritmos de Mudança de Débito Binário (DRC), analisando as vulnerabilidades dos algoritmos existentes e propondo soluções para as melhorar. A primeira proposta evita valores altos de taxa de erro de bit (BER) que conduzem a um estado de corte da ligação; a segunda proposta, para além de aumentar a disponibilidade da ligação, também evita oscilações desnecessárias do débito binário. Quando testadas no ambiente de simulação, ambas as propostas mostraram melhores desempenhos que os algoritmos originais. Esta melhoria de desempenho também foi confirmada em condições reais de transmissão, depois de implementar os algoritmos no rádio E/R GRC-525, e de estabelecer uma comunicação HF entre duas estações localizadas em Lisboa e Porto, usando a antena dipolo RF-1936P. Nos testes de propagação no terreno a melhor proposta permite um aumento de 15% na disponibilidade da ligação e de 392% na taxa média de tramas corretas recebidas (*goodput*), em comparação com o algoritmo original.

Palavras-chave: Algoritmo de Seleção de Débito Binário (DRC), Comunicações em HF, Ionosfera, Relação Sinal-Ruído (SNR), Taxa de Erro de Bit (BER).

Abstract

Since the 80s that communications on the high frequency (HF) band have undergone a remarkable technologic evolution, motivated by their potential robustness to catastrophic and emergency situations, and by the high costs involved on the implementation and maintenance of satellite links. For the Portuguese Army, the HF communications are also very important in Theatre of Operations with mountainous regions, like Kosovo and Afghanistan, where this force represents Portugal in United Nations (UN) and North Atlantic Treaty Organization (NATO) missions. In this context, HF communications using radio waves with incidence angles (in Ionosphere) near zero degrees - known as Near Vertical Incidence Sky waves (NVIS) - are often used. Despite the renewed interest on HF communications, there are a lot of challenges involved, like the operation with (typically) very low signal-to-noise ratios (SNR), multipath fading, signal variation due to the changing constitution of the ionosphere, and a limited channel capacity. In order to deal with the variability of the HF channel, several technologies have emerged, like automatic Link Quality Analysis (LQA), Automatic Link Establishment (ALE) and automatic Data Rate Change (DRC), eliminating the need for complex and manual operating procedures.

Motivated by the developed solutions along the last years for DRC algorithms, this Dissertation starts with an overview of the available state-of-the-art, to assess the vulnerabilities of existing algorithms and propose solutions to overcome them. The first proposal avoids high Bit Error Rate (BER) values that lead to a link cut-off state (i.e., disconnection); the second proposal, besides increasing the link availability, also avoids unnecessary data rate oscillations. When assessed on a simulation environment, both proposals showed better performance than the original algorithms. This performance improvement was also confirmed in real transmission conditions, after implementing the algorithms on the E/R GRC-525 radio, and establishing a HF connection between two communication stations located in Lisbon and Oporto, using the RF-1936P dipole antenna. In the field propagation tests, the best proposal allows an increase of 15% on the link availability and of 392% on the average goodput, relatively to the original algorithm.

Key-words: Bit Error Rate (BER), Data Rate Change (DRC) Algorithm, High Frequency (HF) Communications, Ionosphere, Signal-to-Noise Ratio (SNR).

Table of Contents

Acknowledgements	i
Resumo	iii
Abstract	v
List of Figures	xi
List of Tables	xvii
List of Acronyms	xix
Chapter 1 - Introduction	1
1.1. Context and Motivation	1
1.2. Objectives	3
1.3. Main Contributions	3
1.4. Dissertation Structure	3
Chapter 2 - HF Communications	5
2.1. Types of HF Radio Signals	5
2.2. Propagation by the Ionosphere	6
2.2.1. The Ionosphere Layer	6
2.2.2. Near-Vertical Incidence Sky wave	9
2.3. HF Antennas	10
Chapter 3 - HF Communication Standards	13
3.1. Adaptive Techniques in HF Communications	13
3.2. Overview of HF Communications Standards	14
3.3. Physical Layer	15
3.4. Automatic Channel Selection (ACS)	18
3.5. Automatic Link Establishment (ALE)	18
3.6. Automatic Link Maintenance (ALM)	19
3.7. Data Link Protocol	20
3.7.1. High Throughput Data Link	20
3.7.2. Low Latency Data Link	20
3.7.3. High Throughput Data Link+	20
Chapter 4 - State-of-the-art on Data Rate Change Algorithms	23

4.1. DRC algorithm for non-Autobaud Modulations	23
4.2. DRC algorithm for Autobaud Modulations	24
4.3. RapidM DRC algorithm	25
4.3.1. RapidM DRC algorithm 1 design	26
4.3.2. RapidM DRC algorithm 1 implementation	29
4.3.3. RapidM DRC algorithm 1 simulation, results and tests	30
Chapter 5 – DRC Algorithm: Assessment of Existing Solutions and Proposals for Improvement ...	33
5.1. DRC Algorithms Simulation System	33
5.2. Previous DRC algorithms: Simulation and Assessment	37
5.2.1. Trinder algorithm Simulation and Assessment	37
5.2.2. RapidM DRC algorithm Simulation and Assessment	39
5.3. Improvements on the Trinder and RapidM Algorithms	41
5.3.1. Avoiding Cut-Off State Algorithm	41
5.3.2. Bit Error Optimization Algorithm	46
5.4. Conclusion	51
Chapter 6 – Field Propagation Tests	53
6.1. Equipment Assembly and Configuration Procedures	53
6.1.1. General Settings and Components	54
6.1.2. Assembly of Bench Tests Circuit	58
6.1.3. Assembly of Field Tests Equipment	59
6.2. Data Rate Change Software Application	60
6.2.1. User Application Configuration	60
6.2.2. Output Files and Graphical Views	62
6.3. Field Propagation Tests: Environment Conditions and Results	63
6.3.1. Meteorological and Ionospheric Conditions for Test Days	64
6.3.2. Algorithms Performance in Real Test Conditions	64
6.4. Relation between Simulations and Field Propagation Values	68
Chapter 7 – Summary and Future Work	73
7.1. Summary	73
7.2. Future Work	74
Appendix A – Radio E/R GRC-525 datasheet	75

Appendix B – Dipole antenna RF-1936P datasheet	77
Appendix C – Results from Algorithms Assessments.....	79
Appendix D – HF Communications Electrical Message.....	87
Appendix E – Assembly of the Dipole Antenna 1936P	89
Appendix F – Results from the Field Propagation Tests.....	91
Appendix G – Ionospheric Conditions for the Test Days	111
Bibliography	113

List of Figures

Figure 1.1 - Example of HF channel propagation waves [1].	1
Figure 1.2 – Image of the E/R GRC-525 [2].	2
Figure 2.1 – Radio Spectrum [8].	5
Figure 2.2 – The Ionosphere Layers [10].	6
Figure 2.3 – Ionosphere behaviour: a) reflection depending on the frequency; b) reflection depending on the day time [13].	7
Figure 2.4 – Reflection of type M [14].	7
Figure 2.5 – Reflection of type N [14].	7
Figure 2.6 - Example of an Ionogram: a) real [16]; b) schematic.	8
Figure 2.7 – Example of a Global Real Time Ionospheric foF2 Map [17].	8
Figure 2.8 – NVIS propagation and its characteristic "umbrella" shape [19].	9
Figure 2.9 – Change of the critical frequency during the day, and on winter [16].	10
Figure 2.10 – Antennas used in NVIS: a) horizontal dipole antenna [15]; b) circular loop antenna [21].	11
Figure 2.11 – Gain of three different antennas used in NVIS propagation [16].	11
Figure 2.12 – Use of the Whip antenna for NVIS communication [16].	12
Figure 3.1 – ARCS process cycle [18].	14
Figure 3.2 – The HF house of standards [18].	15
Figure 3.3 – Frame structure for all modulations [24].	16
Figure 3.4 – Synchronous dwell structure in 3 rd Generation ALE [22].	18
Figure 3.5 – The 3 rd Generation ALE call [22].	19
Figure 3.6 - HDL+ Header [29].	21
Figure 4.1 – ARQ throughput as a function of SNR [6].	24
Figure 4.2 – RapidM DRC algorithm1 system of inputs and outputs [3].	26
Figure 4.3 – RapidM DRC Algorithm1 flowchart (Adapted from [3]).	27
Figure 4.4 – The fitted line through the 10 – 5 BER points [3].	28
Figure 4.5 – Input and Output system of the RapidM DRC algorithm 1 implementation (Adapted from [3]).	29
Figure 4.6 – BER channel profile [3].	30
Figure 5.1 – Simulation system flowchart.	33
Figure 5.2 – BER as a function of SNR for m-QAM modulation, with a straight line (in green) representing a BER variation of 1 decade per dB (Adapted from [32]).	34
Figure 5.3 – Channel measurements time diagram.	34
Figure 5.4 – Downward sinusoidal SNR variation.	36
Figure 5.5 – Upward sinusoidal SNR variation.	36
Figure 5.6 – Sinusoidal SNR variation.	36
Figure 5.7 – Step-wise SNR variation.	36
Figure 5.8 – Trinder algorithm data rate variation, for an upward sinusoidal SNR variation.	38

Figure 5.9 – Trinder algorithm: BER vs Data Rate variation, for an upward sinusoidal SNR variation using an ITU Poor channel.....	39
Figure 5.10 – Original RapidM algorithm data rate variation, for an upward sinusoidal SNR variation.	40
Figure 5.11 – RapidM DRC algorithm: BER vs Data Rate variation, for an upward sinusoidal SNR variation using an ITU Poor channel.....	40
Figure 5.12 – Avoiding Cut-Off State algorithm flowchart.....	42
Figure 5.13 – Trinder algorithm with ACOS data rate variation, for an upward sinusoidal SNR variation.	42
Figure 5.14 – Trinder algorithm with ACOS: BER vs Data Rate variation, for an upward sinusoidal SNR variation using an ITU Poor channel.....	44
Figure 5.15 – RapidM algorithm with ACOS data rate variation, for an upward sinusoidal SNR variation.	45
Figure 5.16 – RapidM DRC algorithm with ACOS: BER vs Data Rate variation, for an upward sinusoidal SNR variation using an ITU Poor channel.	46
Figure 5.17 – Bit Error Optimization algorithm flowchart.	46
Figure 5.18 – Trinder algorithm with BEO data rate variation, for an upward sinusoidal SNR variation.	47
Figure 5.19 – Trinder algorithm with BEO: BER vs Data Rate variation, for an upward sinusoidal SNR variation using an ITU Poor channel.....	48
Figure 5.20 – RapidM algorithm with BEO data rate variation, for an upward sinusoidal SNR variation.	49
Figure 5.21 – RapidM DRC algorithm with BEO: BER vs Data Rate variation, for an upward sinusoidal SNR variation using an ITU Poor channel.	50
Figure 6.1 – Dipole antenna RF-1936P from Harris Corporation.	53
Figure 6.2 – Critical frequency of F2 layer in real time for the 28 th of August 2017 (Consulted on [17]).	54
Figure 6.3 – Real time Ionospheric data for the 28 th August 2017: a) MUF values in percentage during the day (Consulted on [36]); b) Warnings that may influence the HF communications (Consulted on [17])......	55
Figure 6.4 – Process of downloading the mission on the radio: a) Fill Gun HQ produced by EID; b) Data transfer from the Fill Gun HQ to the E/R GRC-525.	55
Figure 6.5 – Wattmeter used to verify the reflected wave power of each frequency: a) Image of the wattmeter produced by Bird Electronic Corporation; b) Practical use of the wattmeter.	56
Figure 6.6 – ATU learning process: a) ATU learning the group of eight available frequencies; b) Message when the tuning is performed successfully.	56
Figure 6.7 – Hardware components used in the experiments: a) Assembly of a computer running the DRC application on the radio; b) RS232/USB cable used as serial and data port, produced by EID; c) Micro-headset from the E/R GRC-525 radio, produced by EID; d) Several meters of coaxial cable.	57
Figure 6.8 – Hardware components used specifically for bench experiments: a) Variable HF attenuator, produced by EID; b) Fixed attenuator of 30 dB to assembly on the transmitter output.	58

Figure 6.9 – Schematic of the bench circuit used to test the DRC application.	58
Figure 6.10 – Physical assembly of the bench tests circuit: a) Output system with a TX station and the fixed attenuator of 30 dB; b) Input system with the RX station and the variable HF attenuator.....	59
Figure 6.11 – Location of the HF stations: a) Station one located in Logistics Support Unity, <i>Paço de Arcos</i> , Lisbon; b) Station two located in the Signals Regiment, <i>Viso de Baixo</i> , Oporto.	59
Figure 6.12 – Image of the two dipole antennas RF-1936P used to perform the field propagation tests: a) Antenna located in the Signals Regiment, <i>Viso de Baixo</i> , Oporto; b) Antenna located in Logistics Support Unity, <i>Paço de Arcos</i> , Lisbon.	60
Figure 6.13 – Output tab page of the DRC application.	61
Figure 6.14 – Configuration tab page from the DRC application: a) Parameters to open the remote control port and starting the channel sounding; b) Signal when the remote control is open: green light when the remote control port is open and red light when it is closed; c) Fields to set the interleaver size.	61
Figure 6.15 – Algorithms tab page from the DRC application: a) Type of algorithm, type of channel and number of version settings; b) Process to open the data send port.	62
Figure 6.16 – Handling files in the DRC application: a) Create a file with a defined name and size; b) Sending the created file.	62
Figure 6.17 – DRC application graphical view with the interval of SNR measures and data rate settings.	63
Figure 6.18 – Data rate adaption for a SNR variation measured in 30 th August 2017, using the original DRC RapidM algorithm.	65
Figure 6.19 – Data rate adaption for a SNR variation measured in 31 st August 2017, using the DRC RapidM algorithm with ACOS.	66
Figure 6.20 – Data rate adaption for a SNR variation measured in 1 st September 2017, using the DRC RapidM algorithm with BEO.	66
Figure 6.21 – Data rate adaption for a SNR variation measured in 4 th September 2017, using the original Trinder algorithm.	67
Figure 6.22 – Data rate adaption for a SNR variation measured in 5 th September 2017, using the Trinder algorithm with ACOS.	67
Figure 6.23 – Data rate adaption for a SNR variation measured in 7 th September 2017, using the Trinder algorithm with BEO.	68
Figure 6.24 – Cross-correlation coefficient values between the field propagation tests and the expected results provided by the simulation system (graphic representation).....	69
Figure 6.25 – Simulated values for the 5 th September 2017, using Trinder algorithm with ACOS and assuming an AWGN channel which corresponds to the best cross-correlation fit.	70
Figure 6.26 – Simulated values for the 4 th September 2017, using original Trinder algorithm and assuming an AWGN channel which corresponds to the worst cross-correlation fit.	70
Figure C.1 – Trinder algorithm data rate adaptation for an AWGN channel using downward sinusoidal SNR variation.....	79

Figure C.2 – Trinder algorithm data rate adaptation for a GOOD channel using downward sinusoidal SNR variation.....	79
Figure C.3 - Trinder algorithm data rate adaptation for a POOR channel using downward sinusoidal SNR variation.....	79
Figure C.4 – Trinder algorithm data rate adaptation for an AWGN channel using upward sinusoidal SNR variation.....	80
Figure C.5 – Trinder algorithm data rate adaptation for a GOOD channel using upward sinusoidal SNR variation.....	80
Figure C.6 – Trinder algorithm data rate adaptation for a POOR channel using upward sinusoidal SNR variation.....	80
Figure C.7 – Trinder algorithm data rate adaptation for an AWGN channel using sinusoidal SNR variation.....	81
Figure C.8 – Trinder algorithm data rate adaptation for a GOOD channel using sinusoidal SNR variation.	81
Figure C.9 – Trinder algorithm data rate adaptation for a POOR channel using sinusoidal SNR variation.	81
Figure C.10 – Trinder algorithm data rate adaptation for an AWGN channel using discontinues SNR variation.....	82
Figure C.11 – Trinder algorithm data rate adaptation for a GOOD channel using discontinues SNR variation.....	82
Figure C.12 – Trinder algorithm data rate adaptation for a POOR channel using discontinues SNR variation.....	82
Figure C.13 – RapidM algorithm data rate adaptation for an AWGN channel using downward SNR variation.....	83
Figure C.14 – RapidM algorithm data rate adaptation for a GOOD channel using downward SNR variation.....	83
Figure C.15 – RapidM algorithm data rate adaptation for a POOR channel using downward SNR variation.....	83
Figure C.16 – RapidM algorithm data rate adaptation for an AWGN channel using upward SNR variation.	84
Figure C.17 – RapidM algorithm data rate adaptation for a GOOD channel using upward SNR variation.	84
Figure C.18 – RapidM algorithm data rate adaptation for a POOR channel using upward SNR variation.	84
Figure C.19 – RapidM algorithm data rate adaptation for an AWGN channel using sinusoidal SNR variation.....	85
Figure C.20 – RapidM algorithm data rate adaptation for a GOOD channel using sinusoidal SNR variation.....	85
Figure C.21 – RapidM algorithm data rate adaptation for a POOR channel using sinusoidal SNR variation.....	85

Figure C.22 – RapidM algorithm data rate adaptation for an AWGN channel using discontinues SNR variation.....	86
Figure C.23 – RapidM algorithm data rate adaptation for a GOOD channel using discontinues SNR variation.....	86
Figure C.24 – RapidM algorithm data rate adaptation for a POOR channel using discontinues SNR variation.....	86
Figure E.1 – Assembly of the station one images: a) Unroll the dipole wires; b) Attaching the copper bar to perform the ground of the system; c) Wire that connect the radio with the antenna; d) Fixing the base of the antenna to the ground; e) Hoist the mast of the antenna; f) Stretching the coaxial cable to the radio station.....	89
Figure G.1 – Ionospheric conditions for the 30 th August 2017: a) foF2 real measure in red colour, and foF2 predicted value in white colour during the day; b) MUF values during the day.....	111
Figure G.2 – Ionospheric conditions for the 31 st August 2017: a) foF2 real measure in red colour, and foF2 predicted value in white colour during the day; b) MUF values during the day.....	111
Figure G.3 – Ionospheric conditions for the 1 st September 2017: a) foF2 real measure in red colour, and foF2 predicted value in white colour during the day; b) MUF values during the day.....	111
Figure G.4 – Ionospheric conditions for the 4 th September 2017: a) foF2 real measure in red colour, and foF2 predicted value in white colour during the day; b) MUF values during the day.....	112
Figure G.5 – Ionospheric conditions for the 5 th September 2017: a) foF2 real measure in red colour, and foF2 predicted value in white colour during the day; b) MUF values during the day.....	112
Figure G.6 – Ionospheric conditions for the 7 th September 2017: a) foF2 real measure in red colour, and foF2 predicted value in white colour during the day; b) MUF values during the day.....	112

List of Tables

Table 3.1 – Modulation used for each data rate (adapted from [24] and [25]).	16
Table 3.2 – SNR requirements for a BER of 10 – 5 using an AWGN channel (Adapted from [3]).	17
Table 3.3 – SNR requirements for a BER of 10 – 5 using an ITU Good channel (Adapted from [3]).	17
Table 3.4 – SNR requirements for a BER of 10 – 5 using an ITU Poor channel (Adapted from [3]).	17
Table 4.1 – FER threshold values used for DRC algorithm for Autobaud Modulations [6]......	25
Table 4.2 – RapidM DRC algorithm 1 input parameters [3].	26
Table 4.3 – Number of frames received after 127s interval and frame length of 250 bytes (Adapted from [3])......	26
Table 4.4 – BER decision threshold for RapidM DRC algorithm 2 (Adapted from [3]).	28
Table 4.5 – Simulation constants (Adapted from [3]).....	31
Table 4.6 – Test settings for RapidM DRC algorithm 1 (Adapted from [3]).	31
Table 4.7 – Results for data throughput test for Trinder and RapidM DRC algorithms (Adapted from [3]).	31
Table 4.8 – Results for acquisition time test for Trinder and RapidM DRC algorithms (Adapted from [3]).	32
Table 5.1 – Trinder algorithm simulation results for each channel type.	38
Table 5.2 – RapidM DRC algorithm simulation results for each type of channel.	39
Table 5.3 – Relative variation between RapidM DRC and Trinder algorithm.	41
Table 5.4 - Trinder algorithm with ACOS simulation results for each channel type.	43
Table 5.5 – Relative variation between Trinder with ACOS and original Trinder algorithm.....	43
Table 5.6 – RapidM DRC algorithm with ACOS simulation results for each channel type.	44
Table 5.7 – Relative variation between RapidM DRC algorithm with ACOS and its original version....	45
Table 5.8 – Trinder algorithm with BEO simulation results for each channel type.	47
Table 5.9 – Relative variation between Trinder algorithm with BEO and the original version.	48
Table 5.10 – RapidM DRC algorithm with BEO simulation results for each channel type.....	49
Table 5.11 – Relative variation between RapidM DRC algorithm with BEO and the original version.	50
Table 6.1 – Meteorological conditions and Ionospheric warnings for test days.	64
Table 6.2 – Overall results of the field propagation tests.....	64
Table 6.3 – Cross-correlation coefficients values between the field propagation tests results and the excepted results provided by the simulation system.	68
Table 6.4 – Relation between the field propagation results and the expected values for each channel provided by the simulation system.....	71
Table F.1 - Results from the Field Propagation Tests on 30 th August 2017 using the DRC RapidM algorithm.....	91
Table F.2 – Results from the Field Propagation Tests on 31 st August 2017 using the DRC RapidM algorithm with ACOS.....	93
Table F.3 – Results from the Field Propagation Tests on 1 st September 2017 using the DRC RapidM algorithm with BEO.	97

Table F.4 – Results from the Field Propagation Tests on 4 th September 2017 using the Trinder algorithm.	100
.....
Table F.5 – Results from the Field Propagation Tests on 5 th September 2017 using the Trinder algorithm with ACOS.	102
.....
Table F.6 – Results from the Field Propagation Tests on 7 th September 2017 using the Trinder algorithm with BEO.	107
.....

List of Acronyms

2G	2 nd Generation
3G	3 rd Generation
3G-ALE	3 rd Generation Automatic Link Establishment
ACK	Acknowledgement
ACOS	Avoiding Cut-Off State
ACS	Automatic Channel Selection
ALE	Automatic Link Establishment
ALM	Automatic Link Maintenance
ARCS	Automatic Radio Control System
ARQ	Automatic Repeat Request
ATU	Antenna Tuning Unity
AWGN	Additive White Gaussian Noise
BEO	Bit Error Optimization
BER	Bit Error Rate
BLOS	Beyond Line-of-Sight
BW6	Burst Waveform 6
CM	Connection Management
CRC	Cyclic Redundancy Check
CSMA	Carrier-Sense-Multiple-Access
DCSI	<i>Direção de Comunicações e Sistemas de Informação</i>
DRC	Data Rate Change
DTS	Data Transfer Sub-layer
E/R GRC-525	Portuguese Military Radio
EID	<i>Empresa de Investigação e Desenvolvimento de Eletrónica</i>
EPM	Electronic Protection Measures
EW	Electronic Warfare
FER	Frame Error Rate
foF2	Critical Frequency of the F2 Layer
HDL	High Throughput Data Link
HDL+	High Throughput Data Link+
HF	High-Frequency
HFCS	High Frequency Channel Simulator
IRE	Institute of Radio Engineers
IRI	International Reference Ionosphere
IT	<i>Instituto de Telecomunicações</i>
ITU	International Telecommunications Union
LDL	Low Latency Data Link
LM	Link Maintenance
LOS	Line-of-Sight

LQA	Link Quality Analysis
LSU	Link Setup
LUF	Lowest Usable Frequency
MIL-STD	United States Military Standard
MUF	Maximum Usable Frequency
NATO	North Atlantic Treaty Organization
NFO	National Force Outstanding
NLOS	Non-Line-Of-Sight
NVIS	Near Vertical Incidence Sky wave
OSI	Open Systems Interconnection
PDUs	Protocol Data Units
PSK	Phase Shift Keying
PU	Participating Unit
RX	Receiver
SIC-T	<i>Sistemas de Informação e Comunicação - Tático</i>
SNMP	Simple Network Management Protocol
SNR	Signal-to-Noise Ratio
STANAG	NATO Standardisation Agreement
TM	Traffic Management
TO	Theatre of Operations
TX	Transmitter
UHF	Ultra High-Frequency
UN	United Nations
UV	Ultraviolet
VHF	Very High-Frequency
WRC-97	1997 World Radiocommunication Conference

Chapter 1 - Introduction

This chapter presents the motivation and the context of the problem to be solved; the main characteristics of high frequency (HF) signals and the importance of these signals in military communications are also described. Finally, the objectives, the main contributions and the structure of the Master Dissertation are outlined.

1.1. Context and Motivation

HF communications have been used by military organizations since the end of the First World War. These communications use the range of radio frequencies of the electromagnetic spectrum between 3 MHz and 30 MHz, known as HF band, allowing long distance transmissions (e.g., inter-continental) without the need of repeaters.

Before the 60s, HF radio signals were the primary source of long-range communications; in the 60s and 70s the HF transmissions declined because satellite communications allowed much higher data rates. However, satellites are vulnerable to physical damage and it is expensive to build and maintain them. In the beginning of the new millennium, the development of Automatic Link Establishment (ALE) technologies, including automated frequency selection and high speed modems (up to 9600 bit/s) for HF communications, have led to a renaissance in the HF usage.

HF frequencies are refracted by the Ionosphere, enabling beyond line-of-sight (BLOS) communications; this atmosphere layer is a region of electrically charged particles and it is situated, approximately, between 50 to 600 kilometres above the earth's surface. This layer refracts the signal back to earth several times, depending on the amount of ionization, before the signal reaches its destination, acting like a natural satellite.

The HF signals propagate, generally, in two ways: ground waves and sky waves (Figure 1.1). The ground waves can be direct, surface or ground reflected waves. Depending on the time of the day, of the atmosphere conditions and on the operating frequencies, sky waves can be refracted returning to the Earth surface hundreds or thousands of kilometres away, allowing long-range communications; this dissertation considers mainly this type of waves.

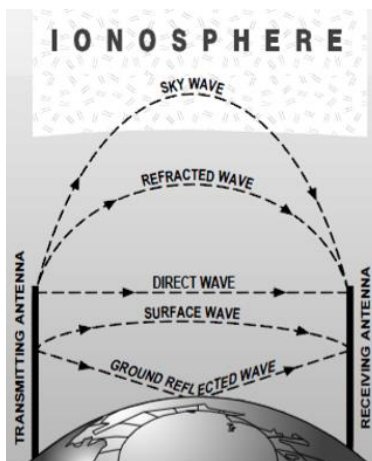


Figure 1.1 – Example of HF channel propagation waves [1].

The sky waves with most interest for military operations are the Near Vertical Incidence Sky waves (NVIS), which are characterized by having high tilt angles, typically between 60° and 89°. There are several advantages in the use of the NVIS, like the possibility of communication over hilly terrain without the need for repeaters; additionally, this form of propagation needs only one operator in the field using a small antenna, like a simple dipole antenna, which is very practical for military operations. For these reasons, the NVIS communication in HF band is often used in emergency situations and in the Theatre of Operations (TO).

The Portuguese Army participates in several National Force Outstanding (NFO), and the most common NFOs locations are situated in hilly terrain, like those in Afghanistan and Kosovo. The NVIS communications are used in NFO since 1996, in the Bosnia and Herzegovina's mission, and supported mainly by the military radio E/R GRC-525. This radio was developed by the Portuguese Army and by the company EID¹; Figure 1.2 shows a picture of it.



Figure 1.2 – Image of the E/R GRC-525 [2].

Despite the renewed interest on HF communications, there are a lot of challenges involved, like the operation with (typically) very low signal-to-noise ratios (SNR), multipath fading, signal variation on a time interval that may correspond to an hour, a season or a sun cycle, due to the changing constitution of the ionosphere, and a limited channel capacity [3]. In order to deal with the variability of the HF channel, several technologies have emerged, like automatic Link Quality Analysis (LQA), Automatic Link Establishment (ALE) and automatic Data Rate Change (DRC), eliminating the need for complex and manual operating procedures [2]. The LQA measures, assesses and analyses the link parameters, such as the bit error rate (BER) and the signal-to-noise ratio (SNR). These measurements are stored at, and exchanged between, stations and used for deciding about link establishment and maintenance [4]. ALE is a feature in a HF communications radio transceiver system that enables the radio station to establish a connection between itself and another HF radio station or network of stations. The purpose is to provide a reliable and fast method of calling and connecting during constantly changing HF ionosphere propagation conditions, reception interference, and shared (and sometimes congested) spectrum of HF channels, using the BER and the SNR values provided by the LQA [5]. The main purpose of a DRC algorithm is to select the highest possible data rate, based on the channel conditions (e.g., measured BER and/or SNR at the receiving side), and to change that data rate based upon changing channel conditions [3].

¹ EID - <http://www.eid.pt/>

In recent years, some DRC algorithms were implemented, but this technology was poorly developed with only two structured algorithms: Trinder [6] and RapidM DRC algorithm 1 [3], as these algorithms were developed in 2001 and 2005, respectively, there is a large margin for improving these solutions based on data rate adaptation failures. Both of these algorithms were tested in a High Frequency Channel Simulator (HFCS) which produces three classified channel types: Additive White Gaussian Noise (AWGN) channel, International Telecommunications Union (ITU) Good channel and ITU Poor channel. The HFCS works in conjunction with a SNR generator signal which produces the desired SNR function.

1.2. Objectives

As mentioned before, at the beginning of the 2000 decade some algorithms were developed to improve the HF communications efficiency, the main topic of this dissertation. The DRC algorithm for HF communications, available on the literature, were not implemented and tested on the field, with real propagation conditions.

Therefore, the main objective of this dissertation is to design, implement and test on the field an improved solution of a DRC algorithm for an efficient data transfer in the HF band, using the E/R GRC-525 radio. This shall be done by first implementing, in a simulation system, existing DRC algorithms, in order to assess them, find out their eventual vulnerabilities, and make the necessary improvements. The next step is to implement the DRC algorithms (original versions and improved ones) on the E/R GRC-525 radio and test them in real propagation conditions, and with a considerable distance between communicating stations, representing a conventional battlefield scenario.

1.3. Main Contributions

The main contributions of this dissertation are the new improved versions of existing DRC algorithms: the avoiding cut-off state (ACOS) version and the bit error optimization (BEO) version; comparatively to the original algorithms, the new proposed versions improve the link quality parameters such as the link availability, the average throughput (bit/s) and goodput (frames/s), the average BER and the average frame error rate (FER). The original algorithms and their improved versions were implemented in a military radio, and validated in a real HF transmission scenario, over a distance of approximately 300 km - in the existing literature, the original algorithms were just validated in simulation systems.

1.4. Dissertation Structure

This dissertation is organized in seven chapters, with this first one introducing the dissertation work in terms of context, motivation, objectives and main contributions.

Chapter 2 presents an overview of the HF communications and relevant concepts, such as the types of HF radio signals, the Ionosphere structure and how it is possible to know the usable communication frequencies; finally, an overview of the typical HF antennas is presented.

Chapter 3 describes the current adaptive techniques used in HF communications, and implemented by the E/R GRC-525 radio. Firstly, an overview of the important standards is presented; next, the

physical layer characteristics and requirements are summarized; finally, a brief explanation of the radio call process is given.

Chapter 4 briefly reviews the state-of-art on DRC algorithms; besides presenting the algorithms design, implementation and results, their main positive aspects and limitations are identified.

Chapter 5 describes the original DRC algorithms implementation, their assessment results and identified vulnerabilities; next, the design, implementation and evaluation of improved versions are presented; finally, a comparison between original and improved versions of the DRC algorithms is done.

Chapter 6 describes the field propagation tests, as the environment measures, the equipment assembly and the DRC software application developed. Finally, the main results are presented and a comparison with the expected values of the simulation system, described in Chapter 5, is performed.

Chapter 7 concludes this dissertation with a summary and suggestions for future work.

Chapter 2 - HF Communications

This chapter describes the different types of HF signals used in radio communications and the associated antennas; the main characteristics of the ionosphere propagation, with emphasis on the NVIS waves, are also overviewed.

2.1. Types of HF Radio Signals

In radio communications it is usual to consider three types of signals, according to the used carrier frequency: HF signals (High-Frequency), VHF signals (Very High-Frequency) and UHF signals (Ultra High-Frequency).

The UHF designates a range of electromagnetic waves between 300 MHz and 3 GHz, for which the wavelength varies from 1 metre to 10 centimetres. The UHF band is typically used for the transmission of television signals and in modern mobile phones signals; this band is also used by public service agencies for radio communications using narrowband frequency modulation.

The VHF corresponds to the frequency range between 30 MHz and 300 MHz, with wavelengths ranging from 10 meters to 1 meter. Unlike in the HF band, the ionosphere does not reflect the VHF waves and the transmissions are restricted to local areas. VHF waves are less affected by racket and interference from electrical equipment.

The HF band is situated between 3 MHz and 30 MHz, with wavelengths ranging from 100 to 10 metres; it allows long-distance transmission using reflection by ionosphere layer. The military forces use this frequency band because the transmission via satellite is expensive and it is easier to block using Electronic War (EW). Accordingly, the HF band is the most important band for military communications and it is used by ships, aircraft, non-line-of-sight (NLOS) radio networks and military operations in the field [7]. Figure 2.1 shows the main applications for the different types of HF communications.

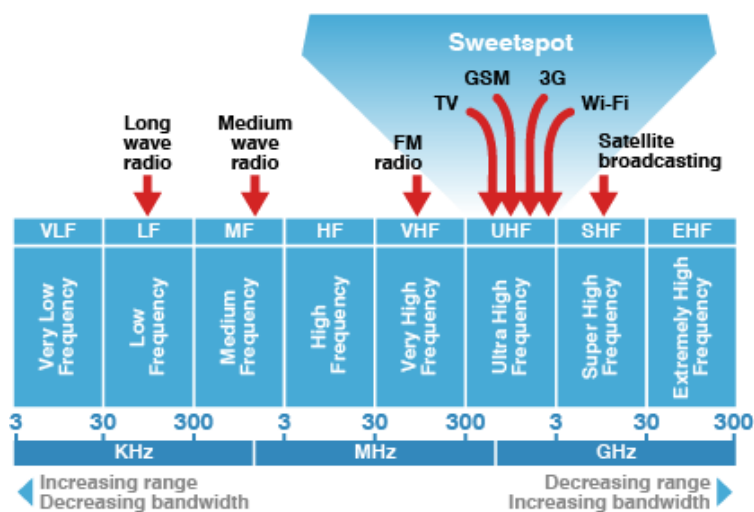


Figure 2.1 – Radio Spectrum [8].

2.2. Propagation by the Ionosphere

The Ionosphere is an atmosphere layer composed by a cold plasma, ionized by the ultraviolet radiation coming from the Sun, and occupies a range from 50 km to 600 km from the Earth's surface. It contains a great amount of electrons and ions that affect the radio waves and the electromagnetic signals, which justifies its name, that was coined in 1950 by the Institute of Radio Engineers (IRE) [9]. In the next section the characteristics of the Ionosphere and its relations with NVIS communications are described.

2.2.1. The Ionosphere Layer

The ionization of the atoms in the Ionosphere layer is the result of the cosmic radiation and solar radiation. During periods of high solar activity, the ultra-violet (UV) rays and other types of radiation influence the Ionosphere composition and its interaction with electromagnetic waves; therefore, it is necessary to permanently find out the optimum communication frequencies, which can be accomplished with the help of an ionospheric model. This model is a mathematical description of the ionosphere as a function of location, altitude, day of year, phase of the sunspot cycle and geomagnetic activity. The state of the ionospheric plasma may be described by four parameters: electron density, electron and ion temperature and ionic composition. Radio propagation depends uniquely on electron density [10].

One of the most widely used ionospheric model is the International Reference Ionosphere (IRI) [11]; this model divides the Ionosphere into four layers (or five, if the sporadic E_s layer is also considered), based mainly on the electronic density [12]; those layers are (see Figure 2.2):

- **Layer D:** it begins at 50 km high and finishes at 90 km, this is the closest layer to the Earth's surface. This layer causes attenuation of radio signals, low frequencies are attenuated more than higher ones, and heavy ionization only results in absorption of HF signals.
- **Layer E:** situated between 90 km and 140 km from the Earth's surface. HF radio signals are reflected in this layer back towards the Earth.
- **Layer F:** this layer is divided in **sub-layer F₁**, starting at 140 km to 300 km, and **sub-layer F₂**, starting at 300 km to 600 km from the Earth's surface. Most forms of sky wave propagation use the normal and cyclic ionization properties of this layer. It is a dual layer during the day, single at night.

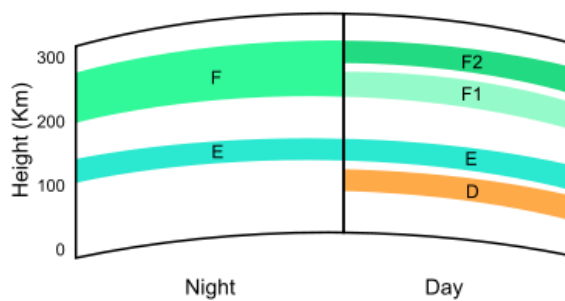


Figure 2.2 – The Ionosphere Layers [10].

When frequency is high enough it penetrates the E region it then may be reflected back by the F₁ region, the first part of the F region of the ionosphere, then with higher frequency F₁ is penetrated and F₂ is reflective (see Figure 2.3). Signals can hop more than once, they can be bounced back to the ground, then reflected back up to the ionosphere once again for another hop, sometimes several more times, and water should be used to reflect to do that hop, because it reflects much better than land.

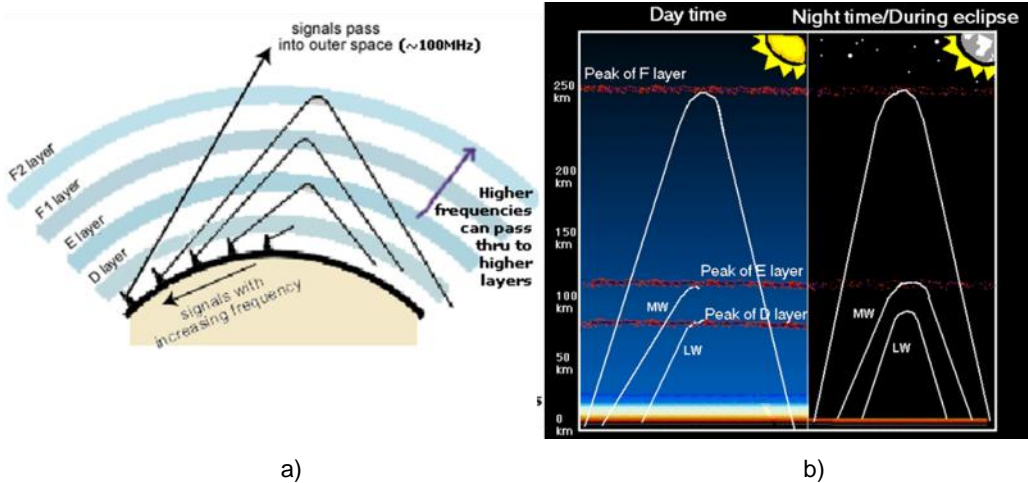


Figure 2.3 – Ionosphere behaviour: a) reflection depending on the frequency; b) reflection depending on the day time [13].

The D layer is the first layer of the ionosphere; it is the densest layer in the ionosphere and acts like an attenuator for HF signals with frequencies below 15 MHz. Since this layer disappears after the sunset, the lowest frequencies can only propagate at night.

The E layer is situated between 90 km and 140 km and is similar to D layer, because it is ionized only at day, with a maximum at noon. Normally, this layer can only reflect radio waves having frequencies lower than 10 MHz and may contribute a bit to absorption on frequencies above. There is a layer that appears rarely and it is named E sporadic (E_S); that layer appears in periods with high solar activity and is very slim, with a short period of existence (can be minutes or hours); it may contribute with a partial reflexion of the radiation [14], given raise to the so called M and N reflection types, showed in Figure 2.4 and Figure 2.5, respectively.

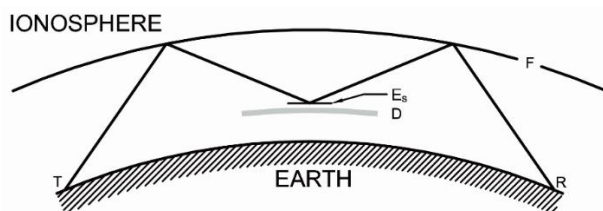


Figure 2.4 – Reflection of type M [14].

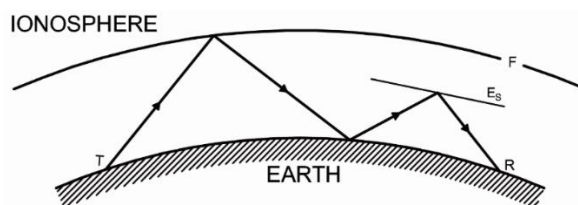


Figure 2.5 – Reflection of type N [14].

The layer F is divided into two distinct layers, *F*1 and *F*2. The *F*1 layer is situated between 140 km and 300 km and has an ionization level higher than layers E and D [14]; it suffers great modifications in the summer and with the effect of ionospheric storms [15]. The *F*2 layer is situated between 300 km and 500 km, with a maximum ionization level near 300 km from the Earth's surface. Like the other layers, the *F*2 varies with the hour of the day and attains the peak level at noon. At night, it fuses with *F*1, forming a unique layer. The *F* layer is always present in the Ionosphere and for that reason is considered as the most important for HF communications

The study of the Ionosphere's behaviour is very important due to its frequent layer changes, which condition the frequencies that should be used in HF communications. The study of the Ionosphere's behaviour is possible with ionograms (an example is given in Figure 2.6) that are obtained with an instrument - ionosonde - that measures the atmosphere ionization. The combination of all these ionosondes measurements around the planet allows to create a global real time map of the critical reflection frequency in the Ionosphere, as showed in Figure 2.7.

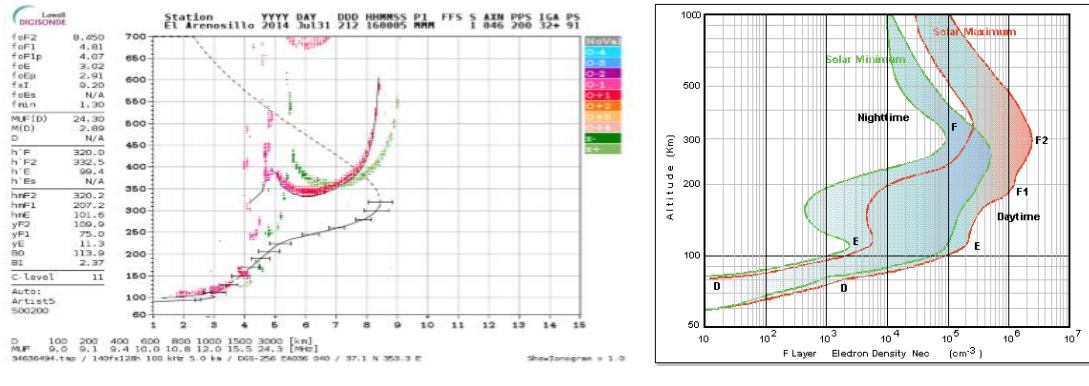


Figure 2.6 - Example of an ionogram: a) real [16]; b) schematic.

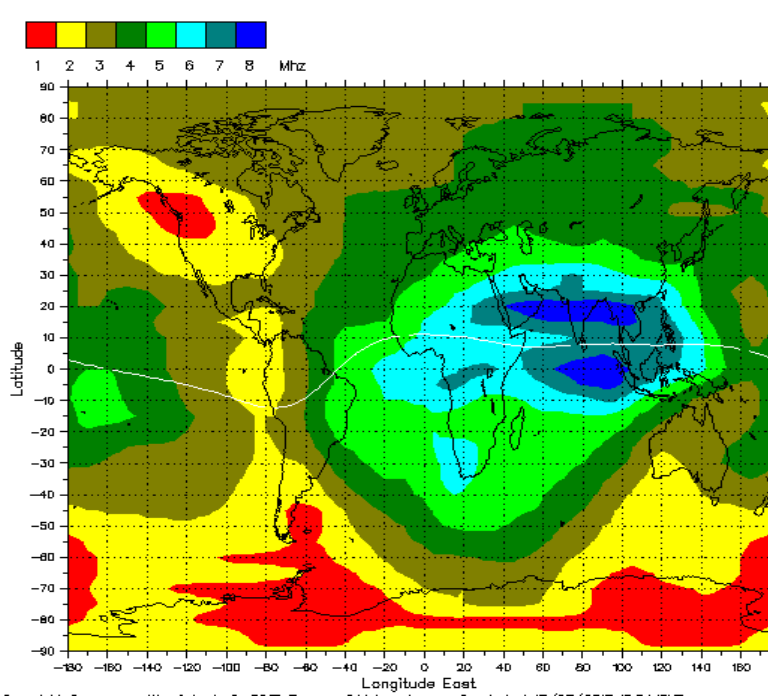


Figure 2.7 – Example of a Global Real Time Ionospheric foF2 Map [17].

Since the radio propagation conditions on the Ionosphere layer depend of the time of the day, the period of the year and the Sun activity cycle, these define the Maximum Usable Frequency (MUF) and Lowest Usable Frequency (LUF), with the following main characteristics [18]:

- MUF values are larger during the day than in the night.
- For layer F, MUF values are larger in the winter than in the summer, and for other layers it is the opposite, i.e., MUF values are larger in the summer than in the winter.
- MUF values are larger during a strong Sun activity cycle.
- LUF for short distances reach their maximum values in the afternoon and leave out the HF range during the night. LUF values are irregular for long distances.

2.2.2. Near-Vertical Incidence Sky wave

The NVIS is a radio sky wave used for military communications, broadcasting and by radio amateurs. This sky wave uses high tilt-angles (between 60° and 89°) and the Ionosphere to reflect the signals back to Earth. If the frequency is too high, the electromagnetic wave breaks the Ionosphere and continues the propagation to space; if the frequency is too low, the signal is reflected back to Earth in all possible angles (including the Zenith angle) resulting in an omnidirectional radiation [16]. Figure 2.8 shows the use of NVIS and how it allows to overpass the obstacles.

In NVIS, the Ionosphere reflects the energy according to an "umbrella" shape diagram (see Figure 2.8); this may cause fading on the received signal, although choosing a good antenna may reduce this effect [16]. The distance range of a NVIS signal depends on the Ionosphere's height and on the antennas tilt-angles, and the propagation loss varies between 110 dB and 120 dB [16]; this loss value is close to the free space propagation loss, because the beams arrive to the receiver in a vertical plane, so there are not effects from the Earth and the obstacle attenuation is null.

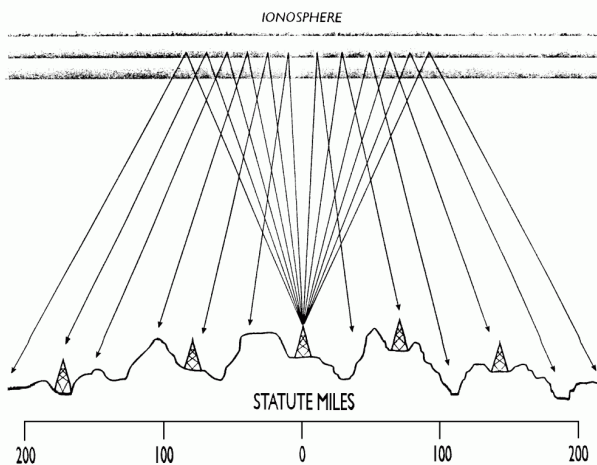


Figure 2.8 – NVIS propagation and its characteristic "umbrella" shape [19].

There are three important factors to consider in NVIS communications: interference between the Earth's wave and the Sky wave, high tilt-angles and choice of the critical frequency. In telecommunications, the critical frequency means the limit value of frequency, below which the wave is reflected by the Ionosphere layer, and above which the wave penetrates the Ionosphere [20]. The interference between the Earth's waves and the Sky waves is a problem because the Earth's wave can

have a destructive effect and break the communication. The high tilt-angles can be a problem because to have vertical radiation it is necessary to be careful with the selection of an antenna and the installation's local to minimize the Earth's wave and maximize the vertical radiation direction. It is also necessary to be careful to select the critical frequency, because in NVIS, if the frequency is above the critical frequency it is not possible to reflect the wave in the Ionosphere [16]. There is one direct relation between the incidence angle and the reflection angle in the Ionosphere².

Figure 2.9 shows the variation of the critical frequency during a period of 24 hours - with the increase of the UV intensity, the critical frequency also increases.

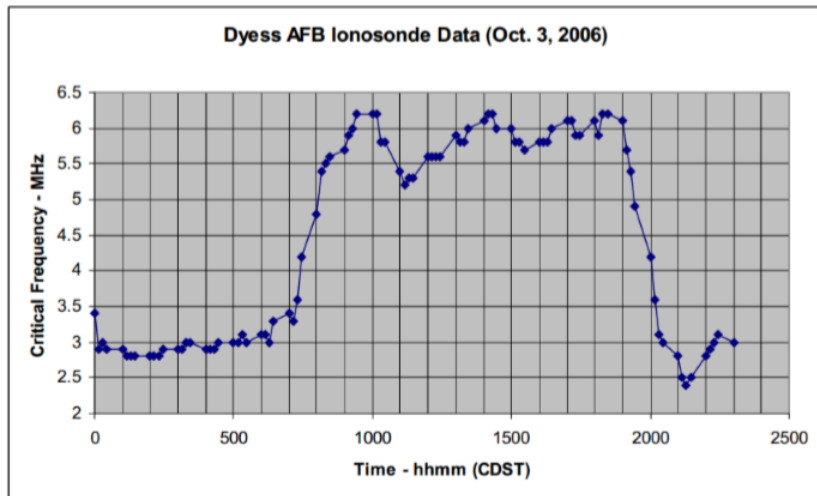


Figure 2.9 – Change of the critical frequency during the day, and on winter [16].

2.3. HF Antennas

Transmission antennas transform the electrical energy from the radio transmitter into electromagnetic waves to be propagated in the environment. Although the channel (Ionosphere) provides good conditions to propagate the radio waves over long distances, HF transmitter operates with thousands of watt, therefore the antenna must handle this high power [7]. As small HF antennas do not give a good impedance for the transmission system, some reactive elements, like capacitors and coils, should be introduced between the transmitter and the antenna [7].

One of the types of antennas that is used in NVIS is a horizontal half-wave dipole antenna, because it has the maximum radiation for high incidence angles. Another type of antenna used in NVIS is a circular loop antenna, because it has a high flow of power when it is placed on the vertical plane yz . Depending of the characteristics of the military operation it is possible to choose one of these two antennas to communicate in NVIS. The horizontal dipole antenna is not appropriate for mobile communications because its size is too big to be attached to one vehicle, but in turn, the horizontal dipole can be used by troop on feet because it is easy to assembly and disassembly, it is easy to carry on the backpack of a soldier and it can be placed on a safety zone to communicate. The circular loop antenna is more appropriate to use in mobile communications, attached to the vehicles, due to its

² Snell-Descartes' Law: $n1 \cdot \sin\theta i = n2 \cdot \sin\theta r$

dimensions. Otherwise, it is more difficult to carry by Special Forces [21]. Figure 2.10 shows a horizontal dipole antenna and a circular loop antenna.

Figure 2.11 shows the gain of three antennas often used in NVIS by military forces. The horizontal resonant dipole is situated 4.5 m above the ground, and the Whip antenna has a 4.5 m height. The graphic in Figure 2.11 shows that the horizontal resonant dipole is the ideal solution for NVIS communications because the gain is very constant along a wide frequency range; this is also confirmed by studies from the United States Army [16]. The Whip antenna is often used in vehicles by the Portuguese Army, but its gain changes a lot with the frequency. One of the methods to improve the efficiency of the Whip antenna is to put the antenna with an angle of 45° relatively to the vertical axis of the vehicle, transforming the Whip in an almost horizontal dipole antenna [16]; Figure 2.12 describes the method to transform the Whip antenna in a dipole.



Figure 2.10 – Antennas used in NVIS: a) horizontal dipole antenna [15]; b) circular loop antenna [21].

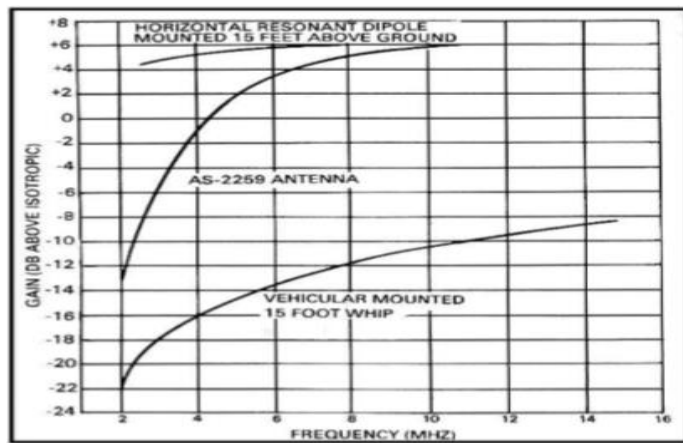


Figure 2.11 – Gain of three different antennas used in NVIS propagation [16].

When working in NVIS it is not necessary to have concerns about the orientation of the dipole antenna, since all energy is propagated in the vertical direction and returns to the Earth with an omnidirectional “umbrella” shape diagram. Therefore, to install the dipole antenna it is not necessary to know the receiver’s localization. However, when operating near the Equator line, the dipole should be installed in the North-South magnetic direction to improve the signal reception of all NVIS connections [16].

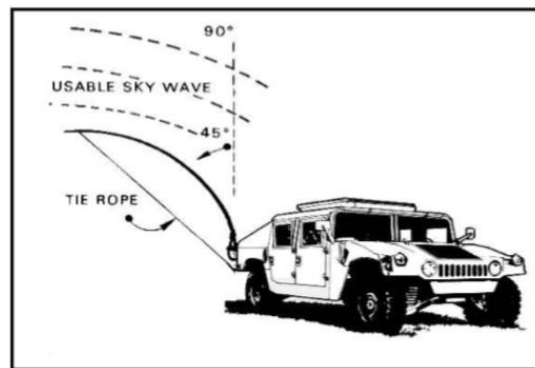


Figure 2.12 – Use of the Whip antenna for NVIS communication [16].

Chapter 3 - HF Communication Standards

3.1. Adaptive Techniques in HF Communications

The use of HF communications is governed by the natural changing of ionospheric propagation conditions so the signal carrier frequency has to be changed several times in a day. In the past, to assure optimal transmission conditions, frequency scheduling updates had to be implemented by human operators according to existing propagation conditions. The first adaptive techniques in HF systems were developed in the late 70s and the early 80s; control equipment was available at reasonable costs and processing power, and the latest radio equipment generation was controlled by computer and it could establish a radio link by selecting one traffic frequency among a small number of selected frequencies. More functionalities were added in the late 80s like full automatic link establishment, link maintenance to ensure the quality of service during message transfer and link disconnection [22].

The advantages of adaptive operation in HF communications were recognized by the 1997 World Radiocommunication Conference (WRC-97) through the adoption of Resolution 729; this resolution sets a number of provisions to ensure the use of appropriate bands, to ensure that interference is minimized, and to safeguard continued use by systems without adaptive techniques. The main characteristics of the adaptive HF systems are:

- **Easy to use:** the adaptive systems establish, maintain and disconnect the HF link without the need for a radio operator.
- **High reliability:** the time interval during which the adaptive systems provide high quality service is higher than in traditional fixed frequency systems, due to adaptive frequency selection, automatic repeating on request and more robust modulations.
- **Flexibility:** an adaptive system continuously analyses and updates the link quality assessment information selecting the best frequency for each particular instant, using quality analysis techniques. This adaptive technique minimizes the period in which stations cannot communicate and provides low power stations in both fixed and mobile services.

The Automatic Radio Control System (ARCS) process enables HF transmitters to automatically select the channel, and to communicate, establish and maintain a link according to the user requirements [18]. Figure 3.1 shows the tree components of an ARCS process.

The Automatic Channel Selection (ACS) is a process which automatically selects one or more channels from a group of pre-selected channels, in order to match the used modulation to the propagation conditions, and according to the quality requirements. To perform the ACS, the adaptive systems store a set of frequencies, selected by the human operator or by an automatic mechanism that reads from the data base stored by the LQA process. In general, the system stores five to ten frequencies in order to optimize the speed of channel searching, but some adaptive systems have the capability to store up to several hundred of frequencies [22].

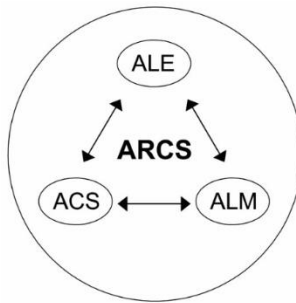


Figure 3.1 – ARCS process cycle [18].

The Automatic Link Establishment (ALE) is a process which automatically establishes a link, using the channel (or channels) selected by the ACS process; it is divided into Link Setup (LSU) and Traffic Management (TM) processes.

The Automatic Link Maintenance (ALM) process provides continuous availability of the established communication link [18].

Four stages can be identified in an adaptive HF communication:

- **Call pre-establishment:** in this stage, the LQA is the only running process, as it is performed only when there is no traffic flow in the station. Once every hour, each station in the network “sounds” every channel, by sending a short transmission to all other stations that contains its identity (ID). Any station may receive the sounding transmission and measure the signal quality. Along the time, each receiving station builds a data base (*LQA data base*) with the following values [23]: Station ID, Time Date Stamp, Channel number and Signal Quality level.
- **Call establishment:** when a call is initiated, the radio automatically checks its LQA data base and selects the best quality channel with the ID of the desired station. It then makes a first attempt to establish a link in that channel and, if not succeed, it will try again on the next best channel in the data base, and so on, until a link is established [23]; this process involves the ALE and ACS systems, simultaneous - the ALE process establishes the link using a channel selected by the ACS.
- **Call maintenance:** once the call has started, the ALM process continuously checks the link quality. If the minimum quality criteria are not attained, the ACS process automatically selects a new transmission channel and the ALE process establishes a link using the new channel.
- **Finishing the call:** when the call between two stations is finished, the LQA process starts again, continuously, until there is a new connection between stations.

3.2. Overview of HF Communications Standards

In the set of standards developed for HF communications, there are two types of military standards: the STANAG and the MIL-STD. The STANAG standard family is developed for countries that belong to NATO; the MIL-STD standard family is developed by the United States for communications in the defence department (although the USA belongs to NATO). As Portugal belongs to NATO force, the standard family adopted for the HF communications with military equipment is the STANAG. The

countries belonging to NATO adopted the STANAG 4538 (new version STANAG 4539), also known as ALE standard, to provide interoperability between systems from different manufacturers.

The HF communication standards implement the three first layers of the OSI model and also provide an interface to higher OSI layers; they can be arranged in the so-called "HF house", that is shown in Figure 3.2. The first HF house's floor (Physical layer) is created by standards that together constitute the concept of multi-modulation which gives two possibilities: use of an appropriate modulation related with the propagation conditions (e.g., SNIR and BER values, Ionospheric conditions) and to add new standards. The second HF house's floor (Link layer and Network layer) is composed by standards with two operations modes: non-Electronic Protection Measures (EPM) mode and EPM mode. The EPM mode is specified in STANAG 4444 and the non-EPM mode is implemented by the standards STANAG 5066 and 4538 [18]. In Figure 3.2, the HF standards relevant for developing a DRC algorithm (the main topic of this report) are signalized in green - they will be detailed in the next sections.

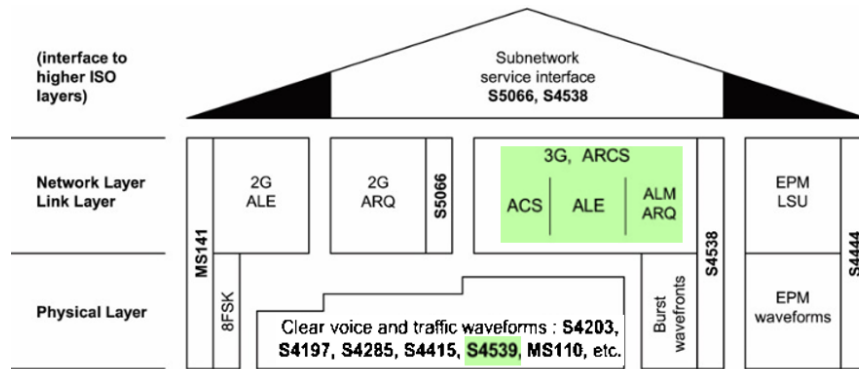


Figure 3.2 – The HF house of standards [18].

3.3. Physical Layer

The STANAG 4539 and MIL-STD-188-110B define the technical rules to use and guarantee the interoperability of land, air and naval HF radio modems [24]. STANAG 4539 describes a set of modems for data transmission rates between 3200 and 12800 bit/s. The used modulations are self-identifying which means that the data rate and the interleaver lengths settings are transmitted as a part of a modulation, and it permits fast adaptation of the modulation to changing channels conditions [1]. Since the communication channel can be in poor conditions and the data rate to use can be lower than 3200 bit/s, STANAG 4285 and MIL-STD-188-110B also describe the modulations to be used with data rates of 75, 150, 300, 600, 1200 and 2400 bit/s. Table 3.1 shows the respective modulation for each data rate.

The frame structure is shown on the top of in Figure 3.3. An initial preamble with 287 symbols is followed by 72 frames of data and known symbols. Each data frame consists of 256 symbols and is followed by a mini-probe of 31 symbols of known data. After 72 data frames, a 72 symbol subset of the initial preamble is reinserted to facilitate late acquisition, Doppler shift removal and synchronization adjustment. The total length of known data in this segment is actually 103 symbols: the 72 reinserted preamble symbols plus the preceding 31 symbol mini-probe segment which follows the last 256 symbol data block [24].

Table 3.1 – Modulation used for each data rate (adapted from [24] and [25]).

Data rate (bit/s)	75	150	300	600	1200	2400
Modulation	Walsh	BPSK	BPSK	BPSK	QPSK	8PSK
Data rate (bit/s)	3200	4800	6400	8000	9600	12800
Modulation	QPSK	8PSK	16QAM	32QAM	64QAM	64QAM

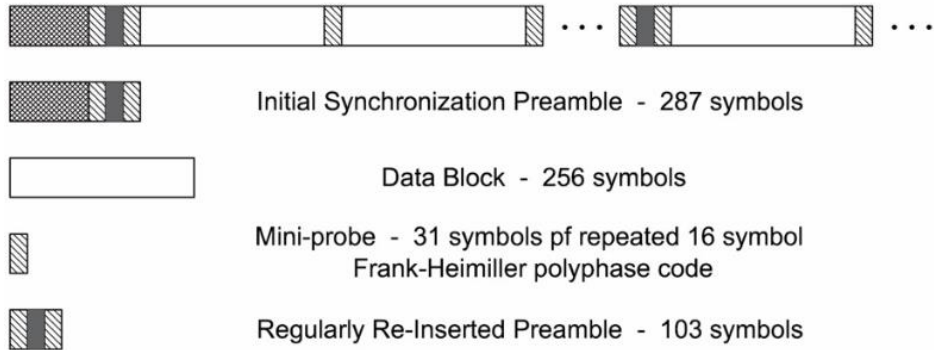


Figure 3.3 – Frame structure for all modulations [24].

There are two types of interleavers in HF communications: block and convolutional interleavers. The block interleaver has the advantage that if the data packets are sized to fit within an interleaver block, no flush is required, but the disadvantage is that it is only possible to synchronize at interleaver block boundaries. With a convolutional interleaver better performance is reached; the disadvantage of using the convolutional interleaver is that it requires a flush to clear out the interleaver at the end of the transmission [26]. The interleaver used is a block interleaver, each block of input data is encoded using a block encoding technique with a code block size equal to the size of the block interleaver. Thus, the input data bits will be sent as successive blocks of bits that span the duration of the selected interleaver length.

The block interleaver used is designed to separate neighbouring bits in the punctured block code over the span of the interleaver with the largest separations resulting for the bits that were originally closest to each other. A flexible interleaver structure is needed because of the 30 different combinations of data rates and interleaver lengths. The interleaver size consists of a single dimension array, numbered from 0 to its size in bits minus 1 [24].

The BER performance of the requirements in the STANAGs was measured using an HF channel simulator programmed to simulate the following channels:

- An AWGN channel, consisting of a single non-fading path, with each different quality test measured for 15 minutes; this channel is representative of ground wave propagation.
- An ITU Good channel, consisting of two independent but equal average power paths, with a fixed period of 2 ms delay between paths; each of the quality test was measured for 2 hours. This channel represents a mixture of the ground and sky wave propagation [27].

- An ITU Poor channel, consisting of two independent but equal average power Rayleigh fading paths with a fixed period of 2 ms delay between paths; each of quality test was measured for 2 hours. This channel represents sky wave conditions.

The measured performance uses the long interleaving period (the 36-frame interleaver) [28]. Table 3.2, Table 3.3 and Table 3.4 show the SNR (dB) requirements for, an AWGN channel, an ITU Good channel and an ITU Poor channel, respectively.

Table 3.2 – SNR requirements for a BER of 10^{-5} using an AWGN channel (Adapted from [3]).

Data Rate (bit/s)	Average SNR (dB) for BER not exceed 10^{-5}
9600	20,48
8000	15,44
6400	14,69
4800	12,29
3200	7,60
2400	10,75
1200	5,25
600	2,02
300	-1,50
150	-4,00
75	-6,75

Table 3.3 – SNR requirements for a BER of 10^{-5} using an ITU Good channel (Adapted from [3]).

Data Rate (bit/s)	Average SNR (dB) for BER not exceed 10^{-5}
9600	42,02
8000	35,56
6400	30,71
4800	25,21
3200	21,40
2400	19,45
1200	14,95
600	12,18
300	5,50
150	2,00
75	1,75

Table 3.4 – SNR requirements for a BER of 10^{-5} using an ITU Poor channel (Adapted from [3]).

Data Rate (bit/s)	Average SNR (dB) for BER not exceed 10^{-5}
9600	29,75
8000	25,50
6400	22,20
4800	19,75
3200	15,00
2400	15,70
1200	10,10
600	7,10
300	1,00
150	-1,00
75	-2,50

3.4. Automatic Channel Selection (ACS)

During the LQA process, the link establishment and the data exchange, the 3rd Generation Automatic Link Establishment (3G-ALE) scans the different channels and saves the corresponding BER and SNR values in a data base [2]. The ACS function uses some combination of propagation conditions prediction, measurements made by the ALE function (that are stored on the data base), and propagation reports provided by external systems to select a frequency that satisfies some requirements such as SNR or BER [22].

3.5. Automatic Link Establishment (ALE)

The last generation of ALE implemented in radio equipment is the 3G-ALE function and it is designed to quickly establish and efficiently broadcast (one-to-one) and multicast (one-to-many) links. It supports trunked-mode operation (separate calling and traffic channels) as well as sharing any subset of the frequency pool between calling and traffic. It uses a specialized Carrier-Sense-Multiple-Access (CSMA) scheme for calling channel access control and regularly monitors traffic channel to avoid interference [22].

The 3G-ALE receivers scan an assigned list of calling channels, listening for 2nd Generation (2G) or 3rd Generation (3G) calls. However, 3G-ALE includes an asynchronous system in the sense that a transmitter station makes no assumption about when a receiver station will be listening to any particular channel and it achieves its highest performance under synchronous operation. Assignment of channels to 3G-ALE scan lists may be static, but may also be managed dynamically via the Simple Network Management Protocol (SNMP) [22]. Figure 3.4 shows a synchronous dwell structure with a nominal duration of 5.4 seconds.

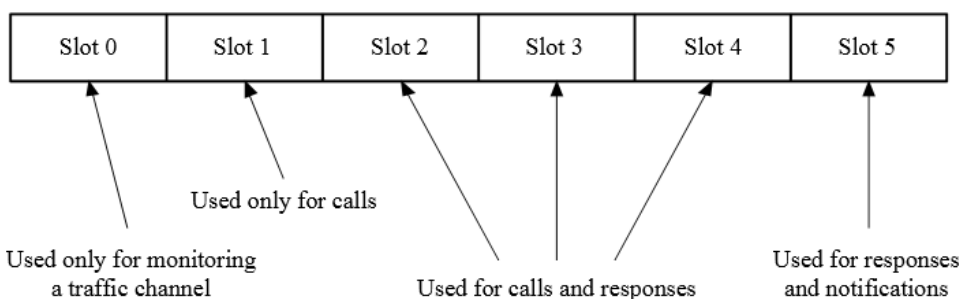


Figure 3.4 – Synchronous dwell structure in 3rd Generation ALE [22].

The Protocol Data Units (PDUs) used in broadcast calling are the Call and the Handshake PDUs. The Call PDU needs to convey sufficient information to the responder so that station will know whether it wants to respond, and what to listen during the traffic channel check. The Call PDU must report: the calling station identification; the priority of the incoming call; what resources will be needed if the call is accepted; and what traffic channel quality is required [22].

The Handshake PDU is used by both transmitter and receiver stations; it is sent only after a Call PDU has established the identities of both stations in a broadcast link establishment, as well as the main characteristics of the traffic that the link will use. The commands carried in Handshake PDUs are: Continue Handshake (link establishment is deferred until a reasonable channel is found); Commence

Traffic Setup (link establishment is finished and data traffic starts to set up); Voice Traffic (link establishment is finished and voice traffic starts) [22].

The point-to-point linking protocol establishes communications on a frequency or pair of frequencies within a few seconds and minimizes channel occupation during the link establishment process. A station will start the link establishment protocol immediately upon receiving a request to establish a link with another station [22]. A 3G-ALE call is showed in Figure 3.5 - the first call occurs in Slot 3, the responder receives the call, but has not identified a traffic channel reasonable for the requested traffic, and therefore sends a Handshake PDU containing a Continuous Handshake command. After the dwell, both stations tune (denoted by cross-hatched areas) during Slot 0, then listen for occupancy on a nearby traffic frequency. The caller selects Slot 1 and the responder has decided that an associated traffic channel was available. When the Call PDU is received by the responder, the measured channel quality is enough for the offered traffic, and the responder sends a Handshake PDU containing a Commerce Traffic Setup command that indicates the traffic channel to be used. Both stations tune to that channel in the following slot, and the caller initiates the traffic setup protocol [22].

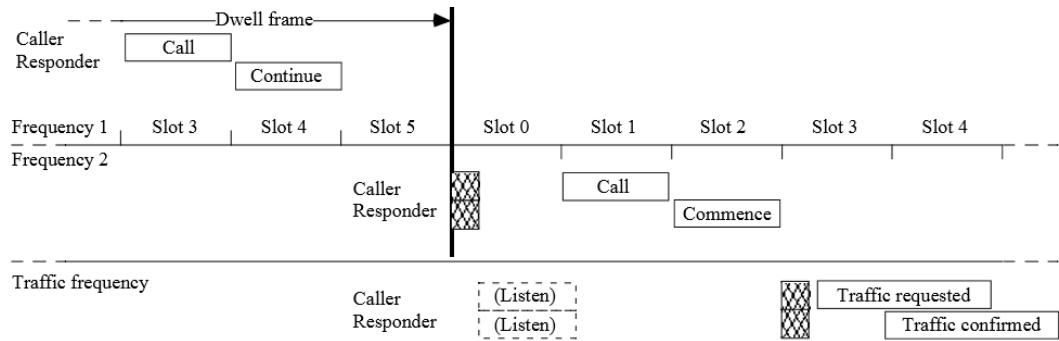


Figure 3.5 – The 3rd Generation ALE call [22].

3.6. Automatic Link Maintenance (ALM)

An ALM mechanism requires the following functions to be satisfied: a reasonable alternative frequency to be discovered; an unambiguous means should be provided to coordinate the changing of both stations to the new frequency; and interference to other stations should be minimized.

The ALM protocol is used by the Connection Management (CM) process to maintain established links. All stations support the mandatory function Link Maintenance (LM) Relink PDU, and the optional functions defined for ARCS process: coordinated departure to reasonable alternative frequencies as required by changing propagation and interference conditions (e.g., SNR, BER and ionospheric conditions); probing of candidate alternative frequencies during traffic; negotiation of frequencies for operating modes other than simplex (i.e., half-duplex or full-duplex); and renegotiation of modulation, data rate, and interleaver [22].

A Countdown field in the LM PDUs contains the number of times the PDU will be resent before the indicated change is to take effect. The sequence of LM PDUs is sent contiguously, ending with the PDU that contains a Countdown with the value of 0. The number of repetitions of the LM PDU is chosen to reduce to a reasonable level the probability that it will be missed by the other station [22].

Coordinated departure to new traffic channel employs the LM Simplex and/or LM Duplex PDUs as appropriate, to indicate a new frequency on which it will listen for traffic. The LM Duplex PDUs indicate that the sending station will continue to send on its current transmit frequency until another frequency is negotiated and the LM Simplex PDUs indicate that the sending station will change its transmit frequency and its receive frequency to that indicated in the LM Simplex PDU [22].

3.7. Data Link Protocol

The nomenclature xDL is the common notion for the two data link protocols defined in STANAG 4538, the High Throughput Data Link (HDL) and the Low Latency Data Link (LDL), that are described next.

3.7.1. High Throughput Data Link

The HDL is the protocol used to transmit large amounts of data over good channels. The data to be transmitted is split into packets of known size; the number of packets contained in one transmitted frame (of the HDL protocol) is given by the number attached to the protocol name (e.g. HDL_24 will transmit 24 HDL packets, 233 bytes in one packet), and the available frame sizes is 3, 6, 12 and 24 packets [29]. The receiving Participating Unit (PU) decodes the packets from each frame and sends an Acknowledge (ACK) message with information about which packets contained errors (selective ACK); this process enables retransmission of failed packets only. The highest data rate is 4800 bit/s which gives an approximate throughput of 3200 bit/s when the maximum amount of packets (24) are sent in each frame [29]. The High Throughput Data Link+ (HDL+) is the new version of the protocol HDL that supports higher data rates.

3.7.2. Low Latency Data Link

The LDL protocol is more robust than the HDL and is better suited for poorer channels and smaller amounts of data; the number of bits to be sent is also designated by a finite set, and only one packet is sent in each frame. The size of the transmission frame can vary from 32 bytes (LDL_32) to 512 bytes (LDL_512). No selective ACK is sent in LDL (as only one packet is sent per frame), and if an error occurs the whole frame is retransmitted. The highest throughput for LDL is approximately 500 bit/s [29].

3.7.3. High Throughput Data Link+

The HDL+ protocol is the combination of the high data rate modulations from STANAG 4539 and the code combining techniques in the data link protocols, achieving a maximum throughput of up to 10 kbit/s in a 3 kHz channel [29].

Each HDL+ forward transmission begins with an informational header transmitted in the most robust Burst Waveform 6 (BW6). The packet size, used modulations and code rate is described in the packet header, with a size of 51 bits. This solution enables the transmitting PU to instantly adapt any of these parameters (modulation, code rate and packet size) between successive frames, making the system highly adaptive to varying channel conditions. The header also contains an estimate of the SNR in the

return channel, information about which packets in the frame are to be sent and a 12 bit size Cyclic Redundancy Check (CRC) to validate the information [29]. As shown in Figure 3.6, the header contains 3 bits to distinguish the data from the ACK messages transmitted with the same BW6; the source address is a 10 bit size identifying the transmitter PU.

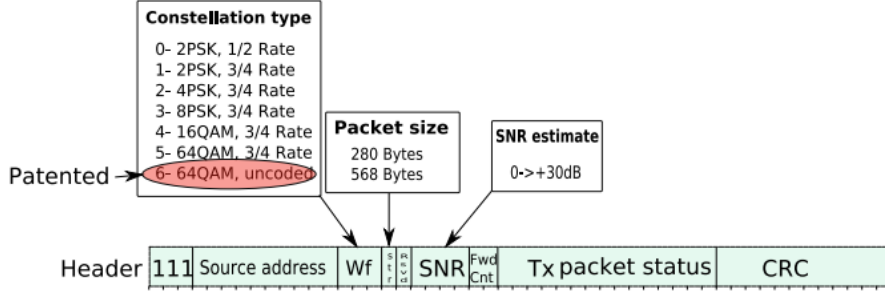


Figure 3.6 - HDL+ Header [29].

The ACK contains information about which packets were received correctly and also estimates of the fade rate and SNR value in the forward channel. This means that the transmitting PU knows which packets to retransmit and how the channel conditions are, so it can adapt the modulation and code rate accordingly [29].

Chapter 4 - State-of-the-art on Data Rate Change Algorithms

In HF communications, to ensure the largest data throughput on a link between two nodes, it is necessary to accomplish the following requirements:

- The best available channel must be used.
- The highest possible data rate must be used.
- The channel utilization should be high.
- The protocol overhead should be low.
- The system must adapt to changing channel conditions and avoid new link setup.

The purpose of a DRC algorithm is to select the highest possible data rate (measured in bit/s), the interleaver size to be used, and to change the data rate and the interleaver size based upon changing channel conditions. The best data rate and interleaver size is selected by the receiving node because it is in the best position to determine what the sending node settings should be when transmitting data [3].

The main requirements for a DRC algorithm are [30]:

- The algorithm should facilitate throughput maximization, avoiding unnecessary data rate changes.
- It should adapt to rapidly change channel conditions, minimizing the time taken to reach optimum data rate.
- It should be robust (i.e., a change to a new data rate should not break the current communications link).

The first DRC algorithms were developed 20 years ago, for Non-Autobaud Modulations (i.e., modulations for data rates between 75 bit/s and 2400 bit/s). The settling of higher data rates, and associated modulations, in adaptive HF systems, motivated the research for DRC algorithms for Autobaud Modulations (i.e., modulations for data rate rates between 2400 bit/s and 9600 bit/s).

This chapter provides an overview of two DRC algorithms: the first one, proposed by Trinder and Brown in 1999 [30], was developed for Non-Autobaud Modulations; the second one, proposed by Schulze and Hancke in 2005 [3], was developed for Autobaud Modulations.

4.1. DRC algorithm for non-Autobaud Modulations

Trinder and Brown proposed, in [30], one of the first DRC algorithms; the main task of the algorithm was to serve as a guideline for implementers of STANAG 5066. The algorithm uses the measure of the received Frame Error Rate (FER) to select the optimum data rate, and according to a simple rule: if the FER is above 50%, than the data rate should be reduced to half of its current value; otherwise, if the FER is zero or close to zero, the data rate should double its value. No mechanism to determine the optimum interleaver size was provided [3].

One of the major problems encountered by Trinder and Brown in their DRC algorithm is the possibility of data rate choice oscillation: if the modem data rate is increased because the FER is zero and in the next transmission interval the FER (at the higher data rate) is greater than 50%, then the modem data rate will be lowered again to the initial value. This oscillating effect can continue indefinitely, even if the

channel conditions remain constant. This effect is especially prevalent in an AWGN channel, which has very abrupt BER curves and thus causes a very sharp change in the FER values, even with a nearly constant SNR [3]. Another problem of the algorithm involves the time required to obtain enough data to estimate the FER with precision. Therefore, it may take a long time to perform the data rate adaptation, losing in efficiency.

Summarizing, the main disadvantages of the Trinder and Brown algorithm are:

- Data rate oscillations.
- Low robustness.
- Slow to performance.
- Inefficient approach.

Otherwise, the main advantages of this DRC algorithm are:

- Simple to implement.
- Independent of the particular modem implementation.

4.2. DRC algorithm for Autobaud Modulations

For Autobaud Modulations the simple rule proposed in [30] (i.e., DRC algorithm based on FER) cannot be applied, because the data rates are not related by a factor of two. Trinder and Gillespie [6] defined a formula to determine the Automatic Repeat Request (ARQ) throughput for the channel (see equations (4.1), (4.2), (4.3), and (4.5)), and it is related with the interleaver, modem latency and data retransmissions.

$$ARQThroughput = \frac{TX_Data}{[(Data_TX_Time + ACK_Time) + 2 \times Latency]} \quad (4.1)$$

$$TX_Data = 128 \times Packet_size(bytes) \times bits_per_byte \quad (4.2)$$

$$Data_TX_Time = \frac{TX_Data}{Modem_DataRate(bit/s)} \quad (4.3)$$

$$ACK_Time \approx Interleaver_Time(s) \quad (4.4)$$

Trinder and Gillespie [6] further studied the ARQ throughput as a function of SNR (see Figure 4.1). The resultant graph can be used to determine the optimum data rate choice for a particular SNR value.

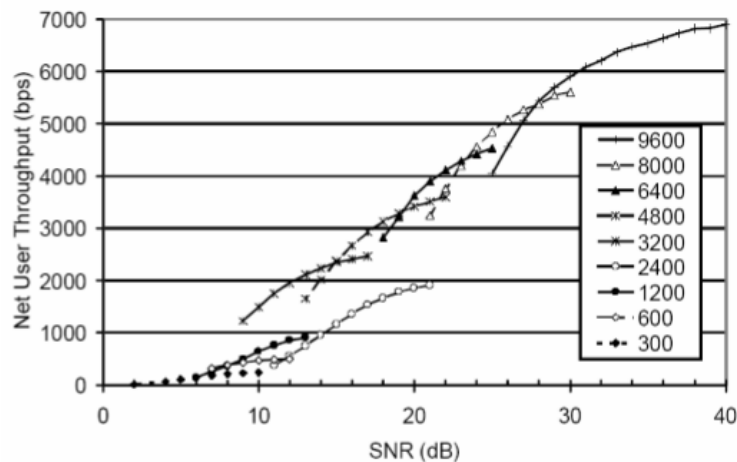


Figure 4.1 – ARQ throughput as a function of SNR [6].

The Trinder algorithm [6] uses the current FER measures. Table 4.1 presents the optimum FER decision threshold values for DRC, at every data rate, for Autobaud Modulations used by the Trinder algorithm. The 2400 bit/s data rate is never used in this algorithm, the transition between Autobaud Modulations and non-Autobaud Modulations is between 3200 and 1200 bit/s data rate values.

Table 4.1 – FER threshold values used for DRC algorithm for Autobaud Modulations [6].

Data Rate (bit/s)	Minimum FER (Decrease Rate)	Maximum FER (Increase Rate)
3200	50%	10%
4800	35%	5%
6400	20%	5%
8000	15%	2%
9600	5%	N/A

Nieto [31] evaluated DRC algorithm for Autobaud Modulations using different packet sizes and varying SNR values, over three types of channels: ITU Poor, ITU Good and AWGN channel. Nieto also indicated that the development of a DRC algorithm is quite complex due to the large number of variables involved like the message size, frame size, current channels conditions including SNR and BER, available modem data rates and interleaver size. The recommendations made by Nieto are [31]:

- Packet sizes should have a size between 750 and 1000 bytes; accordingly, smaller messages should be grouped together into a larger one.
- Use the long and short interleaver for common channels, and the long one for fading channels.
- Data rate changes should be minimized.

The length of the interleaver has an effect on the FER. The choice of which interleaver to use is a trade-off between the latency due to the interleaver delay and the reduced FER. Based on the analysis presented in [6], Trinder and Gillespie recommended to always use the shorter interleaver, except in broadcast data exchange mode, where the long interleaver is preferable.

4.3. RapidM DRC algorithm

The RapidM DRC algorithm was proposed by Schulze and Hancke, in [3], in 2005. A remote station will first create a physical connection to the local station, and the remote station will start to send data to the local station; therefore the local station will be in the receiver (RX) state. After a transmission interval lasting a maximum of 127s the local station responds to data sent by the remote station. When the RX state ends, the local station decides the new data rate and interleaver values, that the remote station will use in the next transmission (TX) interval. The RX interval is the time since that the remote station sends the data until the local station receives it.

The inputs and the outputs of the algorithm are represented and described in Figure 4.2 and Table 4.2. The data rate may take the values represented in Table 3.1 (the value of 12800 bit/s is not included); concerning the interleaver size, the long one is used for data transmission and the short one is used in ACK messages.

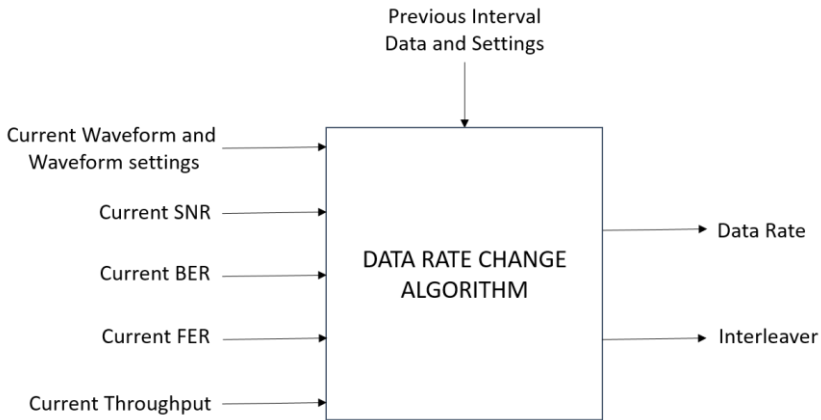


Figure 4.2 – RapidM DRC algorithm1 system of inputs and outputs [3].

Table 4.2 – RapidM DRC algorithm 1 input parameters [3].

Parameter	Description
Interval time (ms)	Total time of the RX interval
Interval throughput (bit/s)	Data throughput achieved in RX interval
FER (%)	FER calculated from data in RX interval
BER	Estimated BER from data in RX interval
SNR (dB)	SNR value for the RX interval

Although the previous algorithms used the FER to determine the current data rate performance, Schulze and Hancke [3] proposed to use the BER, as it reflects the FER, SNR, Doppler spread and multipath effects into one measurable value, and it is measured directly by the HF modem. The relation between FER and BER is given by equation (4.5), where L is the size of the transmission frame, in bits:

$$FER = 1 - (1 - BER)^L \quad (4.5)$$

Table 4.3 gives an indication of frames received in a TX interval that lasts the maximum allowable time of 127s and a frame length of 250 bytes.

Table 4.3 – Number of frames received after 127s interval and frame length of 250 bytes (Adapted from [3]).

Data rate (bit/s)	75	150	300	600	1200	2400
Number of Frames	5	10	20	39	77	153
Data rate (bit/s)	3200	4800	6400	8000	9600	12800
Number of Frames	204	305	407	508	610	N/A

4.3.1. RapidM DRC algorithm 1 design

The RapidM DRC algorithm is based upon four rules [3] and Figure 4.3 describes the flowchart of the algorithm:

- **Rule 1:** will estimate the best data rate based upon the 10^{-5} BER line on a data rate as a function of SNR graph (see Table 3.2, Table 3.3 and Table 3.4).
- **Rule 2:** estimates the data rate based upon the current BER and the average BER.

- **Rule 3:** will estimate the optimum data rate based upon the measured BER and is used when a specific data rate has been acquired and only small data rate changes are made (i.e. increase the rate or decrease the rate by one step).
- **Rule 4:** implements certain safety checks that will limit the change that a DRC rule can make to the current modem data rate, as well as limit the data when the SNR is too low.

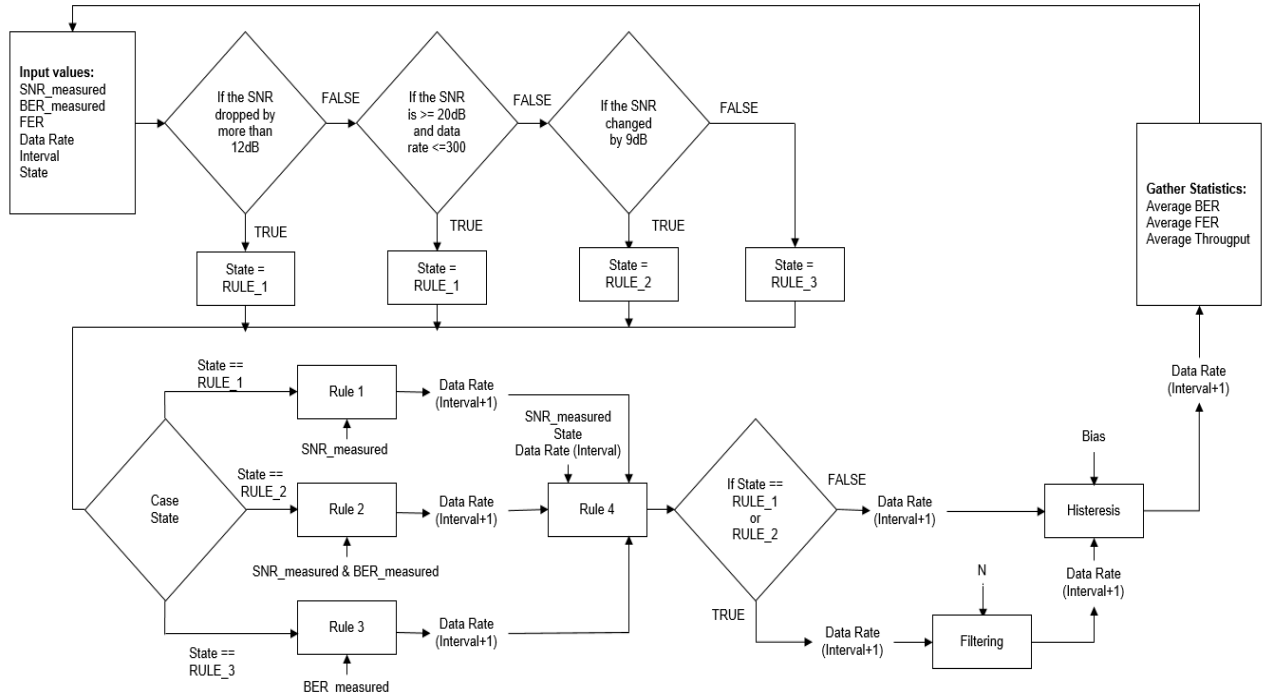


Figure 4.3 – RapidM DRC Algorithm1 flowchart (Adapted from [3]).

4.3.1.1. Rule 1

After a RX interval the inputs of the Rule 1 are the SNR measurement and the current data date. The line through the data points (see Figure 4.4) is found with the least squares method. All the data points are plotted and the best line is in the form of $y = mx + b$. The least squares method works based on y , the value that changes, and x , the value that is known with precision. The best line can be calculated by minimizing the sum of the square of the residual values, and that residual values are calculated in equation (4.6), as the difference between the observed y value and the calculated y value [3].

$$\Delta y = y_{obs} - y_{calc} \quad (4.6)$$

Rule 1 uses the equations (4.7), (4.8), (4.9) and (4.10) to determine the output data rate. This rule assumes that it is used an ITU Good Channel and that the interleaver length is long. The input data rate is determined based on the performance of the HF data modem. The ΔDR value is the difference between consecutive data rates:

$$\Delta SNR = SNR - \left[\frac{10 \times \log_{10}(Data_Rate_IN) - b}{m} \right] \quad (4.7)$$

$$\Delta DR = m \times \Delta SNR \quad (4.8)$$

$$Final_Data_Rate_Log = 10 \times \log_{10}(Data_Rate_IN) + \Delta DR \quad (4.9)$$

$$Data_Rate_OUT = 10^{\left(\frac{Final_Data_Rate_Log}{10} \right)} \quad (4.10)$$

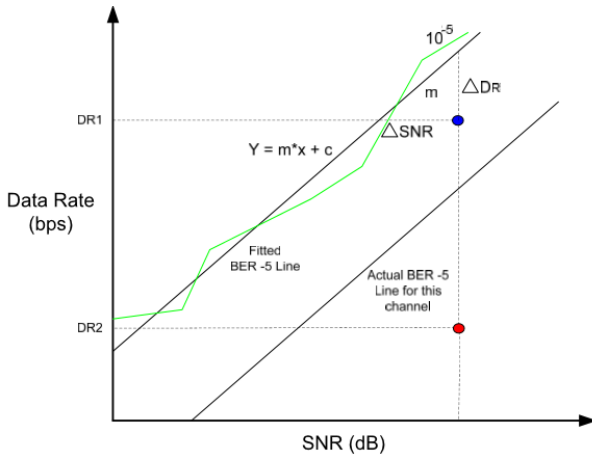


Figure 4.4 – The fitted line through the 10^{-5} BER points [3].

4.3.1.2. Rule 2

The output of rule 2 is a ΔDR value that should be added to the current data rate to produce the new data rate for the next RX interval. This rule can change the data rate in a maximum of two steps up and three steps down, because it is assumed that the change in BER is equal to 1 dB per decade, therefore if the BER is equal to 10^{-4} and the SNR increased 1 dB, the BER will change to 10^{-5} for the same data rate. The change in data rate (ΔDR) is proportional to the change SNR(ΔSNR), which is determined in equation (4.11), in order to keep the FER value low. Rule 2 uses the equations (4.8), (4.9), (4.10) and (4.11) to determine the output data rate [3].

$$\Delta SNR = BER_{measured} - 4 \quad (4.11)$$

4.3.1.3. Rule 3 – RapidM DRC algorithm 2

The rule 3 implements the RapidM DRC algorithm 2. This rule is used to make small data rates changes, like one step up or one step down. The RapidM DRC algorithm 2 is a very simple algorithm and works on the same purpose as the Trinder algorithm. It does not use the FER to decide, but the estimated BER, measured by the HF data modems. Table 4.4 shows how the algorithm works.

Table 4.4 – BER decision threshold for RapidM DRC algorithm 2 (Adapted from [3]).

BER	Equivalent FER	Data Rate Action
Higher than 10^{-4}	18%	Decrease data rate
Lower than 10^{-4} and Higher than 10^{-6}	Between 0,2% and 18%	Keep data rate the same
Lower than 10^{-6}	0,2%	Increase data rate

The BER is a better estimate of the current channel conditions than the FER because the BER is a function of the current SNR, Doppler spread and the multipath and is measured on all incoming data bits, and is not subject to change based on the number of frames received from the remote station. The estimated BER is returned by the HF data modem as a value between 0 and 7 (inverse power of BER), and based on this returned value the data rate will be increased, decreased or remain the same, according with Table 4.4 decision parameters. The frame length will need to remain consistent for all data rates of the algorithm [3].

4.3.1.4. Rule 4

The purpose of rule 4 is to ensure that if the current data rate is changed using rule 2, the rate can only be changed by a maximum of two data rate steps upwards and a maximum of three data rate steps downwards. This rule also sets the data rate to 75 bit/s if the SNR value is smaller than -2 dB [3].

4.3.2. RapidM DRC algorithm 1 implementation

The RapidM DRC algorithm1 was implemented in the Data Transfer Sub-layer (DTS) of the STANAG 5066 station and the algorithm is executed at the end of each RX interval. During this RX interval, the station queries the HF modem measurements according to the current channel conditions. The modem returns the current SNR and BER measurements for the RX signal, and the measurements values are returned periodically to the station which will average there values. When the DRC algorithm is executed, the average SNR and average BER together with the interval number, interval duration and current RX data rate constitute the inputs to the RapidM DRC algorithm 1. The output of the RapidM DRC algorithm 1 will be the RX data rate for the next RX interval (see Figure 4.5) [3].

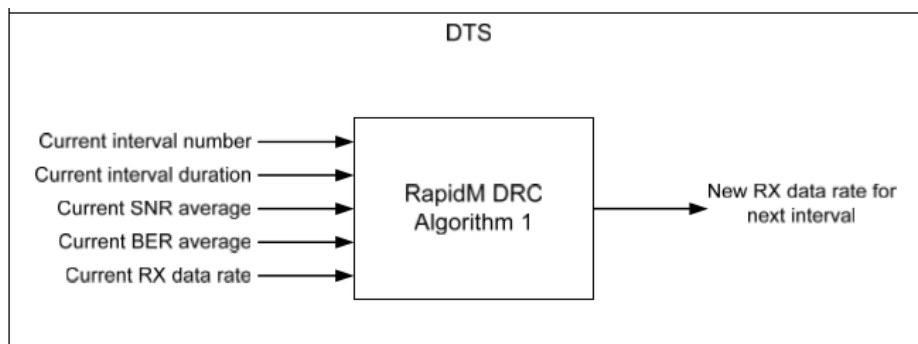


Figure 4.5 – Input and Output system of the RapidM DRC algorithm 1 implementation (Adapted from [3]).

The SNR value returned by the HF modem is calculated using a measurement period of 10 seconds, and this period is also the minimum period that the RX interval has to last for the DRC algorithm to be executed. The value of 10 seconds is used because of the maximum time to send one very long interleaver block with the STANAG 4539 (8.92 seconds). The station also has to average the queried SNR and BER values to reflect the measurement for the entire RX interval. This can be done using equation (4.12) [3]. Also, the BER average and the interval average can be computed using (4.12), with their own values.

$$SNR_{avg}(k) = \frac{\sum_{i=1}^k (SNR(i))}{k} \quad (4.12)$$

The optimum solution proposed by Schulze and Hancke [3] is to design and implement control logic inside the RapidM DRC algorithm 1 that would estimate the BER for each data rate by constructing a channel BER profile (see Figure 4.6). A BER estimate table is constructed that contains the BER estimate for each data rate of the STANAG 4539 waveform, from 75 to 9600 bit/s.

The shifter will shift the current BER estimates table left or right by a certain number of data rates. The number of BER estimates that is shifted depends on the change of SNR from the previous interval to the current interval. The following assumptions are made:

- BER value can range from 10^{-7} to 10^0 .
- The average SNR difference between consecutive data rates is 3 dB.

Therefore, when a BER average value for a data rate is 10^{-7} , then it is assumed that if the rate is increased by one rate step, the next BER average at the same SNR will be 10^{-4} . So, if the SNR changes by more than 3 dB, the entire BER channel profile can be moved left or right by one data rate (see Figure 4.6). The number of data rates to shift is given by equation (4.13). If the SNR change is negative the BER profile shifts to right, and if the SNR change is positive the BER profile shift left (according to Figure 4.6).

$$\text{Number_rates_to_shift} = \left\lceil \frac{\text{SNR_changes}}{3} \right\rceil \quad (4.13)$$

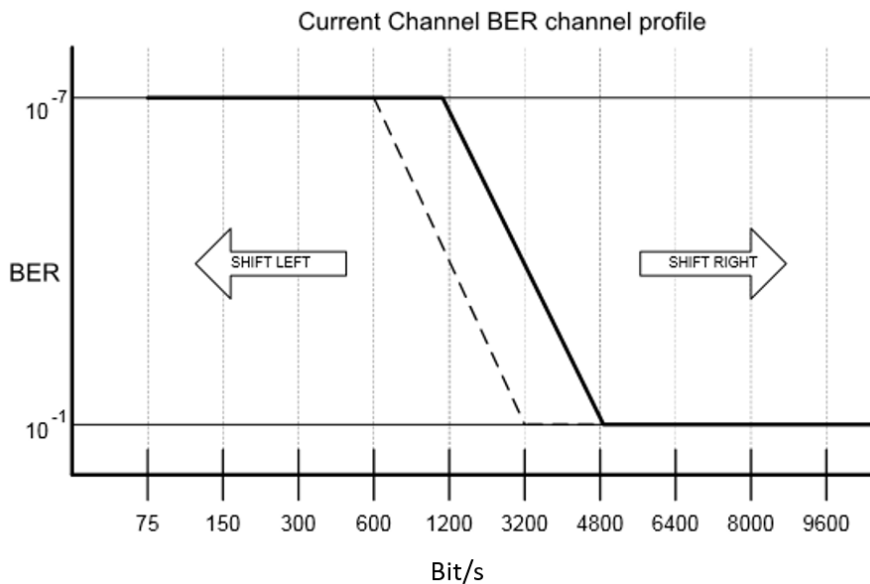


Figure 4.6 – BER channel profile [3].

4.3.3. RapidM DRC algorithm 1 simulation, results and tests

A HFCS was used to simulate the HF channel between two stations, and this channel is characterized by multi-path propagation and signal fading. A SNR generator works in conjunction with the HFCS, and its function is to change the SNR value along time. Table 4.5 shows the constants values used to simulate; the tests setting are represented by Table 4.6 and the following parameters of interest were measured:

- Data throughput - for the entire test duration, measured in bit/s for a RX interval.
- Data rate oscillations - number of data rate oscillations over the entire test duration.
- Algorithm robustness - number of times a data rate change resulted in loss of link during the entire test duration, this value counts the number of times the FER value due to a data rate change is greater than 80 %.
- Average BER - over the entire test duration.
- Average FER - over the entire test duration. This value is computed using equation 4.2.

- Total acquisition time - Required time to reach the optimum data rate for a particular SNR value.

Table 4.5 – Simulation constants (Adapted from [3]).

Description	Value
Number of receive intervals	100
Time of each receive interval (s)	120
Number of bytes in one frame	250
Constant value that will be used to determine the filtering weight	3

Table 4.6 – Test settings for RapidM DRC algorithm 1 (Adapted from [3]).

Data Throughput Test	
Test setting	Test value
HF channel used	AWGN, ITU Poor, ITU Good
PDU frame length	250 bytes
Message size	200-1000 bytes
Test Duration	220 min
SNR start value	-3 dB
SNR end value	35 dB
Acquisition Time Test	
Test setting	Test value
HF channel used	ITU Poor
Message size	200-1000 bytes
Test Duration	220 min

Table 4.7 – Results for data throughput test for Trinder and RapidM DRC algorithms (Adapted from [3]).

AWGN Channel		
Parameter	Trinder Algorithm	RapidM DRC algorithm 1
Number of intervals	160	203
Average BER	$10^{-5,4375}$	$10^{-6,7401}$
Average FER	15,744 %	1,4313 %
Number of oscillations	61	8
Robustness	17	2
Data throughput	2030,167 bit/s	2435,536 bit/s
ITU Poor Channel		
Parameter	Trinder Algorithm	RapidM DRC algorithm 1
Number of intervals	201	180
Average BER	$10^{-5,1207}$	$10^{-6,4429}$
Average FER	18,8088 %	5,768 %
Number of oscillations	52	10
Robustness	18	2
Data throughput	1239,916 bit/s	1776,474 bit/s
ITU Good Channel		
Parameter	Trinder Algorithm	RapidM DRC algorithm 1
Number of intervals	210	201
Average BER	$10^{-4,9556}$	$10^{-6,1017}$
Average FER	23,8089 %	8,2271 %
Number of oscillations	36	9
Robustness	21	4
Data throughput	912,583 bit/s	1191,149 bit/s

The data throughput test results are represented in Table 4.7 for three different types of HF channels; a comparison with the Trinder algorithm [6] is also provided. These results show that the RapidM DRC

algorithm 1 has a higher data throughput, has a lower average BER and FER measurements, has less data rate oscillations and is more robust in every HF channels, than the Trinder algorithm. The acquisition time test results are represented in Table 4.8.

Table 4.8 – Results for acquisition time test for Trinder and RapidM DRC algorithms (Adapted from [3]).

Parameter	Trinder Algorithm	RapidM DRC algorithm 1
Average BER	$10^{-5,3069}$	$10^{-5,9801}$
Average FER	23,5482 %	11,9405 %
Robustness	6	4
Total acquisition time (measured intervals)	49	19

Chapter 5 – DRC Algorithm: Assessment of Existing Solutions and Proposals for Improvement

This chapter presents the simulation and assessment of the DRC algorithms described in the previous chapter. Based on the assessment results, several improvements on those algorithms are then proposed and evaluated.

5.1. DRC Algorithms Simulation System

In order to assess the performance of the DRC algorithms described in Chapter 4, a simulation environment was created in Matlab code, whose flowchart is presented in Figure 5.1.

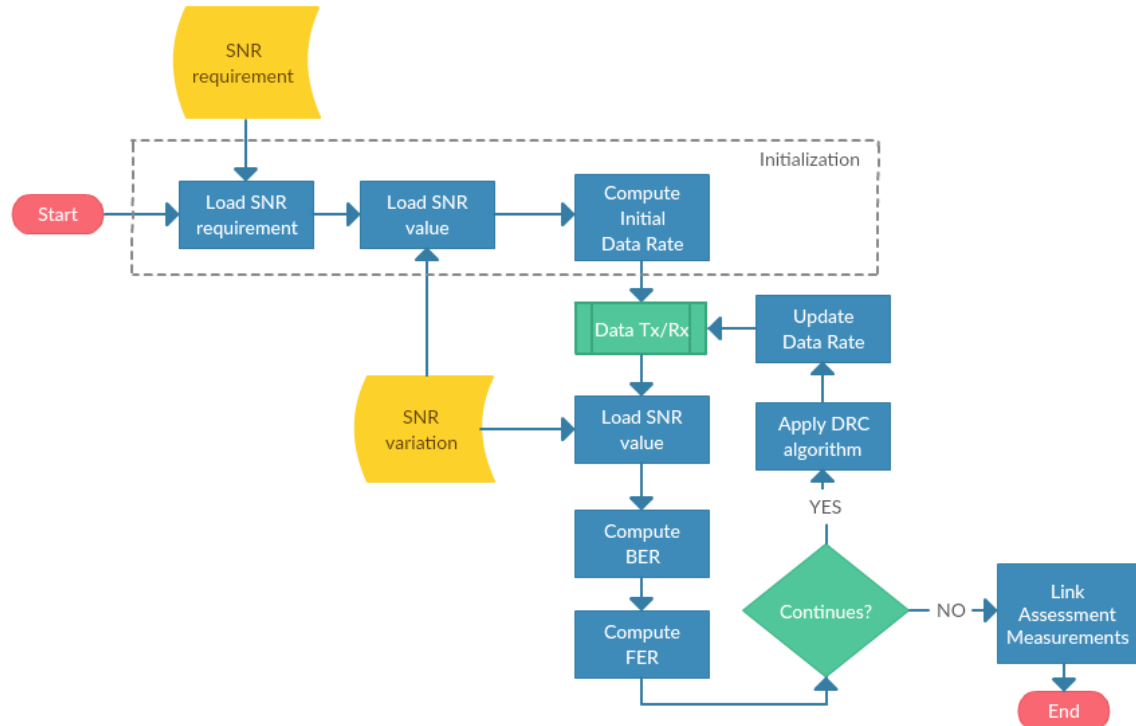


Figure 5.1 – Simulation system flowchart.

The simulation system starts with an initialization process that loads the SNR channel requirements for a BER of 10^{-5} and for the considered channel type, which can be AWGN (cf. Table 3.2), ITU Good (cf. Table 3.3) or ITU Poor (cf. Table 3.4). This process continues with the reading of the current channel SNR, which leads to the computation of the initial data rate by comparing the current SNR with the SNR channel requirements. After this initialization process, the data transmission between stations starts. Periodically, the system reads the current channel SNR and computes the corresponding channel BER and FER using equations (5.1), (5.2) and (4.5); based on these values and on the current data rate, a new data rate value is computed by the DRC algorithm that will be applied to the following transmission interval.

It is worth to note that (5.1) is just an approximation of the BER vs SNR, valid for the range of BER values showing a linear variation with the SNR, in logarithmic units; as shown in Figure 5.2, for BER

values below 10^{-5} the BER decreases by one decade per $+1$ dB variation in SNR, which can be expressed by (5.1).

$$\text{BER} = 10^{-5} \times 10^{-\Delta\text{SNR}} \quad (5.1)$$

$$\Delta\text{SNR} = \text{SNR}_{\text{current}} - \text{SNR}_{\text{requirements}} \quad (5.2)$$

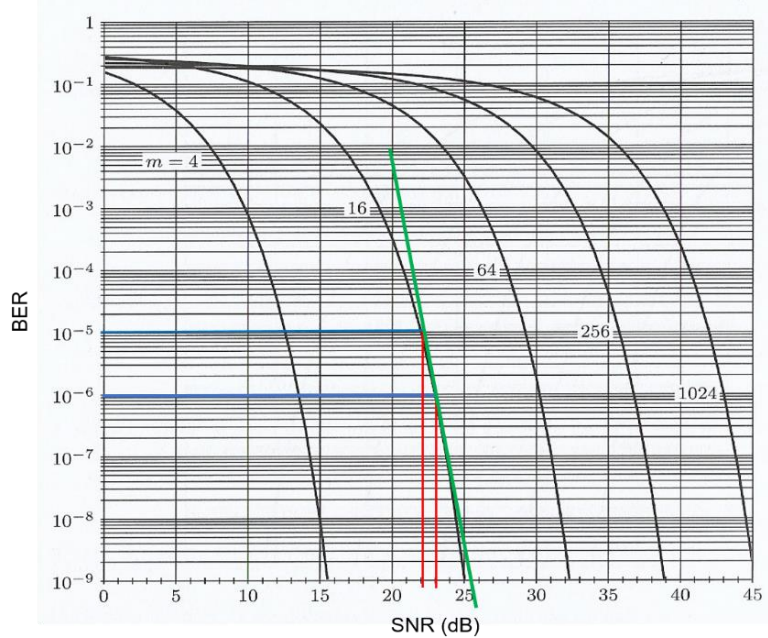


Figure 5.2 – BER as a function of SNR for m-QAM modulation, with a straight line (in green) representing a BER variation of 1 decade per dB (Adapted from [32]).

After the BER and FER computation, the selected DRC algorithm will be applied whenever there is still data to be transmitted; the current data rate will be then updated for the following data transmission interval. The concept of data transmission interval (or time interval) is defined by the period between two SNR measurements. Figure 5.3 shows the time diagram of the channel measurements - at the beginning of each time interval, the computed BER and FER refers to the previous time interval, and the updated data rate refers to the following interval.

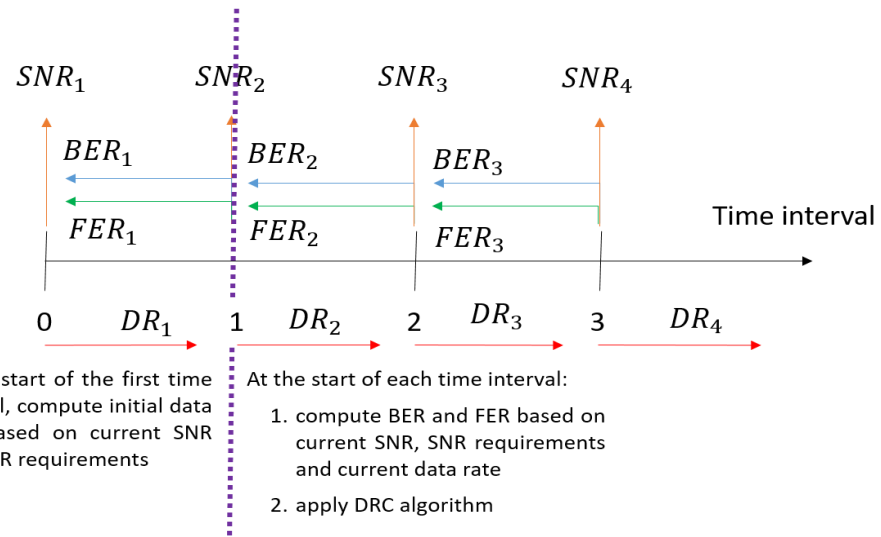


Figure 5.3 – Channel measurements time diagram.

This process shown in Figure 5.3 is applied only in the TX station, because the transmitted frame has a header with the current data rate, and after the RX station read the header it will update this data rate. At the end of the transmission, the following link assessment metrics are computed:

- Average Data Rate (in bits/s) – defined by (5.3), where DR_i is the data rate value for the interval number i , T_i is the interval duration and N is the total number of intervals

$$\overline{DR} = \frac{\sum_{i=1}^N DR_i \times T_i}{\sum_{i=1}^N T_i} \text{ [bit/s].} \quad (5.3)$$

- Average BER – defined by (5.5), where BER_i is the value of the computed BER for interval number i . Whenever the BER value is higher than 10^{-3} , it is considered that the link is in cut-off state; an auxiliary variable, τ_i , computed by (5.4), accounts for the time intervals that are not in cut-off state. This metric is only counted when the link is available

$$\tau_i(BER_i) = \begin{cases} T_i & \text{if } BER_i \leq 10^{-3} \\ 0 & \text{if } BER_i > 10^{-3} \end{cases}, \quad (5.4)$$

$$\overline{BER} = \frac{\sum_{i=1}^N BER_i \times \tau_i(BER_i)}{\sum_{i=1}^N \tau_i(BER_i)}. \quad (5.5)$$

- Average FER (in %) – defined by (5.6), where FER_i is the value of the computed FER for interval number i . As in average BER, this metric is only counted when the link is available

$$\overline{FER} = \frac{\sum_{i=1}^N FER_i \times \tau_i(BER_i)}{\sum_{i=1}^N \tau_i(BER_i)} \times 100 [\%]. \quad (5.6)$$

- Link Availability (in %) – defined by (5.7), is the percentage of time for which the BER value is lower than 10^{-3}

$$LA = \frac{\sum_{i=1}^N \tau_i(BER_i)}{\sum_{i=1}^N T_i} \times 100 [\%]. \quad (5.7)$$

- Average throughput (in bit/s) – defined by (5.8), represents the number of correct bits/s at the receiver

$$\overline{Th} = \frac{\sum_{i=1}^N DR_i \times \tau_i(BER_i) \times (1 - BER_i)}{\sum_{i=1}^N T_i} \text{ [bit/s].} \quad (5.8)$$

- Average goodput (in frames/s) – defined by (5.9), where L is the frame length in bits, represents the number of correct frames/s at the receiver

$$\overline{Gp} = \frac{\sum_{i=1}^N \frac{DR_i}{L} \times (1 - FER_i) \times \tau_i(BER_i)}{\sum_{i=1}^N T_i} \text{ [frames/s].} \quad (5.9)$$

To assess the algorithms, four types of channel SNR variations have been considered: downward sinusoidal, defined by (5.10) and represented in Figure 5.4; upward sinusoidal, defined by (5.11) and represented in Figure 5.5; sinusoidal, defined by (5.12) and represented in Figure 5.6; and step-wise, represented in Figure 5.7 and whose behaviour is the closest to a real channel.

$$SNR(t) = 15 - 25 * \cos\left(\left(\frac{2\pi}{200}\right) \times (t + 100)\right) \text{ [dB]} \quad (5.10)$$

$$SNR(t) = 15 + 25 * \cos\left(\left(\frac{2\pi}{200}\right) \times (t + 100)\right) \text{ [dB]} \quad (5.11)$$

$$SNR(t) = 15 - 25 * \cos\left(\left(\frac{2\pi}{66}\right) \times (t + 100)\right) \text{ [dB]} \quad (5.12)$$

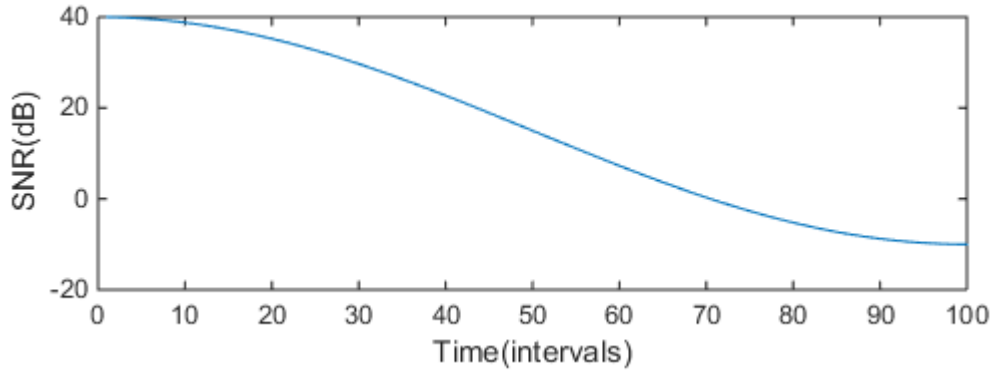


Figure 5.4 – Downward sinusoidal SNR variation.

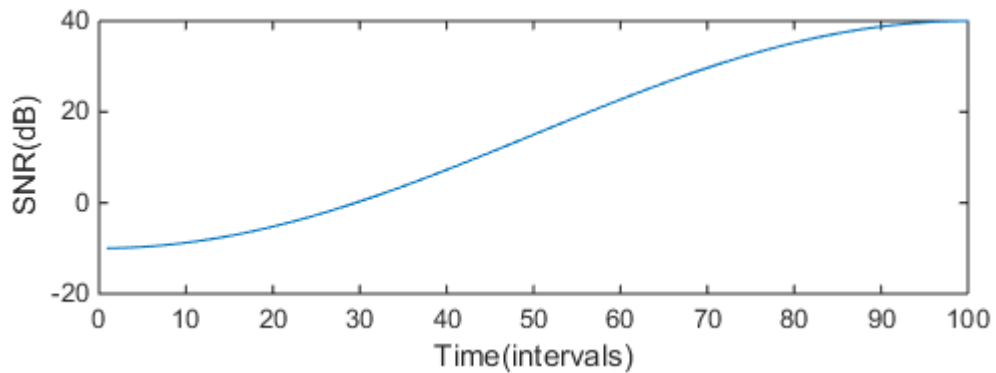


Figure 5.5 – Upward sinusoidal SNR variation.

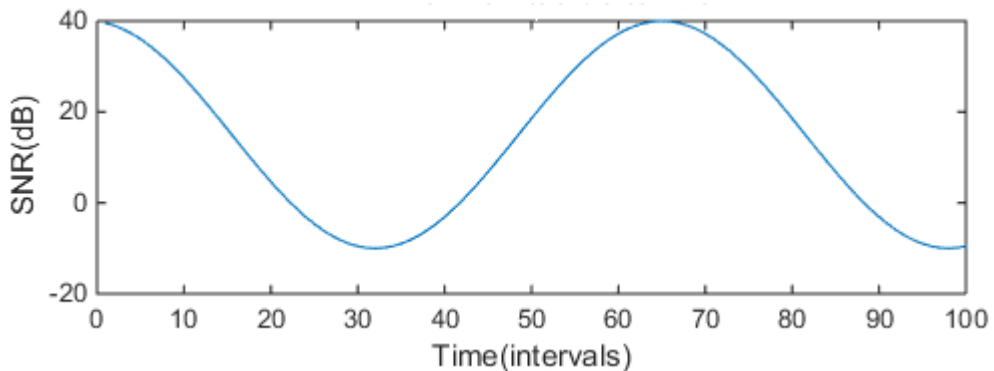


Figure 5.6 – Sinusoidal SNR variation.

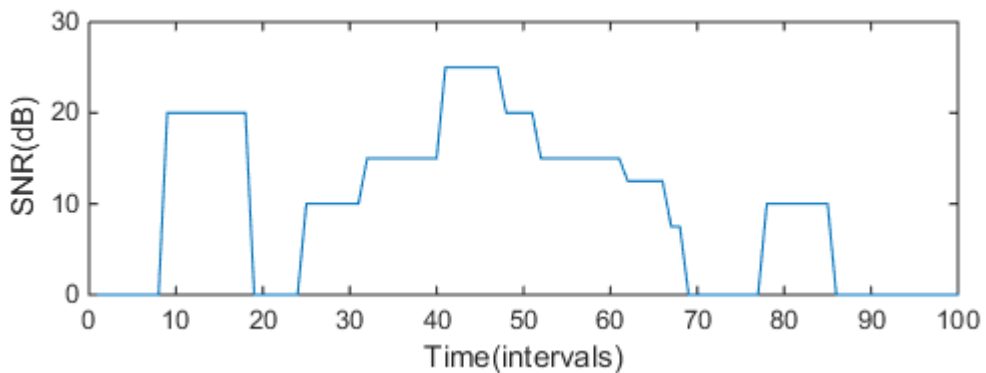


Figure 5.7 – Step-wise SNR variation.

For the algorithms assessment, the following parameters values were used:

- interval duration (T_i) = 120 seconds;
- total number of measurement intervals (N) = 100;
- frame size (L) = 250 bytes.

For these parameters values, equations (5.3) to (5.9) can be rewritten as:

$$\overline{DR} = \frac{\sum_{i=1}^{100} DR_i}{100} \text{ [bit/s]} \quad (5.13)$$

$$\tau_i(BER_i) = \begin{cases} 1 & \text{if } BER_i \leq 10^{-3} \\ 0 & \text{if } BER_i > 10^{-3} \end{cases} \quad (5.14)$$

$$\overline{BER} = \frac{\sum_{i=1}^{100} BER_i \times \tau_i(BER_i)}{\sum_{i=1}^{100} \tau_i(BER_i)} \quad (5.15)$$

$$\overline{FER} = \frac{\sum_{i=1}^{100} FER_i \times \tau_i(BER_i)}{\sum_{i=1}^{100} \tau_i(BER_i)} [\%] \quad (5.16)$$

$$LA = \sum_{i=1}^{100} \tau_i(BER_i) [\%] \quad (5.17)$$

$$\overline{Th} = \frac{\sum_{i=1}^{100} DR_i \times (1 - BER_i) \times \tau_i(BER_i)}{100} \text{ [bit/s]} \quad (5.18)$$

$$\overline{Gp} = \frac{\sum_{i=1}^{100} \frac{DR_i}{250 \times 8} \times (1 - FER_i) \times \tau_i(BER_i)}{100} \text{ [frames/s].} \quad (5.19)$$

5.2. Previous DRC algorithms: Simulation and Assessment

After designing the simulation environment, the DRC algorithms reviewed on Chapter 4, namely Trinder and RapidM algorithms, were reproduced in Matlab code. This section presents the assessments of those algorithms, according to the simulation system described in the section 5.1, to determine the gaps where they can be improved.

5.2.1. Trinder algorithm Simulation and Assessment

In Trinder algorithm, the appropriate data rate is based on FER thresholds; therefore, at the end of each measurement interval the BER and FER values are computed based on the current SNR measure, as depicted in Figure 5.3. The Trinder algorithm assessment results are represented in Table 5.1, for the three considered channel types; Figure 5.8 shows the data rate variation for the considered channels, and for an upward sinusoidal SNR variation.

The main vulnerability detected by combining the analysis of the data rate adaption (in Figure 5.8), the link availability results (in Table 5.1) and the BER versus data rate variation (in Figure 5.9), is the data rate oscillations that lead to many cut-off states, reducing the link availability. If the link availability increases, by reducing the unnecessary oscillations, it is expected that the average BER and FER will also increase. The proposal to improve the link quality is to implement a new version of the Trinder

algorithm that, before updating the data rate evaluates if the new data rate will lead to the cut-off state; if yes, the previous data rate will be kept.

Table 5.1 – Trinder algorithm simulation results for each channel type.

AWGN Channel						
SNR Variation	Data Rate (bit/s)	Availability	BER average	FER average	Throughput (bit/s)	Goodput (frames/s)
Downward	5477,0	72%	6,81E-05	8,93%	4941,38	2,391
Upward	5416,8	79%	4,26E-05	6,10%	5090,44	2,501
Sinusoidal	5437,5	68%	6,82E-05	8,96%	4741,07	2,279
Step	4269,3	66%	8,41E-06	1,64%	3205,20	1,558
ITU Good Channel						
SNR Variation	Data Rate (bit/s)	Availability	BER average	FER average	Throughput (bit/s)	Goodput (frames/s)
Downward	3468,0	39%	1,03E-04	13,05%	1695,39	0,771
Upward	3404,8	46%	7,34E-05	9,42%	1813,92	0,852
Sinusoidal	3371,3	33%	2,83E-05	4,45%	1351,99	0,667
Step	1269,8	38%	4,99E-05	8,00%	582,19	0,244
ITU Poor Channel						
SNR Variation	Data Rate (bit/s)	Availability	BER average	FER average	Throughput (bit/s)	Goodput (frames/s)
Downward	4558,5	57%	6,01E-05	7,93%	3778,65	1,819
Upward	4485,3	66%	4,91E-05	6,59%	4000,67	1,942
Sinusoidal	4456,5	53%	2,61E-05	4,54%	3672,19	1,785
Step	2592,3	54%	3,44E-05	6,33%	1238,23	0,598

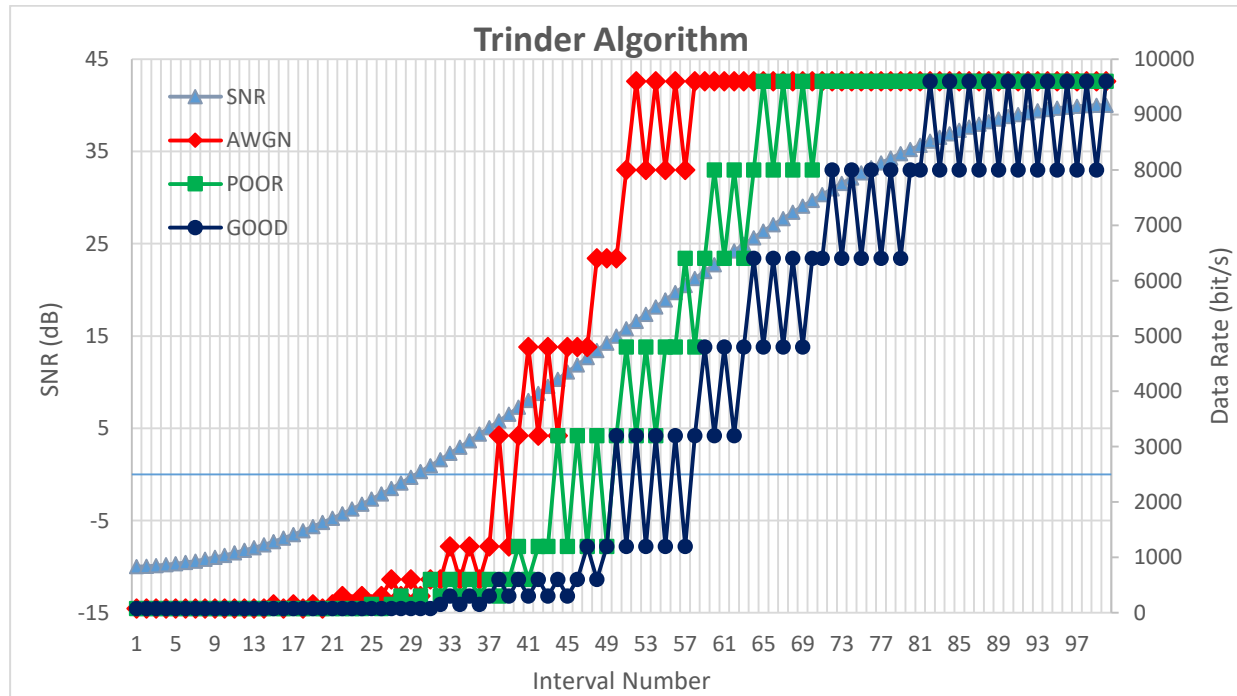


Figure 5.8 – Trinder algorithm data rate variation, for an upward sinusoidal SNR variation.

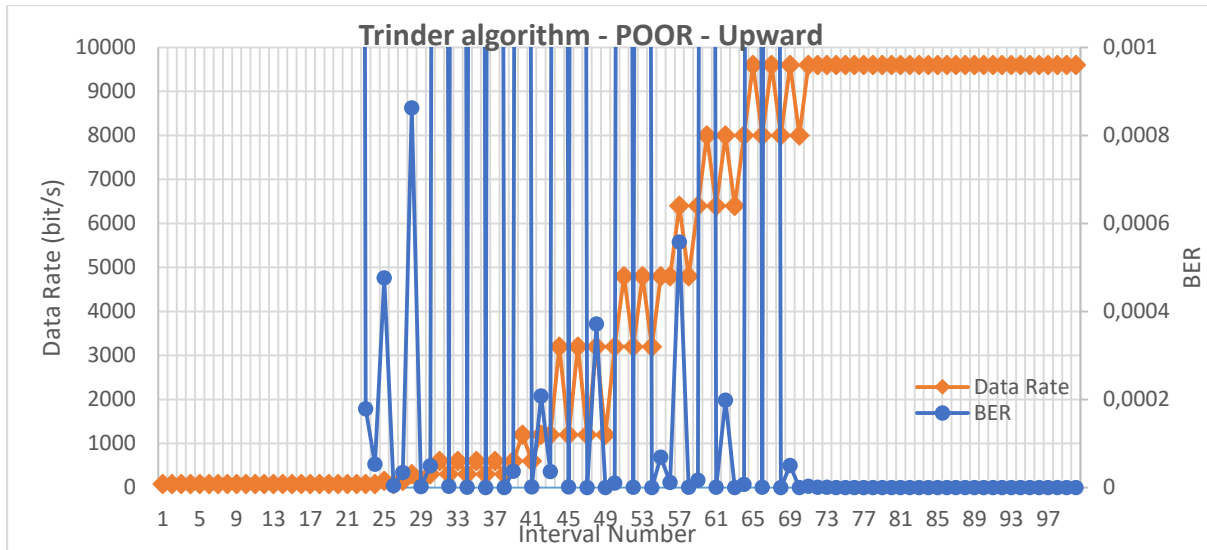


Figure 5.9 – Trinder algorithm: BER vs Data Rate variation, for an upward sinusoidal SNR variation using an ITU Poor channel.

5.2.2. RapidM DRC algorithm Simulation and Assessment

The RapidM DRC algorithm bases the data rate decision in four rules: the first two rules compute the next data rate based on SNR variations; the third rule performs data rate decisions based on the computed BER value, as in Trinder algorithm; and the fourth is a security rule that allows the data rate to increase, at most, two steps at once, and to decrease three steps at once. The link assessment results are represented in Table 5.2 for the three considered channel types; Figure 5.10 shows the data rate variation for the considered channels, and for an upward sinusoidal SNR variation.

Table 5.2 – RapidM DRC algorithm simulation results for each type of channel.

AWGN Channel						
SNR Variation	Data Rate (bit/s)	Availability	BER average	FER average	Throughput (bit/s)	Goodput (frames/s)
Downward	5380,3	83%	4,15E-05	6,48%	5076,41	2,464
Upward	5315,5	88%	3,07E-05	4,50%	5163,95	2,542
Sinusoidal	5267,8	74%	5,92E-05	7,58%	4940,51	2,334
Step	4164,5	68%	7,79E-06	1,52%	3234,46	1,575
ITU Good Channel						
SNR Variation	Data Rate (bit/s)	Availability	BER average	FER average	Throughput (bit/s)	Goodput (frames/s)
Downward	3310,3	48%	4,24E-05	6,81%	1937,94	0,917
Upward	3274,5	55%	4,69E-05	6,14%	2199,90	1,033
Sinusoidal	3242,5	37%	2,20E-05	3,91%	1748,95	0,827
Step	948,8	53%	3,35E-05	5,47%	818,20	0,365
ITU Poor Channel						
SNR Variation	Data Rate (bit/s)	Availability	BER average	FER average	Throughput (bit/s)	Goodput (frames/s)
Downward	4432,0	69%	4,57E-05	7,11%	4139,87	1,969
Upward	4394,0	72%	1,10E-05	1,96%	4188,72	2,066
Sinusoidal	4310,8	56%	2,13E-05	3,69%	3716,94	1,811
Step	2116,0	89%	1,98E-05	3,69%	1743,97	0,847

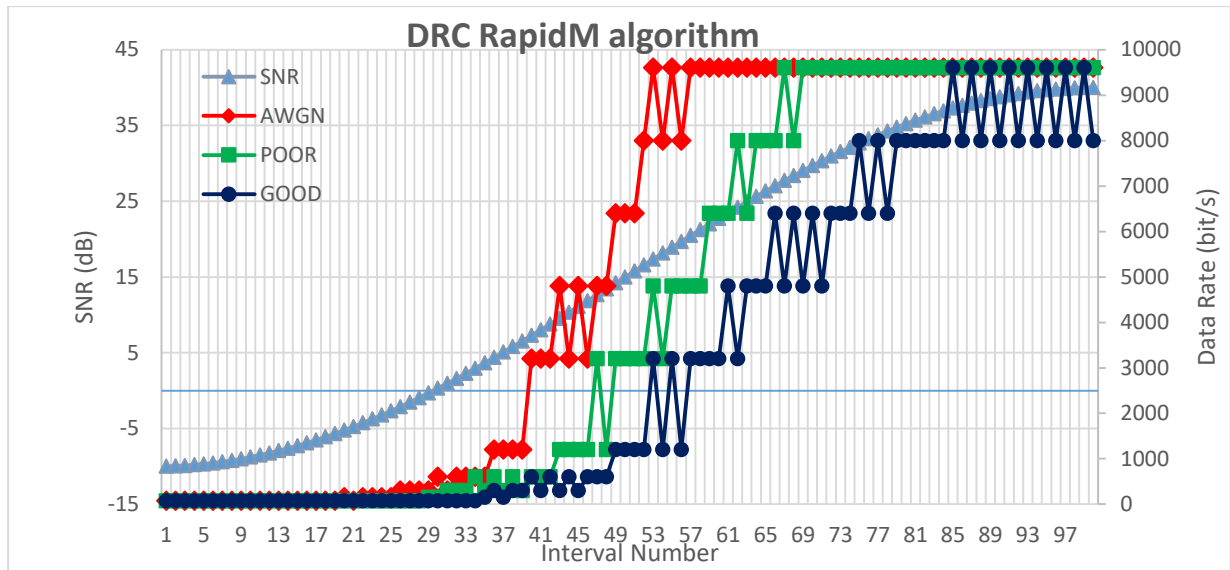


Figure 5.10 – Original RapidM algorithm data rate variation, for an upward sinusoidal SNR variation.

The main vulnerability detected, according to the results presented in Table 5.2, Figure 5.10 and Figure 5.11, is the unnecessary oscillations that reduce the link availability, as also identified in Trinder algorithm. The same proposal to improve the link quality for the Trinder algorithm will be also considered for the RapidM algorithm; if the new data rate leads to the cut-off state, the previous data rate will be kept.

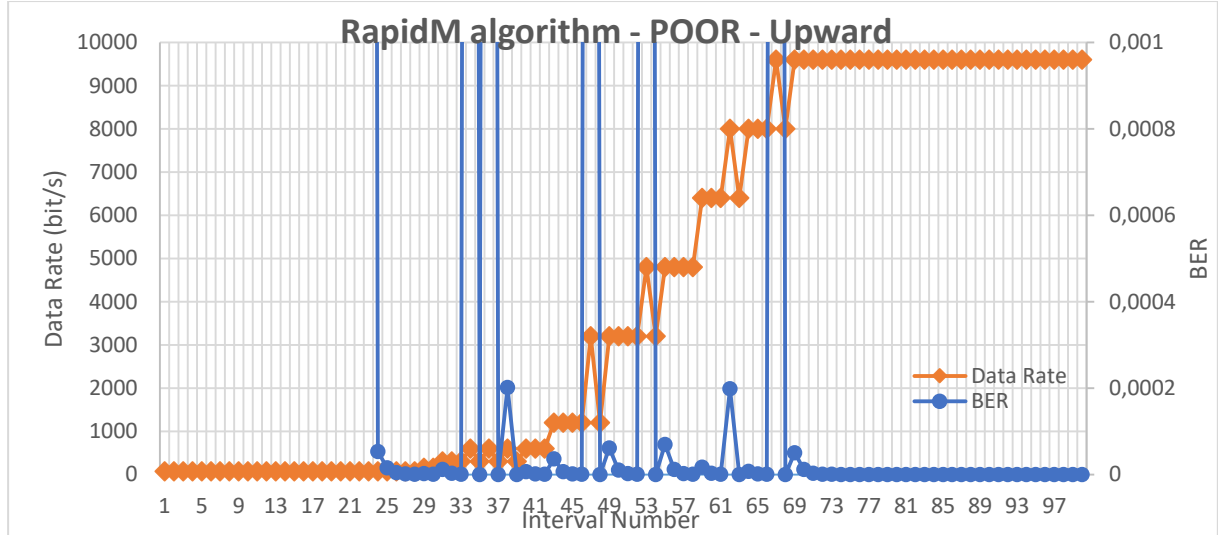


Figure 5.11 – RapidM DRC algorithm: BER vs Data Rate variation, for an upward sinusoidal SNR variation using an ITU Poor channel.

Table 5.2 allows to confirm that, comparatively to the Trinder algorithm, the RapidM DRC algorithm has a better performance, by increasing the link availability, average throughput and goodput, and by decreasing the average BER and FER values. The relative variation of these assessment metrics are represented in Table 5.3, and computed using (5.20), where x is the relative variation in percentage, obj is the RapidM algorithm metric value and ref is the reference value (obtained using the Trinder algorithm)

$$x = \frac{obj - ref}{ref} \times 100 [\%]. \quad (5.20)$$

Table 5.3 – Relative variation between RapidM DRC and Trinder algorithm.

AWGN Channel						
SNR Variation	Data Rate (bit/s)	Availability	BER average	FER average	Throughput (bit/s)	Goodput (10^{-3} frames/s)
Downward	-1,77%	15,28%	-39,13%	-27,43%	2,73%	3,04%
Upward	-1,87%	11,39%	-27,98%	-26,12%	1,44%	1,63%
Sinusoidal	-3,12%	8,82%	-13,22%	-15,46%	4,21%	2,39%
Step	-2,45%	3,03%	-7,40%	-7,27%	0,91%	1,06%
ITU Good Channel						
SNR Variation	Data Rate (bit/s)	Availability	BER average	FER average	Throughput (bit/s)	Goodput (10^{-3} frames/s)
Downward	-4,55%	23,08%	-58,92%	-47,79%	14,31%	18,90%
Upward	-3,83%	19,57%	-36,08%	-34,86%	21,28%	21,33%
Sinusoidal	-3,82%	12,12%	-22,16%	-12,10%	29,36%	23,96%
Step	-25,28%	39,47%	-32,90%	-31,57%	40,54%	49,72%
ITU Poor Channel						
SNR Variation	Data Rate (bit/s)	Availability	BER average	FER average	Throughput (bit/s)	Goodput (10^{-3} frames/s)
Downward	-2,78%	21,05%	-23,99%	-10,29%	9,60%	8,23%
Upward	-2,03%	9,09%	-77,65%	-70,28%	4,70%	6,37%
Sinusoidal	-3,27%	5,66%	-18,35%	-18,56%	1,22%	1,44%
Step	-18,37%	64,82%	-42,44%	-41,79%	40,84%	41,71%

5.3. Improvements on the Trinder and RapidM Algorithms

Based on detected vulnerabilities of the Trinder and RapidM algorithms, two new versions of each algorithm were developed and tested in the Matlab simulation environment described in section 5.1; the first improved version performs a BER prediction to avoid the cut-off link, and was named Avoiding Cut-Off State (ACOS); the second improved version performs an average BER optimization, and was named Bit Error Optimization (BEO).

5.3.1. Avoiding Cut-Off State Algorithm

5.3.1.1. Algorithm design and implementation

The ACOS algorithm is based on the BER predicted value using equation (5.1), just after the DRC algorithm be applied and a new transmission data rate obtained. Figure 5.12 shows the ACOS algorithm flowchart, which should be introduced in the flowchart represented in Figure 5.1. It starts with the new BER computation based on the new data rate selected by the DRC algorithm. After performing the BER prediction, the algorithm verifies if the resulting BER value is greater than 10^{-3} ; if it is false, the data rate is updated to the new value; if this condition is true, a new verification is performed. The algorithm checks if the new data rate is lower than previous one; if it is false, the previous data rate is maintained; if it is true, the new data rate is decreased.

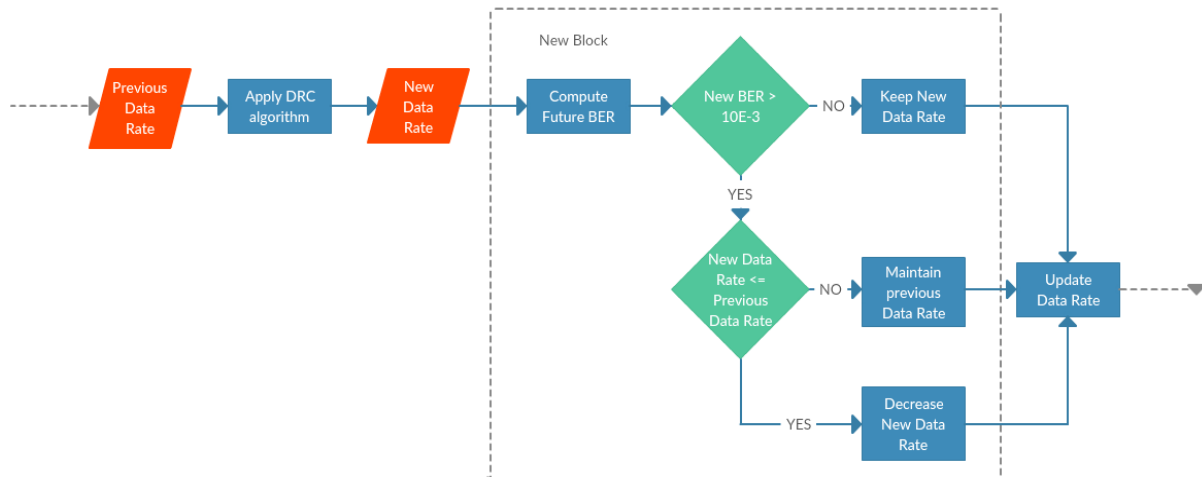


Figure 5.12 – Avoiding Cut-Off State algorithm flowchart.

The ACOS is easy to implement because it is just a BER computation and two condition to be added to the existing solutions.

5.3.1.2. Trinder algorithm with ACOS: simulation and assessment

The link data rate variation for the Trinder algorithm with ACOS is represented in Figure 5.13 (for an upward sinusoidal SNR variation); Table 5.4 presents the assessment metrics values, and Table 5.5 presents the relative variation between both algorithms. The link availability, average throughput and goodput have a great improvement with ACOS, the number of data rate oscillations decrease, although the average BER and FER increase, because the link availability also increase. A graphical comparison between Trinder algorithm with ACOS and the original version is presented in Appendix C.

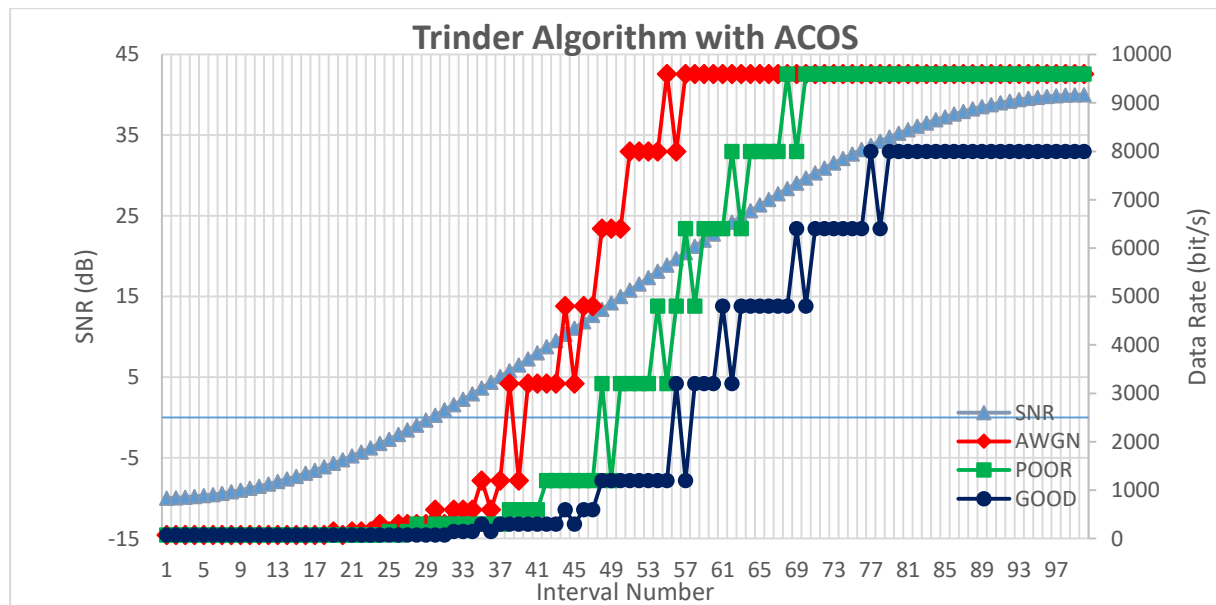


Figure 5.13 – Trinder algorithm with ACOS data rate variation, for an upward sinusoidal SNR variation.

Table 5.4 - Trinder algorithm with ACOS simulation results for each channel type.

AWGN Channel						
SNR Variation	Data Rate (bit/s)	Availability	BER average	FER average	Throughput (bit/s)	Goodput (frames/s)
Downward	5337,8	88%	6,35E-05	8,70%	5328,62	2,580
Upward	5353,8	89%	5,56E-05	7,20%	5345,37	2,592
Sinusoidal	5256,0	79%	7,43E-05	10,01%	4995,00	2,356
Step	4214,3	86%	7,43E-06	1,45%	3760,20	1,831
ITU Good Channel						
SNR Variation	Data Rate (bit/s)	Availability	BER average	FER average	Throughput (bit/s)	Goodput (frames/s)
Downward	3057,0	70%	7,12E-05	9,58%	3034,37	1,425
Upward	3078,3	71%	6,49E-05	8,20%	3056,35	1,435
Sinusoidal	2999,3	61%	3,95E-05	6,73%	2797,94	1,343
Step	1001,3	59%	3,88E-05	6,28%	885,68	0,386
ITU Poor Channel						
SNR Variation	Data Rate (bit/s)	Availability	BER average	FER average	Throughput (bit/s)	Goodput (frames/s)
Downward	4341,3	77%	3,44E-05	8,11%	4323,88	2,077
Upward	4366,3	78%	5,14E-05	7,01%	4349,63	2,091
Sinusoidal	4221,5	71%	2,80E-05	4,93%	4172,67	2,021
Step	2172,3	92%	4,09E-05	7,51%	1938,22	0,938

Table 5.5 – Relative variation between Trinder with ACOS and original Trinder algorithm.

AWGN Channel						
SNR Variation	Data Rate (bit/s)	Availability	BER average	FER average	Throughput (bit/s)	Goodput (frames/s)
Downward	-2,54%	22,22%	-6,80%	-2,61%	7,84%	7,88%
Upward	-1,16%	12,66%	30,53%	18,13%	5,01%	3,66%
Sinusoidal	-3,34%	16,18%	8,91%	11,69%	5,36%	3,38%
Step	-1,29%	30,30%	-11,64%	-11,56%	17,32%	17,47%
ITU Good Channel						
SNR Variation	Data Rate (bit/s)	Availability	BER average	FER average	Throughput (bit/s)	Goodput (frames/s)
Downward	-11,85%	79,49%	-31,01%	-26,57%	78,98%	84,91%
Upward	-9,59%	54,35%	-11,65%	-12,98%	68,49%	68,52%
Sinusoidal	-11,03%	84,85%	39,83%	51,48%	106,95%	101,24%
Step	-21,15%	55,26%	-22,36%	-21,41%	52,13%	58,35%
ITU Poor Channel						
SNR Variation	Data Rate (bit/s)	Availability	BER average	FER average	Throughput (bit/s)	Goodput (frames/s)
Downward	-4,77%	35,09%	-42,79%	2,32%	14,43%	14,14%
Upward	-2,65%	18,18%	4,56%	6,37%	8,72%	7,65%
Sinusoidal	-5,27%	33,96%	7,35%	8,57%	13,63%	13,21%
Step	-16,20%	70,37%	18,93%	18,58%	56,53%	56,92%

The vulnerability detected in the Trinder algorithm with ACOS was the unnecessary oscillations in each data rate value that can be visualized in Figure 5.14, represented by the BER values higher than 10^{-4} . Therefore a new proposal to improve the link quality was considered, that seeks to reduce those oscillations and improve the average BER and FER; this proposal consists on computing the BER value

with the new selected data rate, and verify if this value is greater than the threshold BER, used in the Trinder algorithm to decrease the data rate.

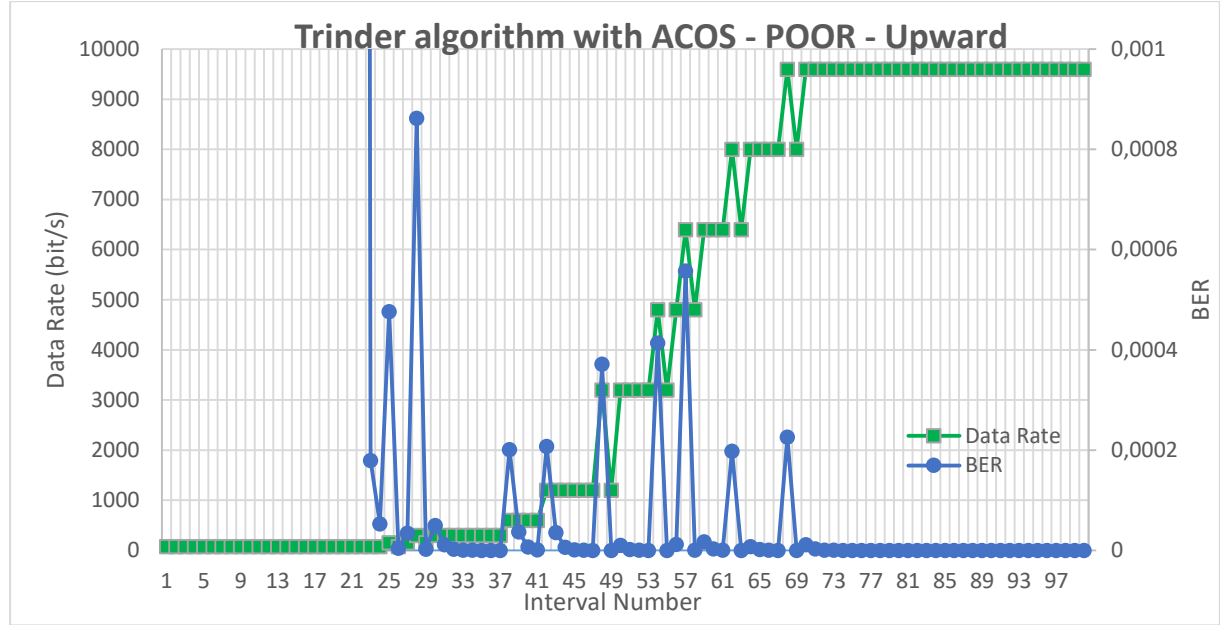


Figure 5.14 – Trinder algorithm with ACOS: BER vs Data Rate variation, for an upward sinusoidal SNR variation using an ITU Poor channel.

5.3.1.3. RapidM DRC algorithm with Avoiding Cut-Off State simulation and results

Table 5.6 presents the assessment metrics values for the RapidM algorithm with ACOS, and the link data rate variation is represented in Figure 5.15 (for an upward sinusoidal SNR variation).

Table 5.6 – RapidM DRC algorithm with ACOS simulation results for each channel type.

AWGN Channel						
SNR Variation	Data Rate (bit/s)	Availability	BER average	FER average	Throughput (bit/s)	Goodput (frames/s)
Downward	5217,3	86%	2,78E-05	4,62%	5206,68	2,545
Upward	5299,5	87%	2,82E-05	3,64%	5289,66	2,590
Sinusoidal	5150,3	84%	5,50E-05	7,21%	5138,00	2,425
Step	3895,5	95%	6,18E-06	1,21%	3695,45	1,802
ITU Good Channel						
SNR Variation	Data Rate (bit/s)	Availability	BER average	FER average	Throughput (bit/s)	Goodput (frames/s)
Downward	3019,8	69%	2,96E-05	4,76%	2996,44	1,445
Upward	3068,5	71%	5,16E-05	6,69%	3046,61	1,434
Sinusoidal	2908,5	65%	2,25E-05	4,05%	2786,94	1,340
Step	894,8	62%	2,89E-05	4,72%	866,20	0,389
ITU Poor Channel						
SNR Variation	Data Rate (bit/s)	Availability	BER average	FER average	Throughput (bit/s)	Goodput (frames/s)
Downward	4355,0	76%	4,16E-05	6,47%	4336,87	2,067
Upward	4336,0	77%	2,11E-05	3,28%	4318,67	2,101
Sinusoidal	4146,3	75%	2,33E-05	4,11%	4127,43	2,007
Step	1979,3	96%	2,06E-05	3,83%	1865,22	0,906

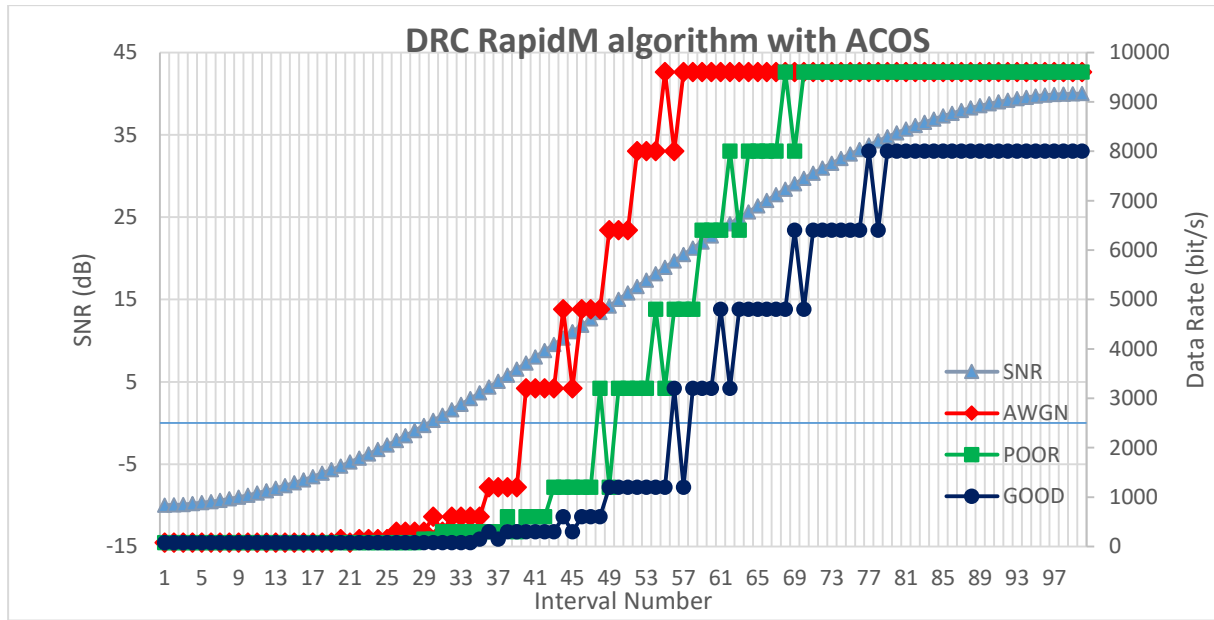


Figure 5.15 – RapidM algorithm with ACOS data rate variation, for an upward sinusoidal SNR variation.

The performance of RapidM DRC algorithm with ACOS is much better than RapidM DRC algorithm original version, as can be seen in Table 5.7 which represents the relative variation between them. As verified for the case of Trinder algorithm, RapidM DRC algorithm with ACOS improves the link availability, average throughput and goodput, although the average BER and FER values increases for the same reason described in Trinder algorithm with ACOS (see Figure 5.16). Therefore the same proposal to get a bit error optimization is assumed for RapidM DRC algorithm.

Table 5.7 – Relative variation between RapidM DRC algorithm with ACOS and its original version.

AWGN Channel						
SNR Variation	Data Rate (bit/s)	Availability	BER average	FER average	Throughput (bit/s)	Goodput (frames/s)
Downward	-3,03%	3,61%	-32,89%	-28,67%	2,57%	3,27%
Upward	-0,30%	-1,14%	-8,19%	-19,22%	2,43%	1,90%
Sinusoidal	-2,23%	13,51%	-7,11%	-4,83%	4,00%	3,92%
Step	-6,46%	39,71%	-20,70%	-20,63%	14,25%	14,44%
ITU Good Channel						
SNR Variation	Data Rate (bit/s)	Availability	BER average	FER average	Throughput (bit/s)	Goodput (frames/s)
Downward	-8,78%	43,75%	-30,15%	-30,08%	54,62%	57,70%
Upward	-6,29%	29,09%	10,05%	8,91%	38,49%	38,79%
Sinusoidal	-10,30%	75,68%	2,41%	3,76%	59,35%	61,97%
Step	-5,69%	16,98%	-13,85%	-13,71%	5,87%	6,54%
ITU Poor Channel						
SNR Variation	Data Rate (bit/s)	Availability	BER average	FER average	Throughput (bit/s)	Goodput (frames/s)
Downward	-1,74%	10,14%	-9,03%	-8,98%	4,76%	4,99%
Upward	-1,32%	6,94%	91,85%	67,30%	3,10%	1,70%
Sinusoidal	-3,82%	33,93%	9,62%	11,33%	11,04%	10,82%
Step	-6,46%	7,87%	4,01%	3,78%	6,95%	7,02%

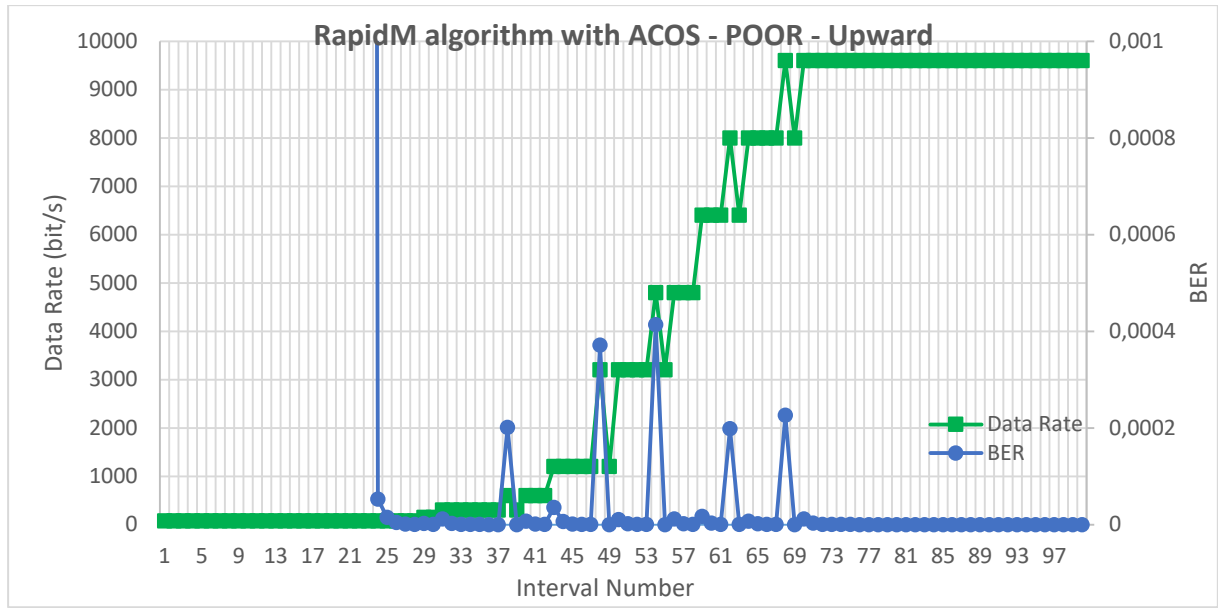


Figure 5.16 – RapidM DRC algorithm with ACOS: BER vs Data Rate variation, for an upward sinusoidal SNR variation using an ITU Poor channel.

5.3.2. Bit Error Optimization Algorithm

5.3.2.1. Algorithm design and implementation

The main difference between ACOS and BEO algorithms is the condition block; in ACOS, the condition avoids the link cut-off. In BEO algorithm, if the predicted BER value is greater than BER threshold defined in the original algorithms, a new condition is verified, otherwise the new data rate is updated. This condition verifies if the new data rate is lower than previous data rate, then the new data rate should decrease. If the condition is false the previous data rate is kept. Figure 5.17 shows the BEO algorithm flowchart, which is introduced in the simulation system flowchart represented in Figure 5.1.

The BEO block was implemented in the simulation environment, mentioned in section 5.1, with the Trinder and RapidM DRC algorithms. As for the ACOS algorithm, the BEO is quite simple to implement.

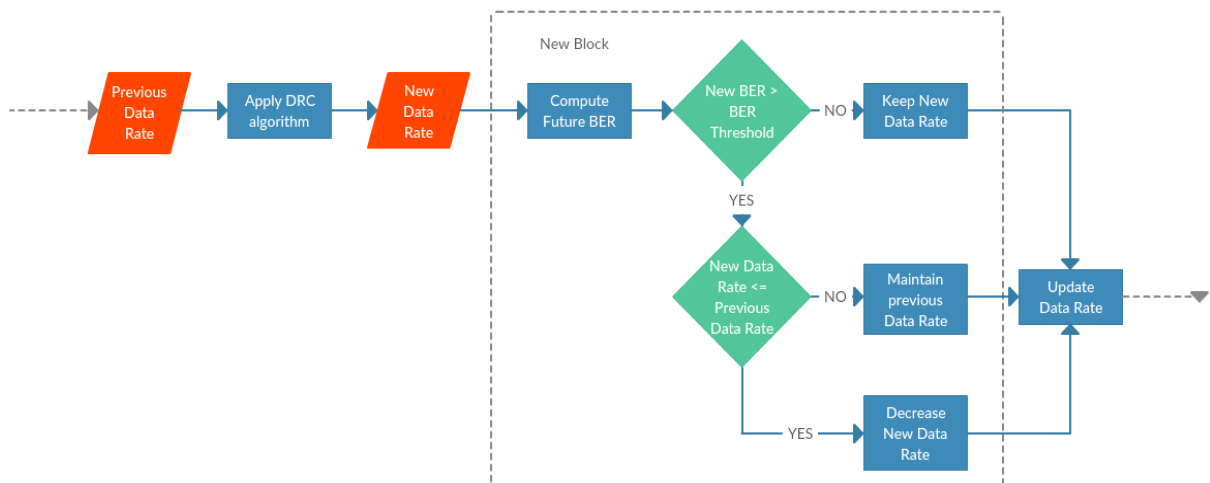


Figure 5.17 – Bit Error Optimization algorithm flowchart.

5.3.2.2. Trinder algorithm with BEO simulation and assessment

The performance results of Trinder algorithm with BEO are presented in Table 5.8 and Figure 5.18 (for an upward sinusoidal SNR variation), for the three considered channel types.

Table 5.8 – Trinder algorithm with BEO simulation results for each channel type.

AWGN Channel						
SNR Variation	Data Rate (bit/s)	Availability	BER average	FER average	Throughput (bit/s)	Goodput (frames/s)
Downward	5264,5	88%	2,60E-05	4,36%	5255,46	2,594
Upward	5337,8	89%	2,10E-05	3,65%	5329,47	2,636
Sinusoidal	5163,0	83%	5,16E-05	7,84%	5126,15	2,493
Step	4039,3	91%	5,71E-06	1,11%	3711,21	1,817
ITU Good Channel						
SNR Variation	Data Rate (bit/s)	Availability	BER average	FER average	Throughput (bit/s)	Goodput (frames/s)
Downward	2983,8	70%	2,29E-05	3,91%	2961,22	1,451
Upward	3062,3	71%	2,19E-05	3,74%	3040,47	1,491
Sinusoidal	2999,3	61%	3,95E-05	6,73%	2797,94	1,343
Step	1001,3	59%	3,88E-05	6,28%	885,68	0,386
ITU Poor Channel						
SNR Variation	Data Rate (bit/s)	Availability	BER average	FER average	Throughput (bit/s)	Goodput (frames/s)
Downward	4255,0	77%	1,98E-05	3,48%	4237,73	2,096
Upward	4350,3	78%	1,95E-05	3,44%	4333,73	2,144
Sinusoidal	4221,5	71%	2,80E-05	4,93%	4172,67	2,021
Step	2172,3	92%	4,09E-05	7,51%	1938,22	0,938

As shown in Figure 5.18, the oscillations were eliminated. The data rate comparison between all versions of Trinder algorithm can be checked in Appendix C; the relative variation between Trinder algorithm with BEO and the original version is presented in Table 5.9.

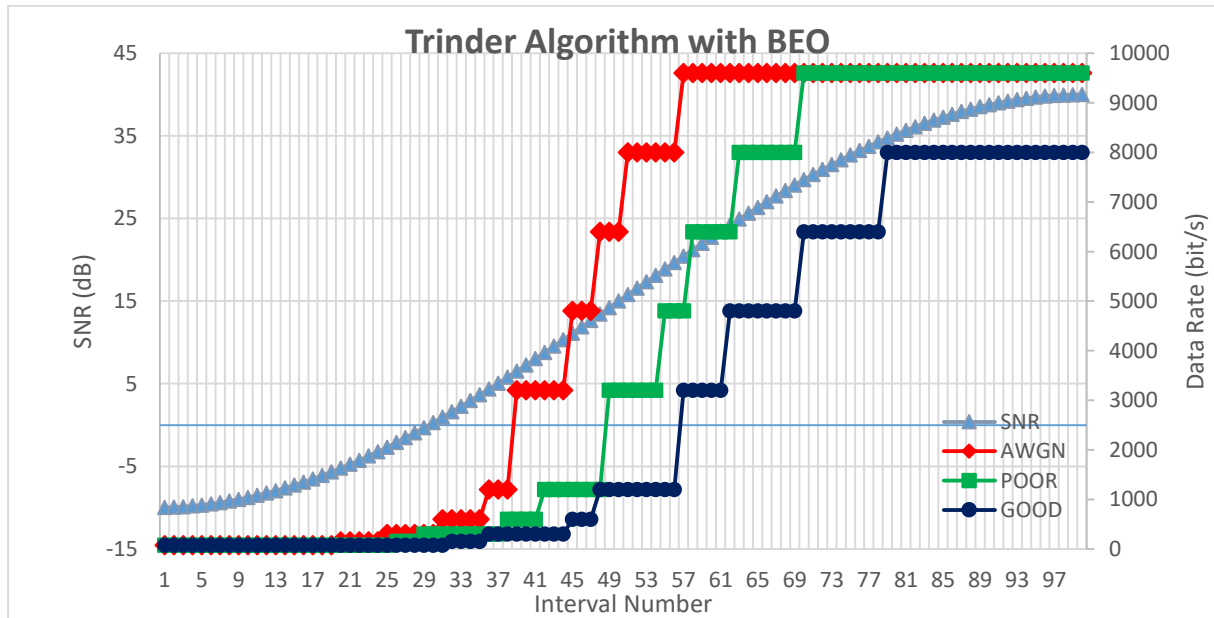


Figure 5.18 – Trinder algorithm with BEO data rate variation, for an upward sinusoidal SNR variation.

The elimination of the data rate oscillations resulted in the best performance of average goodput, BER and FER in the set of solutions presented for Trinder algorithm; this can be checked by the relative variations presented in Table 5.5 and Table 5.9. The Trinder with ACOS and the Trinder with BEO algorithms have similar link availability values, but the first one has better average throughput performance. Figure 5.19 shows how the BER is maintained below the BER threshold, resulting in an elimination of the data rate oscillations.

Table 5.9 – Relative variation between Trinder algorithm with BEO and the original version.

AWGN Channel						
SNR Variation	Data Rate (bit/s)	Availability	BER average	FER average	Throughput (bit/s)	Goodput (frames/s)
Downward	-3,88%	22,22%	-61,79%	-51,14%	6,36%	8,46%
Upward	-1,46%	12,66%	-50,63%	-40,14%	4,70%	5,41%
Sinusoidal	-5,05%	22,06%	-24,28%	-12,54%	8,12%	9,37%
Step	-5,39%	37,88%	-32,07%	-31,95%	15,79%	16,62%
ITU Good Channel						
SNR Variation	Data Rate (bit/s)	Availability	BER average	FER average	Throughput (bit/s)	Goodput (frames/s)
Downward	-13,96%	79,49%	-77,79%	-70,00%	74,66%	88,24%
Upward	-10,06%	54,35%	-70,17%	-60,29%	67,62%	75,08%
Sinusoidal	-11,03%	84,85%	39,83%	51,48%	106,95%	101,24%
Step	-21,15%	55,26%	-22,36%	-21,41%	52,13%	58,35%
ITU Poor Channel						
SNR Variation	Data Rate (bit/s)	Availability	BER average	FER average	Throughput (bit/s)	Goodput (frames/s)
Downward	-6,66%	35,09%	-67,09%	-56,11%	12,15%	15,21%
Upward	-3,01%	18,18%	-60,23%	-47,85%	8,33%	10,40%
Sinusoidal	-5,27%	33,96%	7,35%	8,57%	13,63%	13,21%
Step	-16,20%	70,37%	18,93%	18,58%	56,53%	56,92%

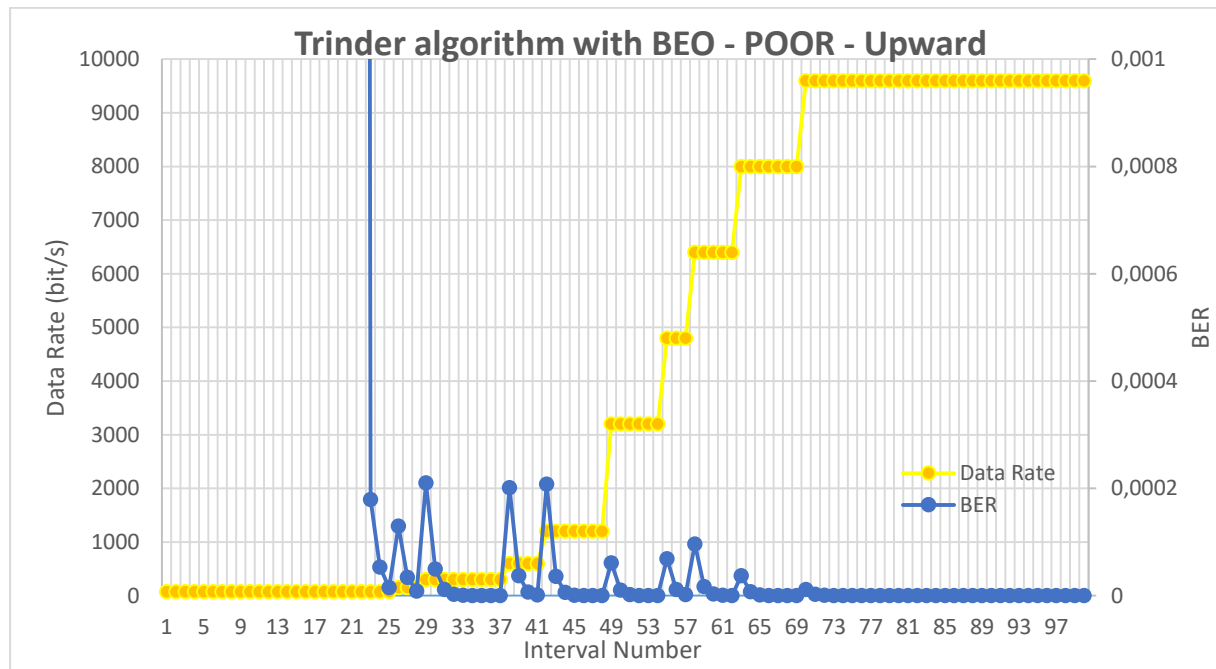


Figure 5.19 – Trinder algorithm with BEO: BER vs Data Rate variation, for an upward sinusoidal SNR variation using an ITU Poor channel.

5.3.2.3. RapidM algorithm with BEO simulation and assessment

The performance results of the RapidM algorithm with BEO are represented in Table 5.10 and Figure 5.20 (for an upward sinusoidal channel), for the three types of channels. According to the results, the oscillations were eliminated (like in Tinder algorithm with BEO), and the average BER and FER had great performance improvements.

The relative variation between the RapidM algorithm with BEO and the original version is represented in Table 5.11, and Figure 5.21 shows how the BER is maintained below the BER threshold of RapidM DRC algorithm.

Table 5.10 – RapidM DRC algorithm with BEO simulation results for each channel type.

AWGN Channel						
SNR Variation	Data Rate (bit/s)	Availability	BER average	FER average	Throughput (bit/s)	Goodput (frames/s)
Downward	5217,3	86%	6,92E-06	3,83%	5206,73	2,588
Upward	5280,5	87%	6,54E-06	1,25%	5270,74	2,622
Sinusoidal	5077,3	84%	9,51E-06	1,80%	5065,22	2,508
Step	3895,5	95%	6,18E-06	1,21%	3695,45	1,802
ITU Good Channel						
SNR Variation	Data Rate (bit/s)	Availability	BER average	FER average	Throughput (bit/s)	Goodput (frames/s)
Downward	2940,5	69%	6,93E-06	1,32%	2917,23	1,444
Upward	3017,5	71%	1,05E-05	1,85%	2995,73	1,483
Sinusoidal	2860,5	66%	1,49E-05	2,74%	2834,97	1,390
Step	794,8	62%	8,60E-06	1,54%	766,24	0,370
ITU Poor Channel						
SNR Variation	Data Rate (bit/s)	Availability	BER average	FER average	Throughput (bit/s)	Goodput (frames/s)
Downward	4259,8	76%	8,58E-06	1,64%	4241,73	2,097
Upward	4336,0	77%	6,05E-06	1,16%	4318,73	2,142
Sinusoidal	4114,3	75%	1,59E-05	2,88%	4095,46	2,016
Step	1979,3	96%	2,06E-05	3,83%	1865,22	0,906

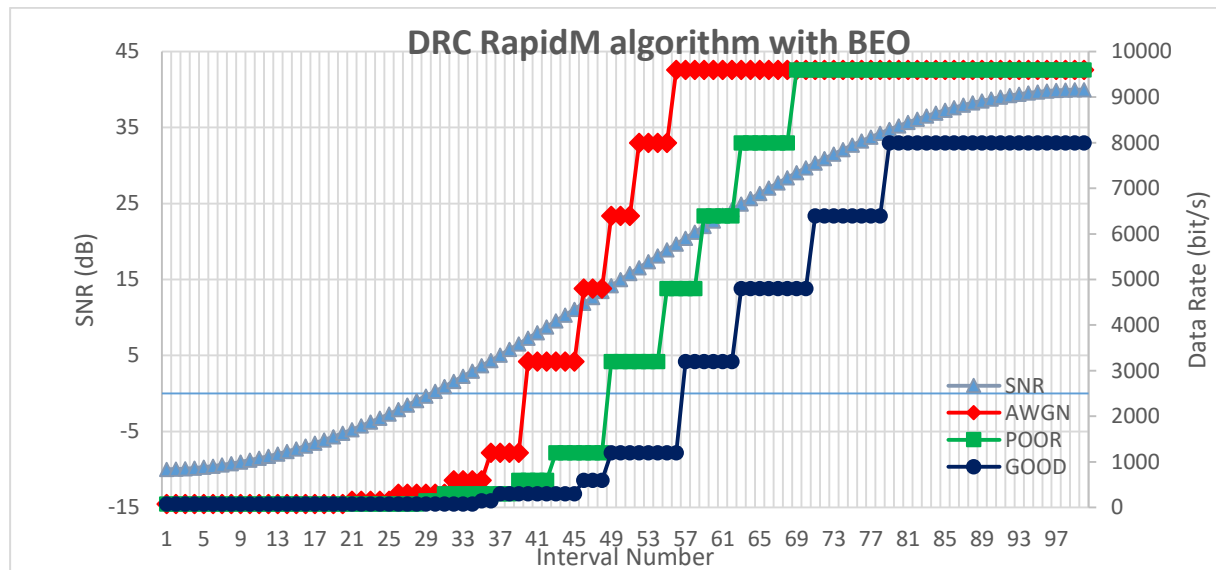


Figure 5.20 – RapidM algorithm with BEO data rate variation, for an upward sinusoidal SNR variation.

Table 5.11 – Relative variation between RapidM DRC algorithm with BEO and the original version.

AWGN Channel						
SNR Variation	Data Rate (bit/s)	Availability	BER average	FER average	Throughput (bit/s)	Goodput (frames/s)
Downward	-3,03%	3,61%	-83,32%	-40,98%	2,57%	5,03%
Upward	-0,66%	-1,14%	-78,68%	-72,23%	2,07%	3,18%
Sinusoidal	-3,62%	13,51%	-83,93%	-76,22%	2,52%	7,47%
Step	-6,46%	39,71%	-20,70%	-20,63%	14,25%	14,44%
ITU Good Channel						
SNR Variation	Data Rate (bit/s)	Availability	BER average	FER average	Throughput (bit/s)	Goodput (frames/s)
Downward	-11,17%	43,75%	-83,65%	-80,56%	50,53%	57,51%
Upward	-7,85%	29,09%	-77,69%	-69,85%	36,18%	43,53%
Sinusoidal	-11,78%	78,38%	-32,38%	-29,78%	62,10%	68,06%
Step	-16,23%	16,98%	-74,33%	-71,92%	-6,35%	1,50%
ITU Poor Channel						
SNR Variation	Data Rate (bit/s)	Availability	BER average	FER average	Throughput (bit/s)	Goodput (frames/s)
Downward	-3,89%	10,14%	-81,22%	-77,00%	2,46%	6,51%
Upward	-1,32%	6,94%	-44,87%	-40,61%	3,10%	3,68%
Sinusoidal	-4,56%	33,93%	-25,27%	-22,15%	10,18%	11,34%
Step	-6,46%	7,87%	4,01%	3,78%	6,95%	7,02%

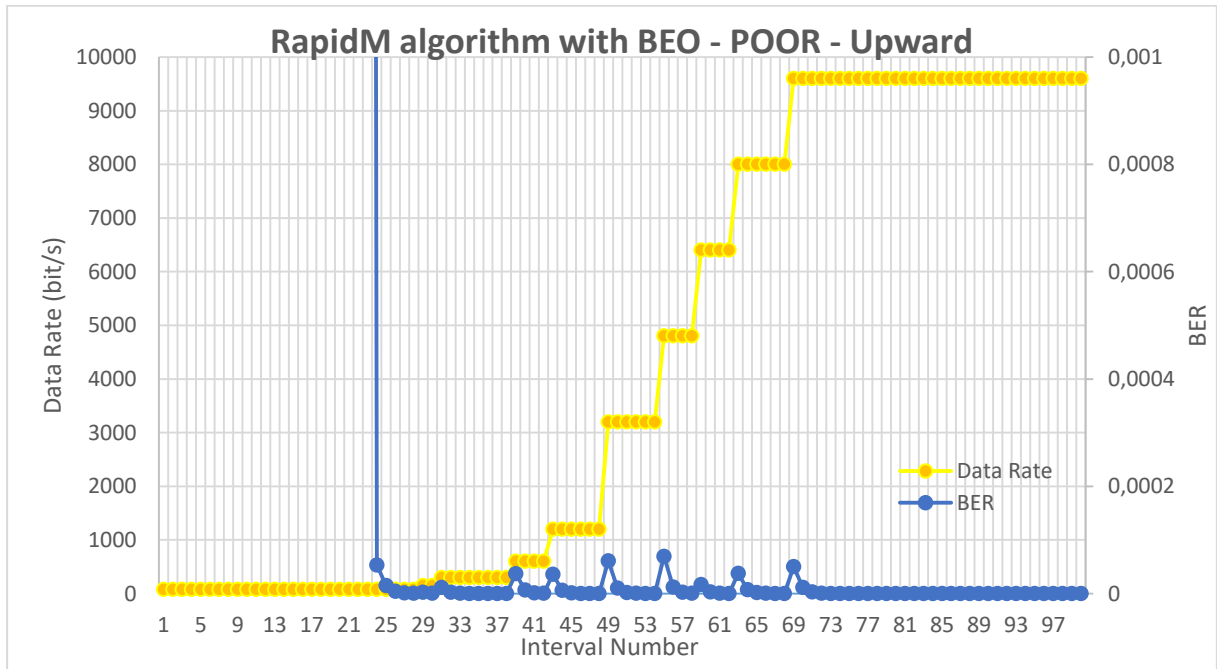


Figure 5.21 – RapidM DRC algorithm with BEO: BER vs Data Rate variation, for an upward sinusoidal SNR variation using an ITU Poor channel.

5.4. Conclusion

The improvements presented in section 5.3 for the Trinder and RapidM algorithms worked as expected and had better outcomes than the existing solutions, for the considered channel types and SNR variations. The following classification for all the improvement proposals and the existing solutions were recorded, based on the relative variation and the simulation results tables, for each type of link assessment metric:

- Lowest average BER – RapidM DRC algorithm with BEO
- Lowest average FER – RapidM DRC algorithm with BEO
- Highest link availability – RapidM DRC algorithm with BEO
- Highest average throughput – Trinder algorithm with ACOS
- Highest average goodput – Trinder algorithm with BEO

As the DRC algorithms main objective is to transmit the largest number of correct frames, to prevent frame retransmission (because of ARQ protocol), the Trinder algorithm with BEO is the algorithm with best performance. For future work it is advisable to implement an algorithm that changes the frame size according to the link quality metrics, since the DRC algorithm assessments were performed with a constant frame size. If the BER increased, the frame size should decrease to keep the same FER value, as can be checked in (4.5).

Chapter 6 – Field Propagation Tests

This chapter presents the hardware and software components involved in the field propagation tests as well as the obtained results. An user interface application was developed in C#, using the Microsoft Visual Studio to allow the radio operator to easily interact with the radio equipment through a serial port. The application was initially tested on a bench circuit for error checking, to test the application functionalities, to evaluate the limits of SNR measurements and the proper behaviour of the algorithms. Finally, field tests were conducted with two stations, each with one E/R GRC-525 radio and one RF-1936P dipole antenna (as showed in Figure 6.1). The two stations were located in the Portuguese cities of Lisbon and Oporto, with a link distance of about 300 km. The E/R GRC-525 radio and RF-1936P antenna datasheets are presented in Appendices A and B, respectively.



Figure 6.1 – Dipole antenna RF-1936P from Harris Corporation.

6.1. Equipment Assembly and Configuration Procedures

The tests of the several DRC algorithms were divided in two phases: the initial bench circuit tests and the field propagation tests. In the first phase it was intended to test the functionality of the developed application, the behaviour of the implemented algorithms, the channel quality for extreme SNR conditions and the behaviour of the radio in terms of the range of the output parameters. To accomplish the goals of the first phase a bench circuit was assembled with a variable attenuator, which allows to test the radio measurements, such as the SNR and BER values, when the LQA Table command is executed. This command is included in a confidential list of commands for radio operation by serial port or over IP (this list was consulted on [33]).

The following phase was to test the algorithms on the field, when all the parameters of the previous phase were already approved, to be sure that the only variable to affect the data rate choice is the propagation conditions. To test the algorithms on a battlefield like scenario, a link was established between the Logistics Support Unity, in Lisbon, and the Signals Regiment, in Oporto, 282 km apart. The tests were performed in a period of nine days, almost at the same time of day, to have similar propagation conditions to compare the performance of the several algorithms.

6.1.1. General Settings and Components

6.1.1.1. Ionospheric Study and Communications Plan

Before proceeding with the stations assembly, it was necessary to plan the communication mission and study the behaviour of the Ionosphere for the testing days. In Portugal, military HF communications require that frequencies are requested to the Direction of Communications and Information Systems (DCSI) which was done using the Electrical Message document, presented in Appendix D. In this document the frequency band limits had to be specified. With this purpose the graph of the Figure 6.2 was analysed and the frequencies selected to be between 4 MHz and 8 MHz, because the tests period were between 9 h and 17 h. In Figure 6.2, the white line corresponds to the expected value during 28th August 2017, and the red line corresponds to the real values measured by the ionosondes. In this case the channel was stable and the measured values match the expected values.

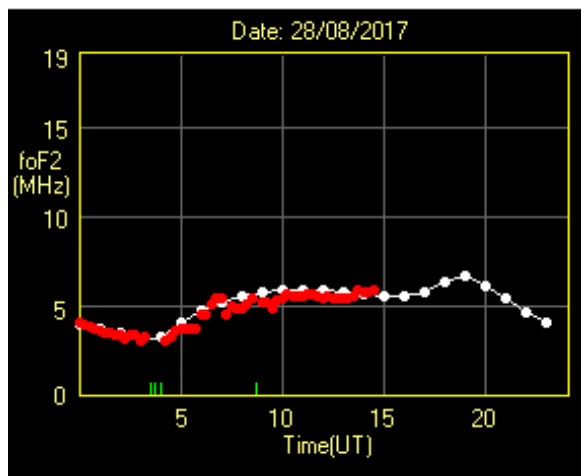


Figure 6.2 – Critical frequency of F2 layer in real time for the 28th of August 2017 (Consulted on [17]).

Another important concern is to verify if the MUF values are stable too, for the time period defined to perform the field propagation tests. Figure 6.3 a) shows three different lines of MUF during the day (28th August 2017) for three different frequencies within the limits defined previously, therefore, with these MUF values it was possible to verify that the HF communications were stable in the time period between 9h and 17h, as shown in Figure 6.3 a).

There are other important facts that may interfere with the stability of the HF communications, and can influence the expected values. These facts are related with the geomagnetic storms, the HF fadeout and the HF communication warnings. A geomagnetic storm is a major Earth magnetic fields disturbance that occurs when there is a very efficient exchange of energy from the solar wind into the space environment surrounding Earth [34] and this results in geomagnetic warnings. The HF fadeout results from the solar flares and it mostly have an onset of a few minutes and a slower decline lasting an hour [35]. The HF communication warning is related with Ionospheric storms or disturbances; these warnings can be verified in Figure 6.3 b).

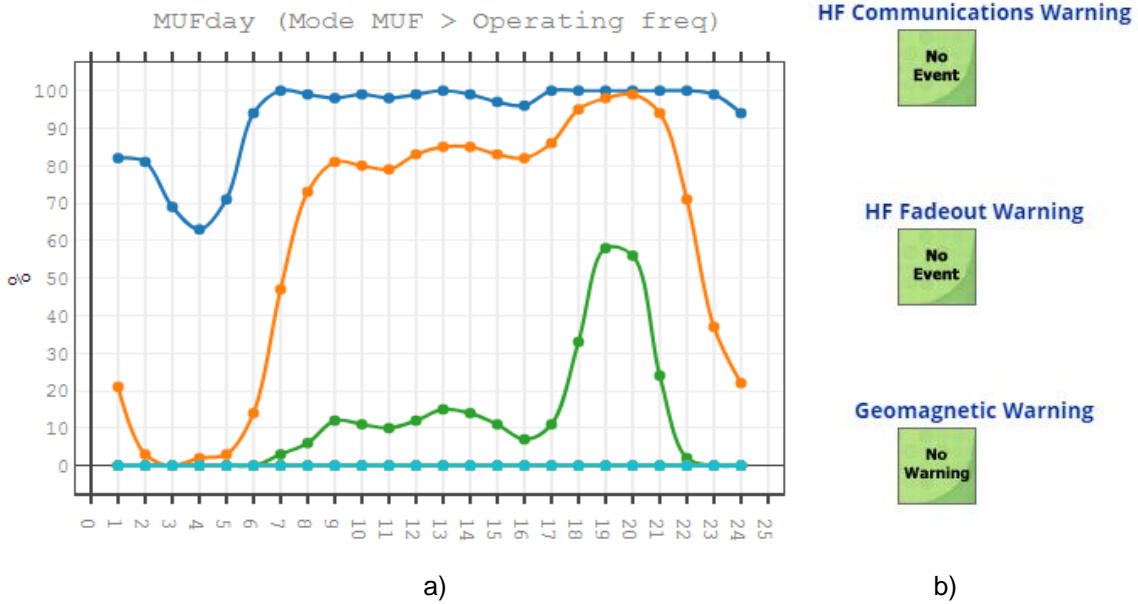


Figure 6.3 – Real time Ionospheric data for the 28th August 2017: a) MUF values in percentage during the day (Consulted on [36]); b) Warnings that may influence the HF communications (Consulted on [17]).

After the Ionospheric study and frequency analysis, the Electrical Message (presented in Appendix D) was submitted to DCSI, requesting frequencies between 4 MHz and 8 MHz. The eight frequencies presented in Appendix H were assigned for the field tests.

With the frequencies scan group already defined, the communication mission was programmed in 3G-ALE mode at the two stations. The chosen interleaver for this HF communication was the long one, with a 250 bytes length of data frame block, as was used in the Matlab simulations, described in Chapter 5, and the LQA exchange time between stations was 5 minutes. A Fill Gun HQ was used to transfer the mission to the radio, as can be seen in the Figure 6.4. The mission was uploaded from the computer to the fill gun, and then it was downloaded from the fill gun into the radio E/R GRC-525.

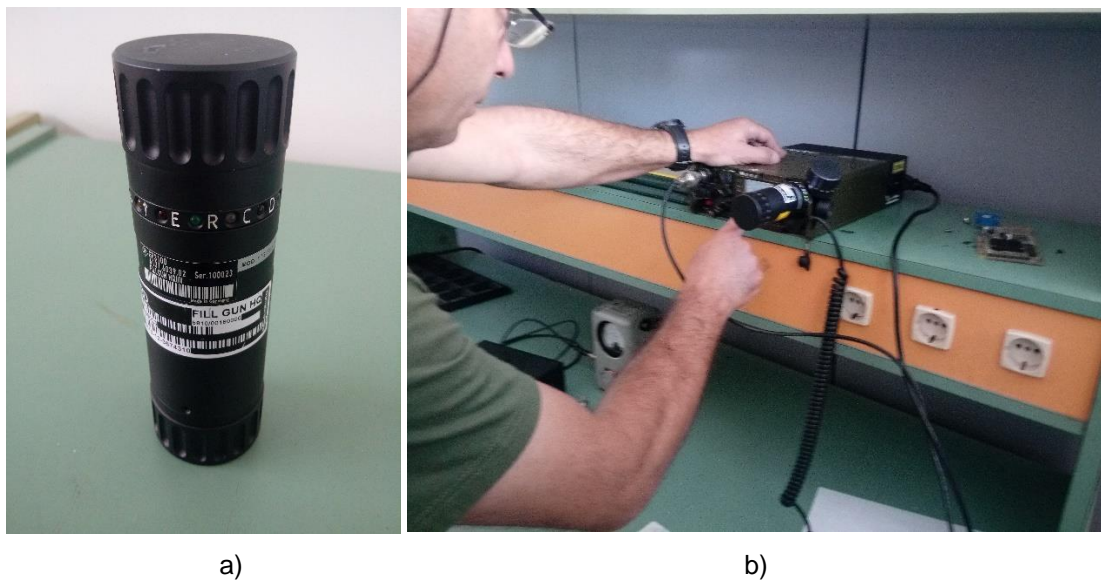


Figure 6.4 – Process of downloading the mission on the radio: a) Fill Gun HQ produced by EID; b) Data transfer from the Fill Gun HQ to the E/R GRC-525.

6.1.1.2. Methodology of Radio Operation

After downloading the communication mission into the radio, it is necessary to verify that the ratio between the reflected wave power and the transmission power is less than 0.1. This fact can be expressed by the condition in equation (6.1), being P_r the reflected wave power (in Watt) and P_T the transmission power (in Watt). The measured reflected wave power is performed with a wattmeter as showed in Figure 6.5.

$$P_r \leq 0.1 \times P_T \quad (6.1)$$

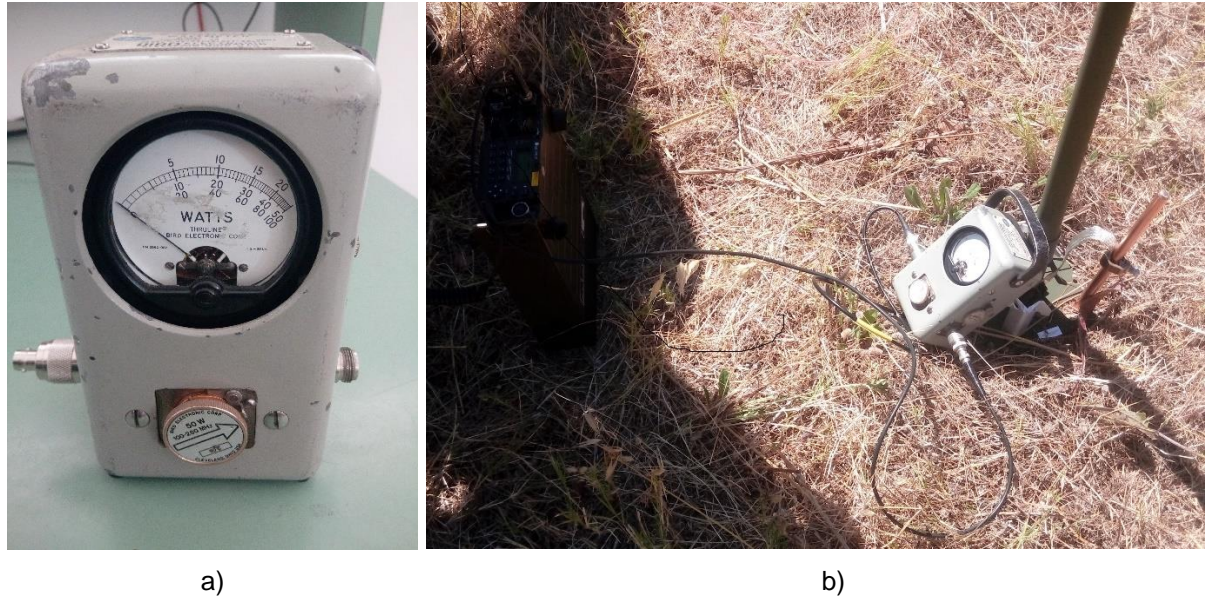


Figure 6.5 – Wattmeter used to verify the reflected wave power of each frequency: a) Image of the wattmeter produced by Bird Electronic Corporation; b) Practical use of the wattmeter.

If everything is fine with the reflected wave power, it is necessary to tune the antenna with the radio. This process is done with the Antenna Tuning Unity (ATU), which is located in the HF/VHF power amplifier. The transmission signal is amplified in the 1.5 MHz to 30 MHz frequency range and it filters the signal harmonics. The ATU process is initialized through the radio menu, as shown in Figure 6.6 a); if the tuning failed the screen shows the following message: “ANTENNA TUNE FAILED”. If the tuning is performed successfully the screen shows the message “ATU LEARN O.K.”, shown in Figure 6.6 b).



Figure 6.6 – ATU learning process: a) ATU learning the group of eight available frequencies; b) Message when the tuning is performed successfully.

6.1.1.3. List of Components Used in the Experiments

The list of components used in the experiments is:

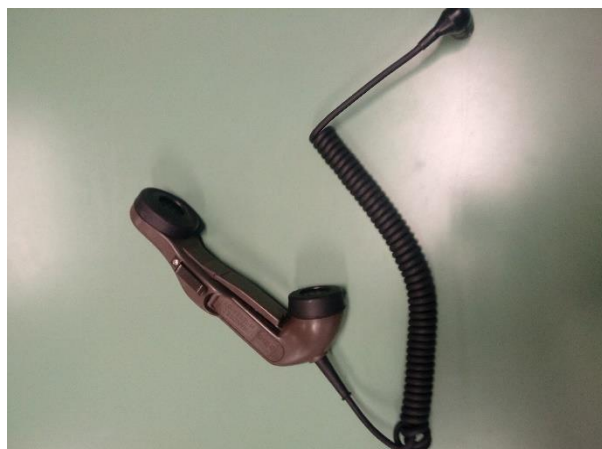
- 2 E/R GRC-525 radios - see Figure 1.2.
- 2 dipole RF-1936P antennas - see Figure 6.1.
- 2 computers with the DRC application - see Figure 6.7 a).
- 2 RS232/USB cable used as serial and data ports - see Figure 6.7 b).
- 2 micro-headset - see Figure 6.7 c).
- 1 Fill Gun HQ with the communication mission - see Figure 6.4.
- 1 wattmeter - see Figure 6.5.
- Several meters of coaxial cable - see Figure 6.7 d).
- 1 variable attenuator - see Figure 6.8 a).
- 1 fixed attenuator of 30 dB - see Figure 6.8 b).



a)



b)



c)



d)

Figure 6.7 – Hardware components used in the experiments: a) Assembly of a computer running the DRC application on the radio; b) RS232/USB cable used as serial and data port, produced by EID; c) Micro-headset from the E/R GRC-525 radio, produced by EID; d) Several meters of coaxial cable.

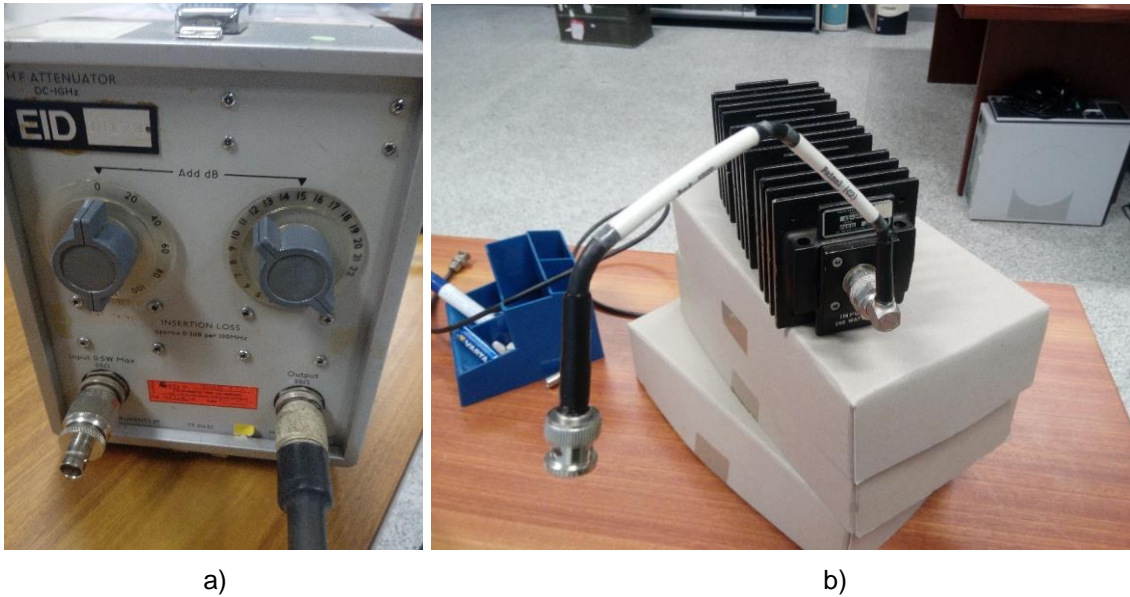


Figure 6.8 – Hardware components used specifically for bench experiments: a) Variable HF attenuator, produced by EID; b) Fixed attenuator of 30 dB to assembly on the transmitter output.

6.1.2. Assembly of Bench Tests Circuit

The bench circuit was assembled to test the application functionalities, such as problems in the functionality of the algorithms, verification of the output files, test the limits of the radio as well the parameters received. As part of the bench test circuit, a 0-90 dB variable HF attenuator (see Figure 6.8 a)) was used to control the output power of the system and simulate the environment changes.

The transmission power used in these bench experiences was 500 mW. The two radio terminals were connected with a 15 m coaxial cable, shown in Figure 6.7 d). It was necessary to put a fixed attenuator at the output of the transmission terminal, as shown in Figure 6.8 b), to avoid high power peaks that can damage the equipment. The schematic of the bench circuit is represented in Figure 6.9. The physical assembly is shown in Figure 6.10 with the two stations, each composed by one computer running the DRC application, one E/R GRC-525 radio, one RS232/USB cable and one micro-headset, implementing what is in the schematic.

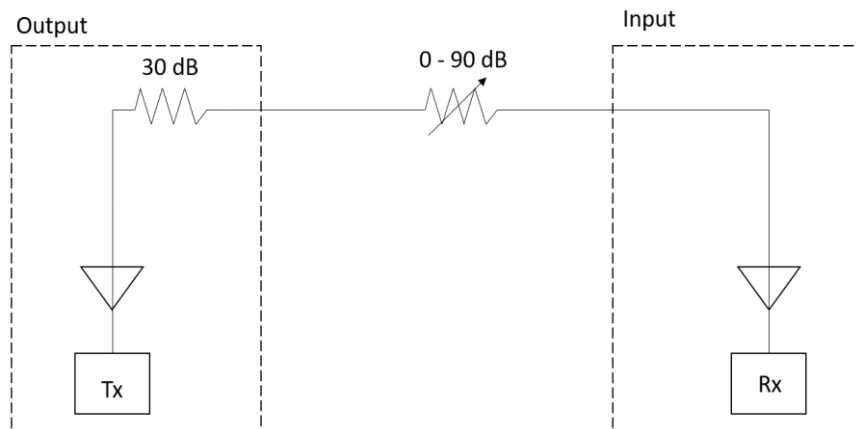


Figure 6.9 – Schematic of the bench circuit used to test the DRC application.



Figure 6.10 – Physical assembly of the bench tests circuit: a) Output system with a TX station and the fixed attenuator of 30 dB; b) Input system with the RX station and the variable HF attenuator.

6.1.3. Assembly of Field Tests Equipment

The main objective of the field propagation tests is to recreate a real battlefield environment where the HF communications can be used; therefore, a BLOS link must be established with a large distance. In Portugal there are two signals units with the appropriate equipment in Lisbon and Oporto, which are separated by almost 300 km.

Both stations are composed by one E/R-GRC525 radio, one dipole antenna RF-1936P, one micro-headset, one RS232/USB cable and one computer with the software application running, named DRC application. The connection distance is 282 km, being the Station 1 located in the Logistics Support Unity, *Paço de Arcos*, Lisbon and the Station 2 located in the Signals Regiment, *Viso de Baixo*, Oporto; the stations locations are represented in Figure 6.11, provided by Google Maps.

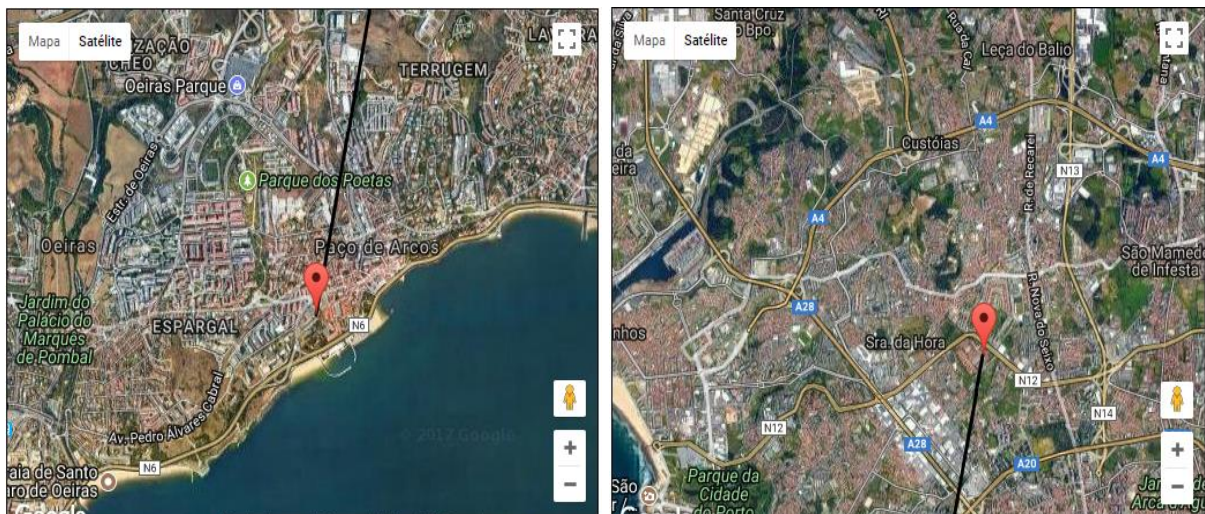


Figure 6.11 – Location of the HF stations: a) Station one located in Logistics Support Unity, *Paço de Arcos*, Lisbon; b) Station two located in the Signals Regiment, *Viso de Baixo*, Oporto.

Appendix E presents some pictures of the station assembly in the Logistics Support Unity, located in Lisbon and all the concerns about the assembly of the dipole antenna used to perform the field propagation tests. Figure 6.12 represents the two stations occupying an area of 225 m² and a height of 4.6 m.



a)

b)

Figure 6.12 – Image of the two dipole antennas RF-1936P used to perform the field propagation tests: a) Antenna located in the Signals Regiment, *Viso de Baixo*, Oporto; b) Antenna located in Logistics Support Unity, *Paço de Arcos*, Lisbon.

6.2. Data Rate Change Software Application

The DRC software application was developed in a Visual Studio environment using the C# programming language, which is object oriented and has specific methods to work with communications using serial ports. The object oriented language is easy to handle and the Visual Studio provides a graphical view to interact with the user. The reference used to learn the base syntax of the C# language was the tutorial in [37].

The C# language was developed by Microsoft, so the application software will not work in other operating systems, unless it is Windows. To run the application on older operating systems, such as Windows 7 and Windows XP, the .NET framework version must be changed according to the Windows requirements.

6.2.1. User Application Configuration

The DRC application has a graphical user interface. When the application runs it shows a window with four tab pages with the following names: Output, Configurations, Algorithms and Graphic View. The first thing to do, after the application initialization, is to fill the directory field identifying where the output files will be created, as shown in Figure 6.13. In the Output tab page there is a field to send commands to interact with the radio remote control and an output window of the radio remote control answers.

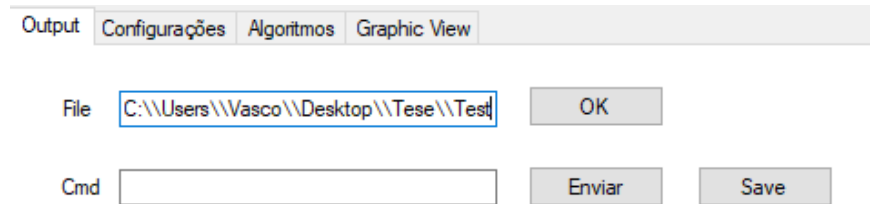


Figure 6.13 – Output tab page of the DRC application.

The next step is to set the communication parameters in the Configurations tab page. For this the remote control port must be opened, choosing the higher port from the list of COM created by the DRC application. After choosing the remote control port, the radio operation mode must be chosen between Monitoring and Operational mode. The Monitoring mode can only be used to record and display the values provided by the radio, while the Operational mode allows to change radio values and set communication parameters. One of the algorithms tasks is to set the radio transmission data rate, so the Operational mode must be used.

Figure 6.14 shows the previously described settings and the radio pre-set pages, which should be chosen in the page with the 3G-ALE mission. When the Open button is pressed, the red colour of the remote control field should change to green. After opening the remote control port, the Starting Sounding button should be pressed and a call must be initiated to the other station, in order to get the communication quality parameters, such as the BER and the SNR. The interleaver size should also be selected in this tab page, as shown in Figure 6.14. For the field propagation tests the long size interleaver must be defined.

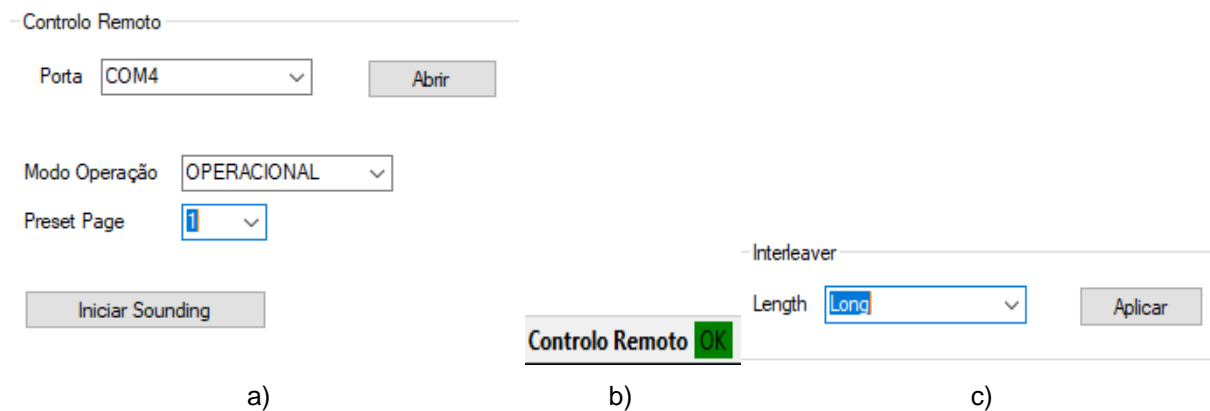


Figure 6.14 – Configuration tab page from the DRC application: a) Parameters to open the remote control port and starting the channel sounding; b) Signal when the remote control is open: green light when the remote control port is open and red light when it is closed; c) Field to set the interleaver size.

The next step is to choose the algorithm to use in the data transmission. It can be done in the Algorithms tab page, identifying the type of channel, type of algorithm and number of version fields. When this is applied, the initial data rate is defined based on the SNR value of the radio sounding. Then, the following step is to open the data send port, which is the COM value before the remote control port value (e.g. if the remote control port value is COM4, then the data send port value is COM3). When the "data send" port value is opened the red colour should switch to green. All this configuration process in the tab page Algorithms is shown in Figure 6.15, which represents the data sending settings.

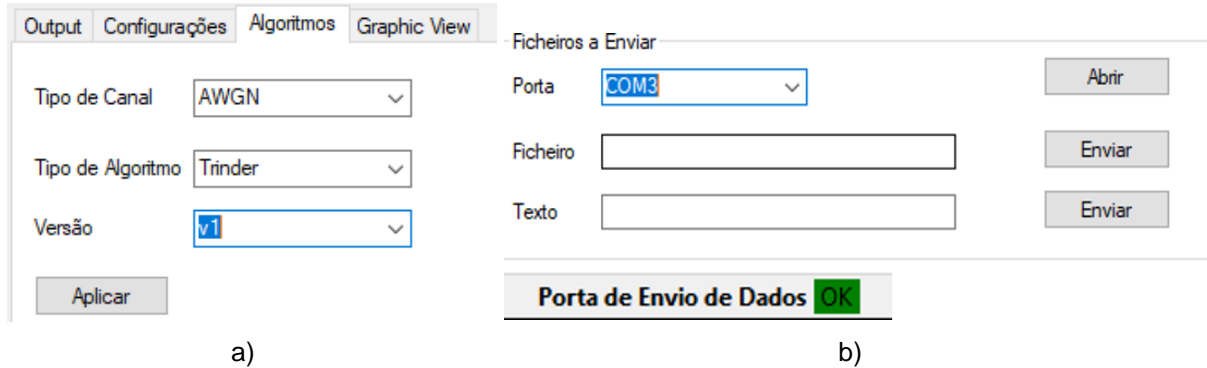


Figure 6.15 – Algorithms tab page from the DRC application: a) Type of algorithm, type of channel and number of version settings; b) Process to open the data send port.

The following step is to send a short message or a file to the other station established in the 3G-ALE mission. The DRC application has the function to create and send a complete file, or exchange short messages like in a chat. The process to create a file is shown in Figure 6.16 a). It requires to fill the fields in the Creating File section, such as the directory of the created file, the name of the file and the size in megabytes. After having the file, it can be sent in the Sending File section, filling the file directory field and pressing the button Send, as shown in Figure 6.16 b). Finally, when the file is being sent, the algorithm will start to perform the data rate transitions according to the SNR and BER values provided by the LQA sounding.

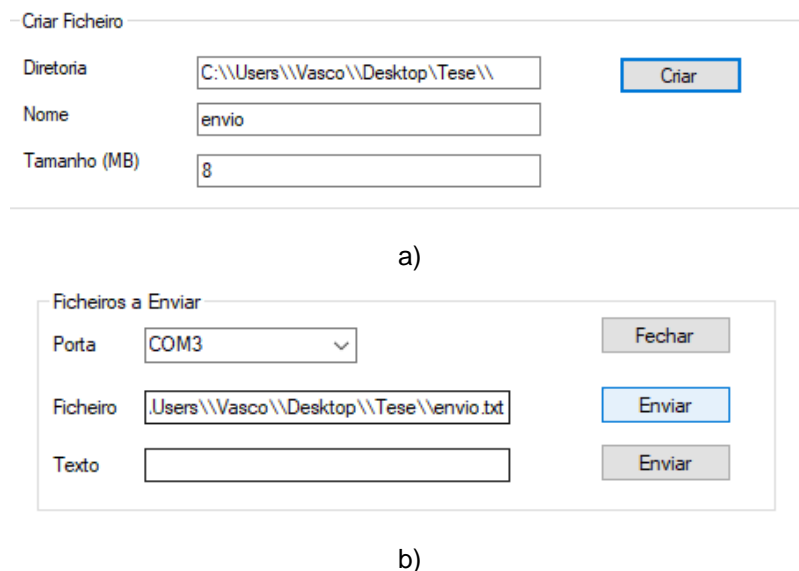


Figure 6.16 – Handling files in the DRC application: a) Create a file with a defined name and size; b) Sending the created file.

6.2.2. Output Files and Graphical Views

The use of output files is to facilitate the understanding and organization of received data; therefore two files were created for handling the information. One of the created files is used to handle the SNR and BER data sent by the radio to the computer. This is a text file created with the current date as the file name (e.g. the file name is “14052017.txt”, corresponding to the file created in May 14, 2017). With this created file the algorithm will read the link quality parameters and set the data rate according to the radio commands, consulted in the Rhode & Schwarz GB2 Platform Protocol [33].

The second created text file has the current data coupled to the word results (e.g. the file name is “Results14052017.txt”, corresponding to the file created in May 14, 2017). This file allows to see the values of data rate used, the time interval, the type of algorithm used, the BER, FER and SNR value for each measure, and the channel used in each communication interval. With these files created on each day of testing, it was possible to organize the results tables presented in the Appendix F, to classify the performance of each algorithm.

The DRC application also has a graphical view to become more “user-friendly”; this view shows the SNR measures and the defined data rate for each time interval and it is an initial prototype to facilitate data understanding for a recent application user; it is shown in Figure 6.17 when the button Plot is pressed.

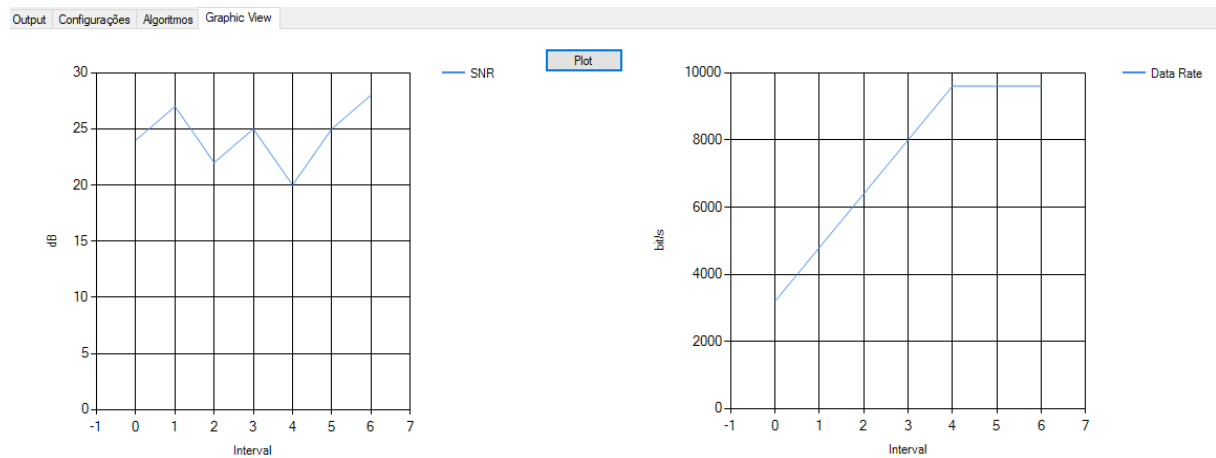


Figure 6.17 – DRC application graphical view with the interval of SNR measures and data rate settings.

This process is only applied in the TX station, because the transmitted frame has a header with the current data rate, and after the RX station read the header it will update this data rate. The RX station only receives the LQA values from the channel sounding.

6.3. Field Propagation Tests: Environment Conditions and Results

The field propagation tests were divided in six days, one day for each algorithm, due to the protection of the equipment, because transmitting with a power of 20 W overheats the radio and can damage the internal hardware circuits. The radio transmits the data without interruption with channel sounding simultaneously, therefore it is important to protect the normal operation of the radio to not overload it.

The meteorological and the ionospheric conditions should be recorded to compare algorithms performances in similar conditions. To have the maximum data of environment conditions the values of meteorological conditions, geomagnetic and fadeout warnings, critical frequency of the F2 layer (f_{0F2}) and MUF were recorded for each day of tests.

During the field propagation tests the following variables were recorded by each station: receiver station, used channel, current time (date-time format), time interval (in seconds), current BER, FER, SNR, data rate, and the computed values of throughput and goodput. These data is presented in Appendix F and allow to correlate the expected values computed by the simulation system, described in Chapter 5, and the obtained values in the field propagation tests.

6.3.1. Meteorological and Ionospheric Conditions for Test Days

This section describes the factors that may influence the communication environment. These factors can be related with meteorological conditions or atmospheric events which change the Ionosphere. The meteorological data was consulted on the Impala Multimedia website [38] and the Ionospheric conditions on the AMSAT-CT website [17]; Table 6.1 shows the important meteorological and Ionospheric factors, and Appendix G the MUF and foF2 measures for each of the test days are presented.

Table 6.1 – Meteorological conditions and Ionospheric warnings for test days.

Day	30/08/2017	31/08/2017	01/09/2017	04/09/2017	05/09/2017	07/09/2017
Algorithm	RapidM DRC	RapidM DRC with ACOS	RapidM DRC with BEO	Trinder	Trinder with ACOS	Trinder With BEO
Start Time (hh:mm:ss)	11:03:02	11:18:40	09:43:09	14:42:41	12:06:40	14:42:32
Finish Time (hh:mm:ss)	12:12:00	12:11:43	10:37:29	15:38:57	12:46:12	15:27:56
Lisbon Temperature (°C)	23,8	25,1	18,5	20,1	24,8	29,3
Porto Temperature (°C)	21,7	23,0	17	21,9	22,0	24,7
Weather Conditions	Cloudy Sky Little Rainfall	Clean Sky	Clean Sky	High Clouds	Clean Sky	Clean Sky
Ionospheric Warnings	Geomagnetic Warning	Geomagnetic Warning	Geomagnetic Warning	Fadeout Warning	Fadeout Warning	Communications Fadeout Geomagnetic Warnings

6.3.2. Algorithms Performance in Real Test Conditions

The overall results of the field propagation tests are shown in Table 6.2, with the worst performance marked in red colour and the best performance in green colour. These overall results are computed with the set of values presented in Appendix F. The Trinder algorithm is the algorithm with the worst performance presenting the average FER, throughput and goodput with the most undesirable values, such as expected in the simulation environment, and the RapidM DRC algorithm with BEO is the algorithm with the best overall performance presenting the link availability, average throughput and goodput with the most desirable values.

Table 6.2 – Overall results of the field propagation tests.

Algorithm	Day	Total Time (s)	Average BER	Average FER	Average SNR (dB)	Throughput (bit/s)	Goodput (frames/s)	Link Availability
RapidM	30/ago/17	4138	5,08E-06	0,89%	9,501	379,60	188,3E-3	83,88%
RapidM ACOS	31/ago/17	3183	6,69E-05	9,26%	9,328	892,22	369,0E-3	95,95%
RapidM BEO	01/set/17	3260	2,76E-04	24,98%	9,548	2425,23	927,1E-3	99,17%
Trinder	04/set/17	3376	3,69E-04	34,03%	3,971	245,61	78,9E-3	83,29%
Trinder ACOS	05/set/17	2372	1,82E-04	18,49%	4,980	1508,52	698,8E-3	86,38%
Trinder BEO	07/set/17	2724	2,68E-04	24,53%	3,383	718,94	228,3E-3	96,44%

In the simulation environment the Trinder algorithm with BEO represents the algorithm with best average goodput, but in these field propagation results it appears in the third worst position of the performance rank. One of the reasons why this happens is because the average SNR presents large differences between the two trials, being the worst case in these field propagation results; therefore it is important to do an analysis again in the simulation system, carrying the real SNR measurements as input values into the simulation system.

To understand the behaviour of the algorithms as well as the differences between the SNR variations during each day of tests, a graphical view of the SNR variation and the data rate adaptation is needed. Figures 6.18 – 6.23 show the data rate adaptation to a SNR variation measured on each test day by the E/R GRC-525 radio station.

According to the figures of the data rate adaptation, for each algorithm in different days, it is possible to see that the Trinder algorithm presents several oscillations cycles, while the RapidM DRC algorithm is more stable and careful in the data rate change, avoiding unnecessary oscillations. Also, it is possible to see the different SNR measurements between the test days, and how the HF communication warnings influence the link quality; as can be seen in Figure 6.23 and in Table 6.2, the average SNR for the 7th September 2017 test is the lowest, because in this day were recorded the highest number of HF communications warnings (HF Communication, HF Fadeout and Geomagnetic warnings).

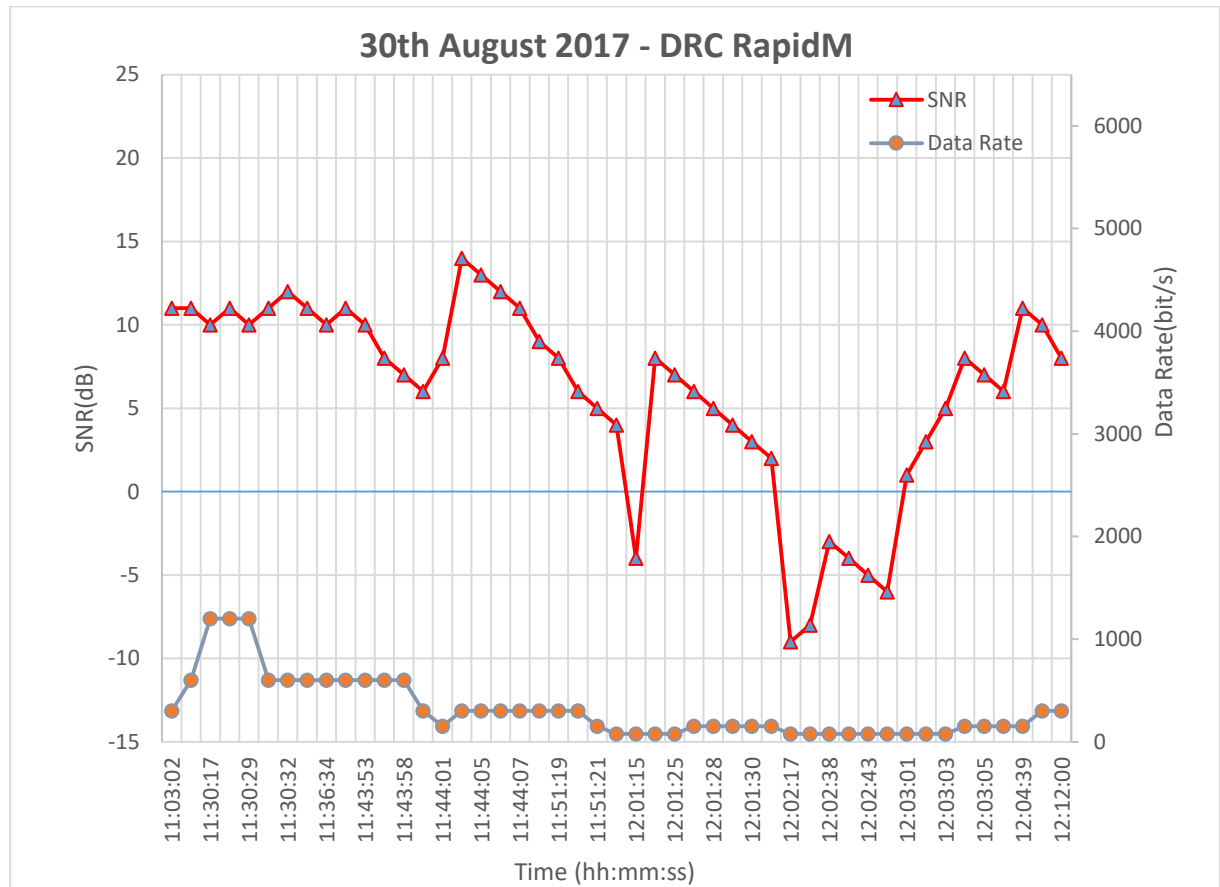


Figure 6.18 – Data rate adaption for a SNR variation measured in 30th August 2017, using the original DRC RapidM algorithm.

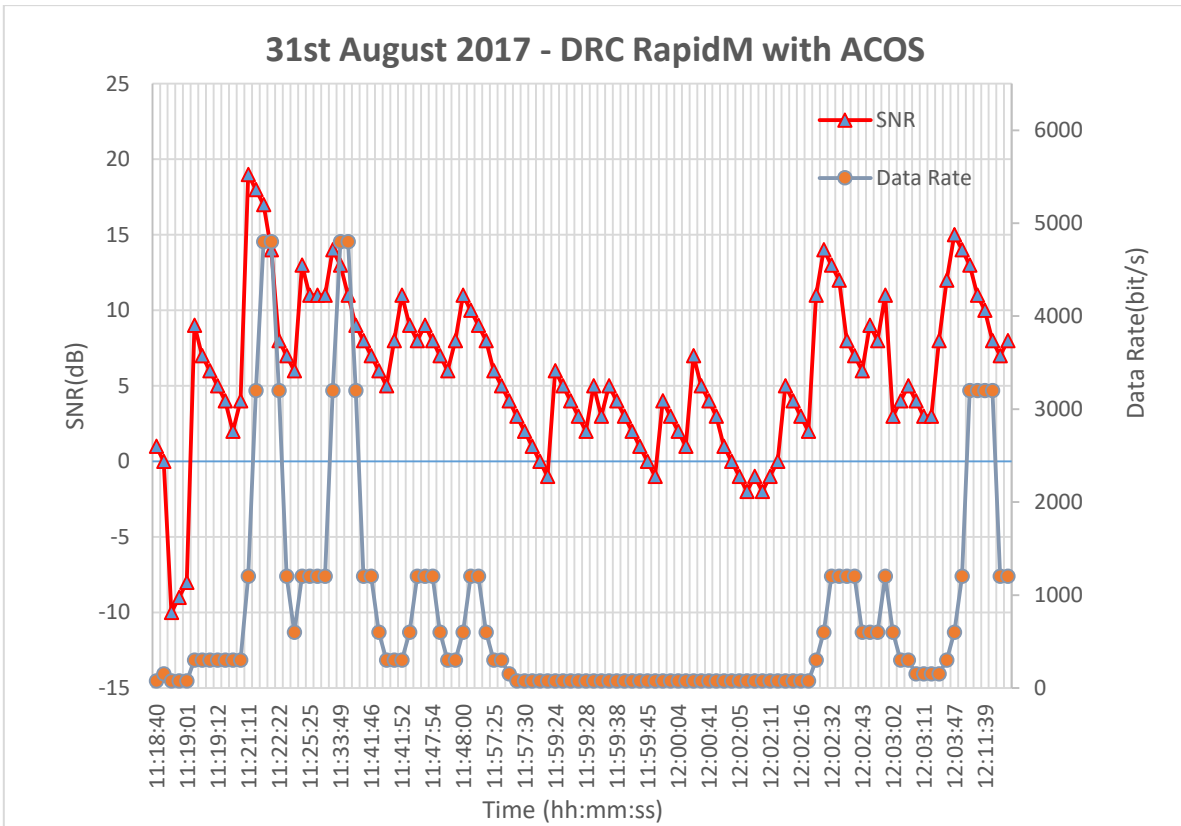


Figure 6.19 – Data rate adaption for a SNR variation measured in 31st August 2017, using the DRC RapidM algorithm with ACOS.

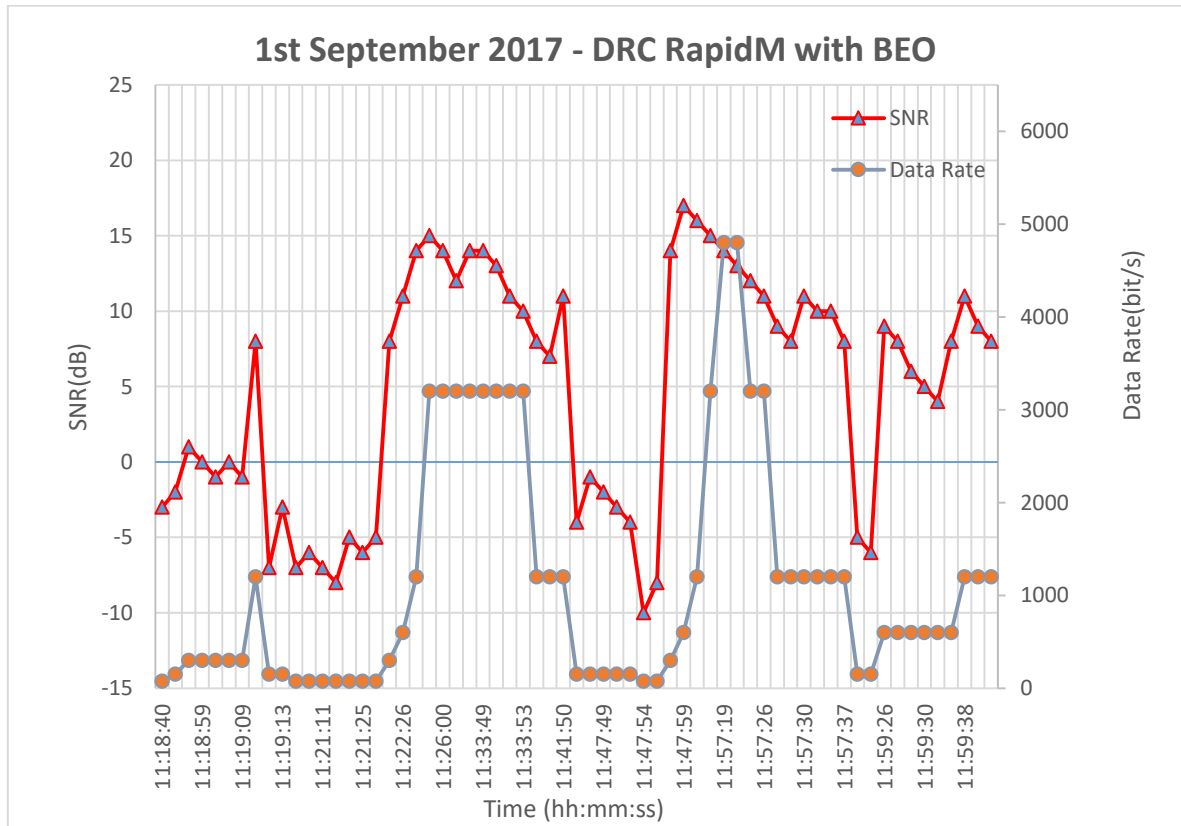


Figure 6.20 – Data rate adaption for a SNR variation measured in 1st September 2017, using the DRC RapidM algorithm with BEO.

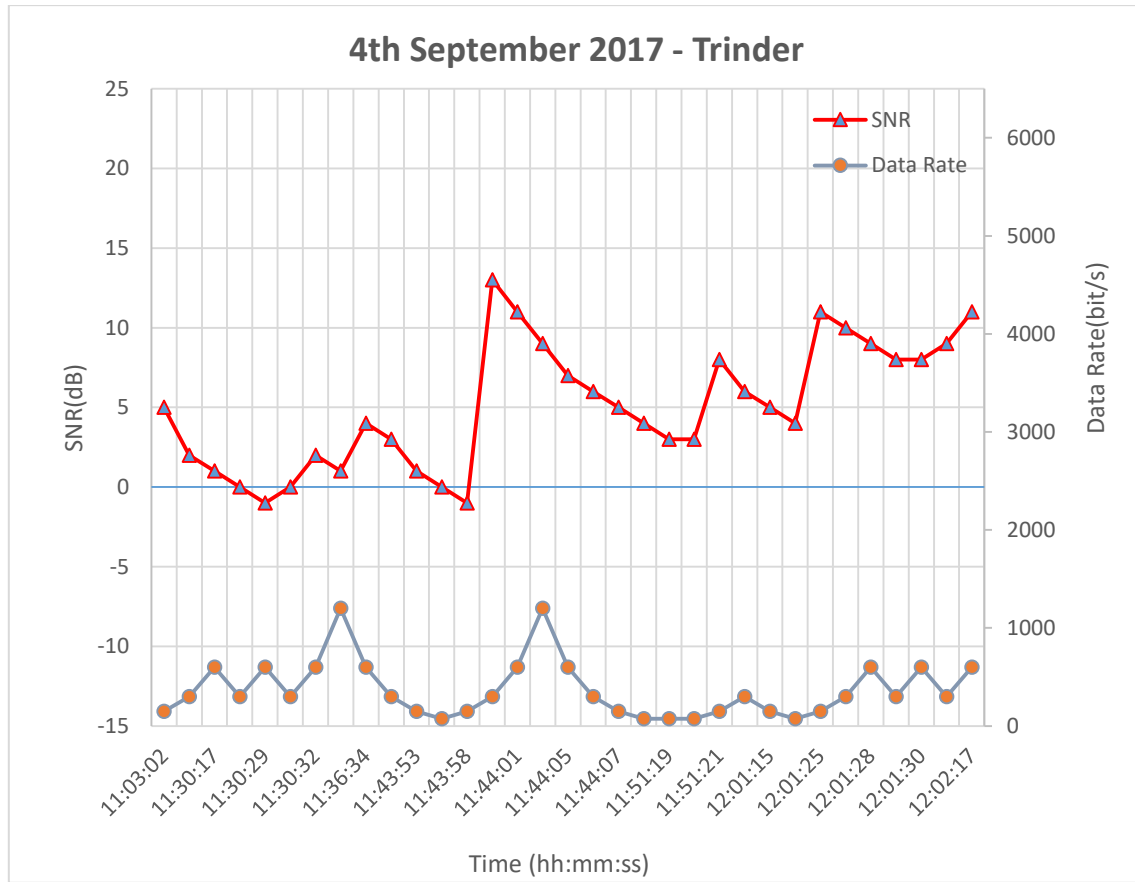


Figure 6.21 – Data rate adaption for a SNR variation measured in 4th September 2017, using the original Trinder algorithm.

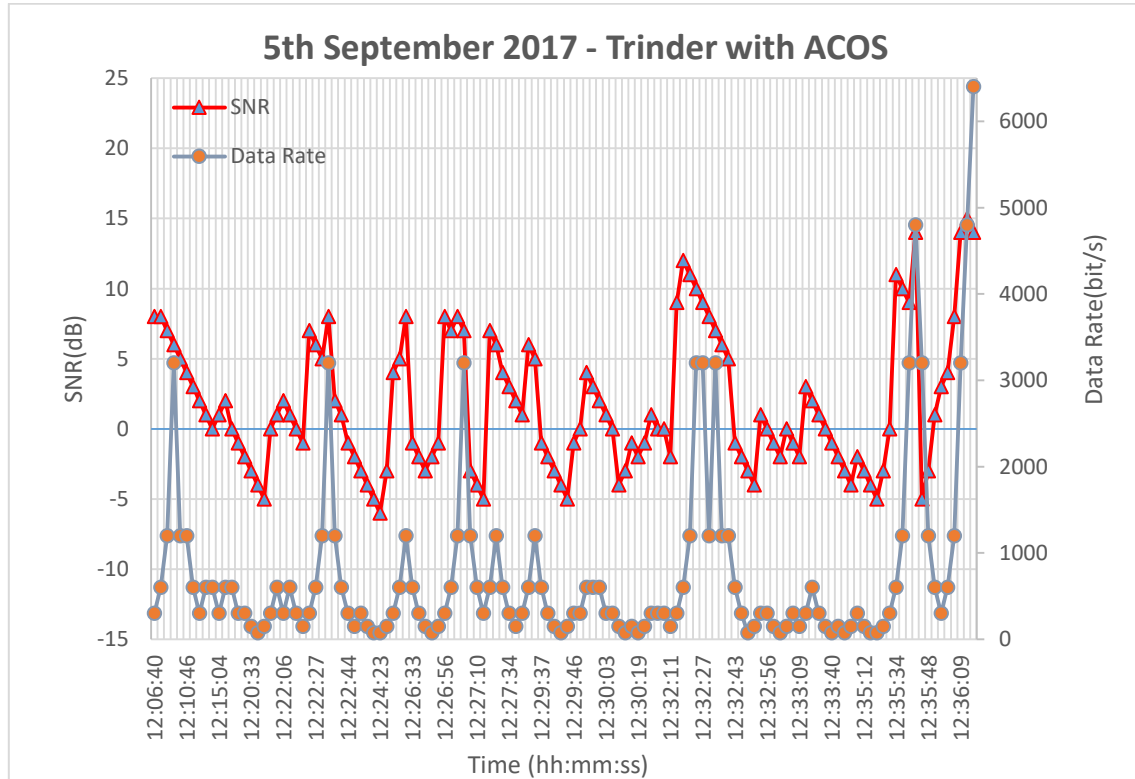


Figure 6.22 – Data rate adaption for a SNR variation measured in 5th September 2017, using the Trinder algorithm with ACOS.

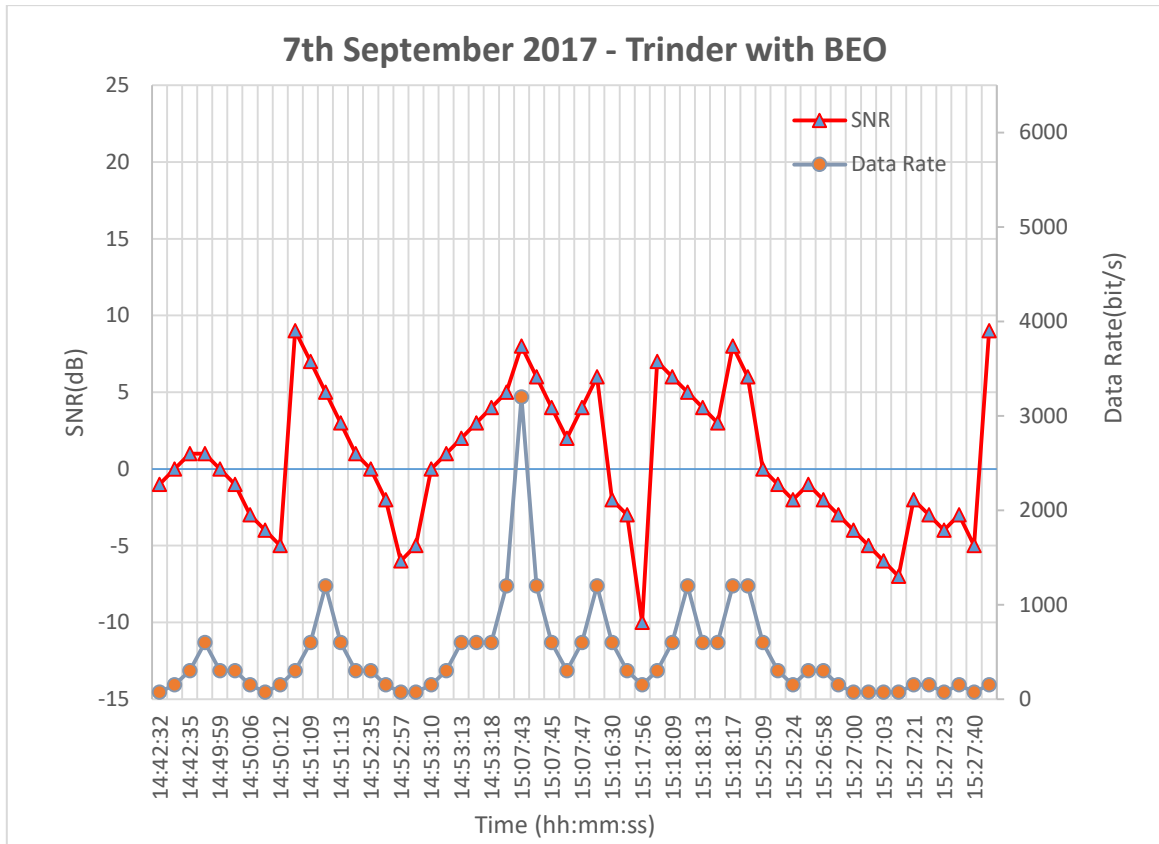


Figure 6.23 – Data rate adaption for a SNR variation measured in 7th September 2017, using the Trinder algorithm with BEO.

6.4. Relation between Simulations and Field Propagation Values

During the field propagation tests the SNR was one of the parameters recorded by the radio station equipment. In order to check the simulation model, these recorded SNR values were given as an input of the simulation system, and the simulation results compared with the field propagation results. This analysis is presented in this section.

The next step was to compute the cross-correlation coefficients between the data rate results of the field propagation tests and the simulated data rate for each channel type. The cross-correlation coefficients are shown in Table 6.3 for each tested algorithm in different days, and the corresponding chart in Figure 6.24.

Table 6.3 – Cross-correlation coefficients values between the field propagation tests results and the expected results provided by the simulation system.

Type of Channel	Type of Algorithm					
	RapidM	RapidM ACOS	RapidM BEO	Trinder	Trinder ACOS	Trinder BEO
30/08/2017	31/08/2017	01/09/2017	04/09/2017	05/09/2017	07/09/2017	
AWGN	0,67766	0,83378	0,85398	0,25174	0,91184	0,84565
POOR	0,59605	0,83946	0,82486	0,16973	0,86288	0,77291
GOOD	0,44352	0,75186	0,87813	0,18590	0,83376	0,73656

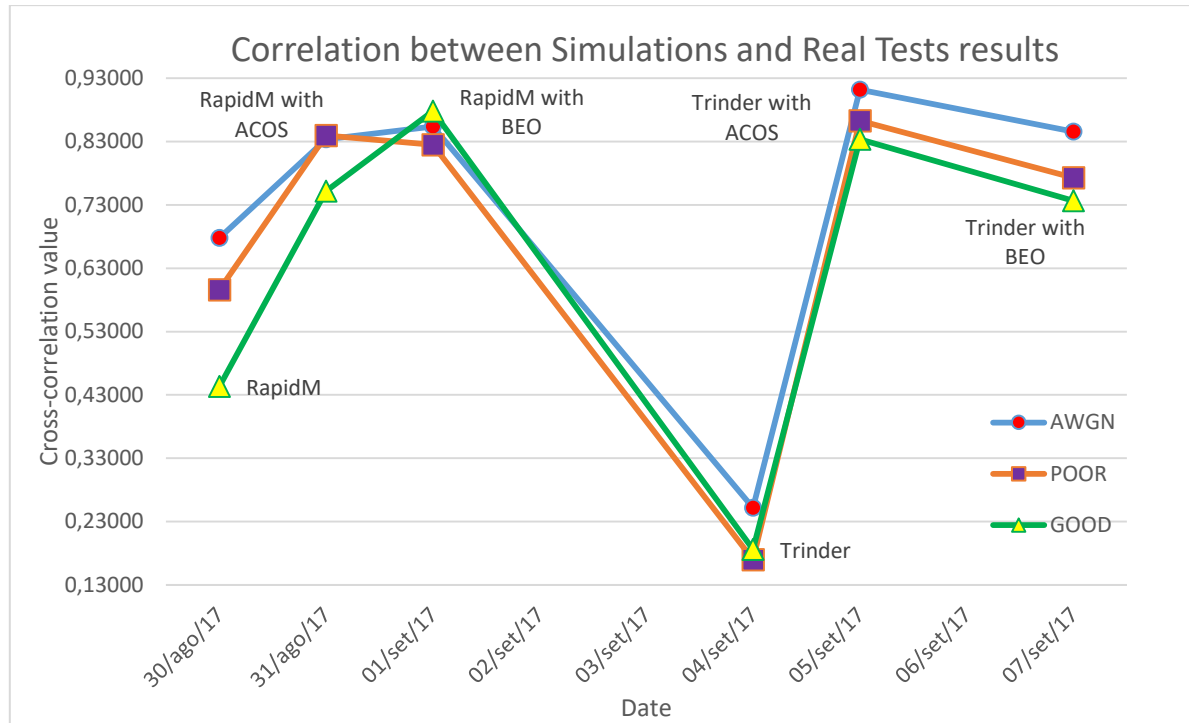


Figure 6.24 – Cross-correlation coefficient values between the field propagation tests and the expected results provided by the simulation system (graphic representation).

According to the cross-correlation coefficient values represented in Figure 6.24 and Table 6.3, the field propagation results corresponds approximately to the expected results provided by the simulation system most of the time. The cross-correlation coefficient value was superior to 0.8 in four out of six test days, presenting one day (31st August 2017) closer to the ITU Poor channel type, another day (1st September 2017) closer to the ITU Good channel type and the two other days (5th September 2017 and 7th September 2017) closer to the AWGN channel type.

The tested algorithms can also be different than simulation predictions, showed by the combining analysis of Figure 6.26 and Figure 6.21, in which the cross-correlation coefficient value is around 0.25, and it presents the worst cross-correlation, for the 4th September 2017, using original version of Trinder algorithm. Otherwise, Figure 6.25 shows the best cross-correlation which can be compared with Figure 6.22, for the 5th September 2017 using the Trinder algorithm with ACOS, with a cross-correlation coefficient value of 0.91.

Table 6.4 shows the relation between the field propagation results and the expected results for each type of channel. It also shows that the original RapidM DRC tested on 30th August 2017 has similar throughput results to the expected for an ITU Good channel type, but the cross-correlation coefficient shows that the field propagation behaviour is closer to the behaviour expected for an AWGN channel. Otherwise, the Trinder algorithm with ACOS tested on 5th September 2017 has a behaviour in agreement with the obtained results. The cross-correlation coefficient shows that the field propagation behaviour is closest to the expected behaviour for an AWGN channel (the results are closest to the expected results for an AWGN channel).

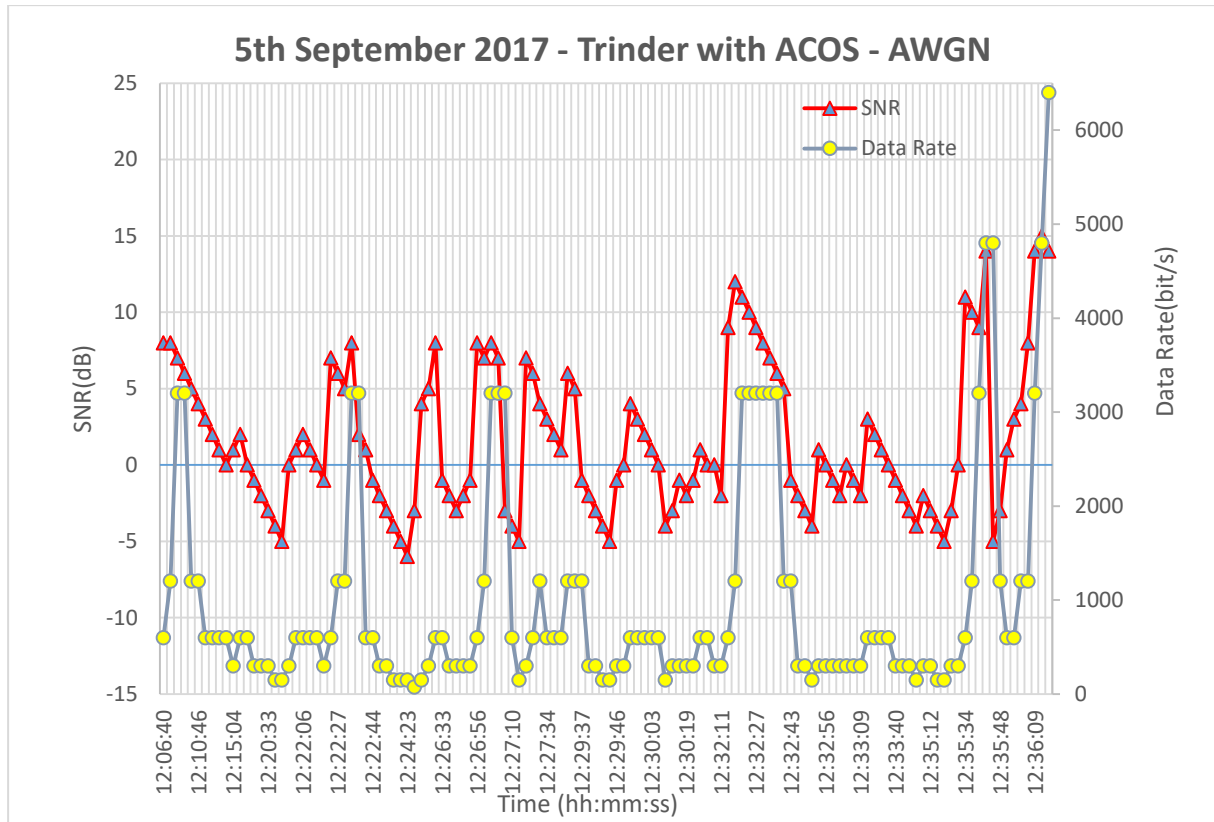


Figure 6.25 – Simulated values for the 5th September 2017, using Trinder algorithm with ACOS and assuming an AWGN channel which corresponds to the best cross-correlation fit.

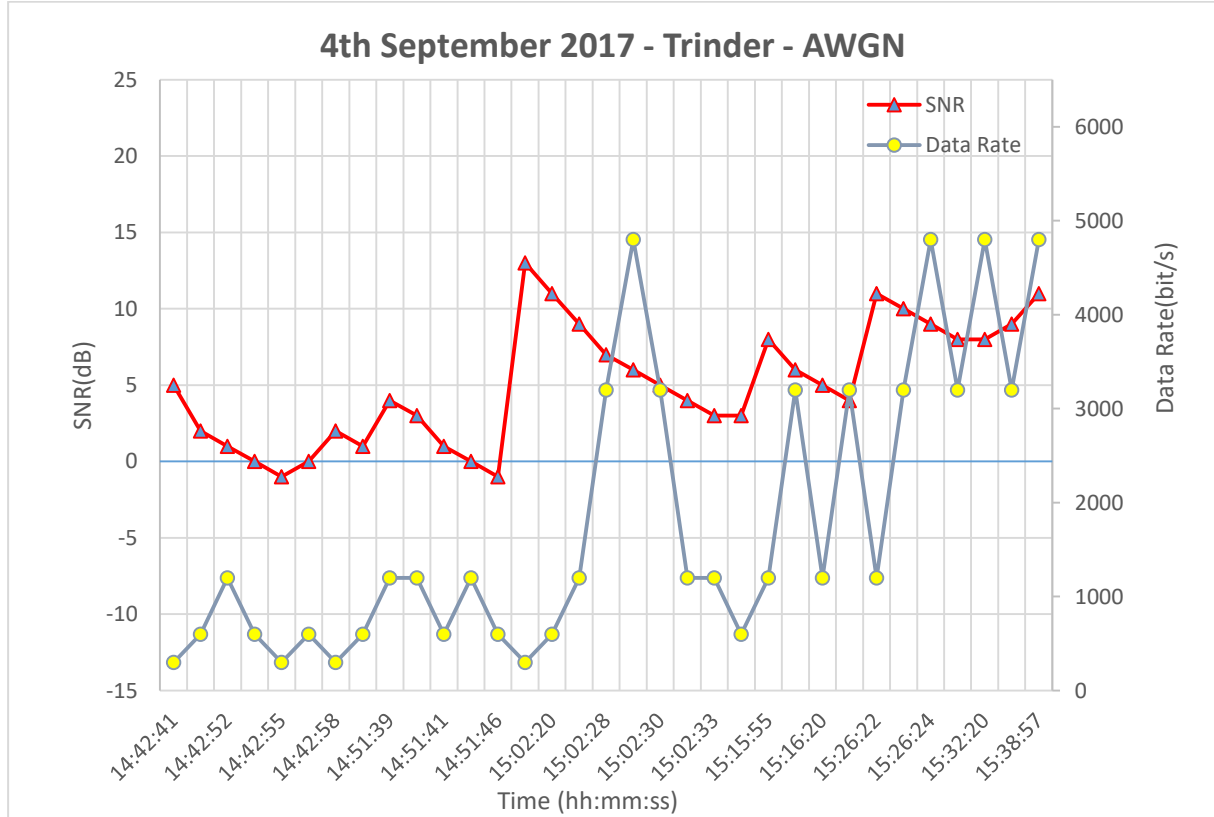


Figure 6.26 – Simulated values for the 4th September 2017, using original Trinder algorithm and assuming an AWGN channel which corresponds to the worst cross-correlation fit.

Table 6.4 – Relation between the field propagation results and the expected values for each channel provided by the simulation system.

		Channel	BER	FER	Throughput (bit/s)	Goodput (frames/s)	LA
Algorithm: RapidM	30/ago/17	AWGN	3,99E-05	6,49%	2887	1,2302	98,99%
		POOR	3,51E-05	6,41%	821	0,4073	83,01%
		GOOD	2,81E-05	4,82%	395	0,1583	87,68%
		Field Test	5,08E-06	0,89%	380	0,1883	83,88%
Algorithm: RapidM with ACOS	31/ago/17	AWGN	2,19E-05	3,68%	2846	1,3464	63,12%
		POOR	5,18E-05	5,81%	893	0,4277	99,43%
		GOOD	1,39E-04	19,81%	418	0,1832	95,66%
		Field Test	6,69E-05	9,26%	892	0,3690	95,95%
Algorithm: RapidM with BEO	01/set/17	AWGN	7,03E-06	1,38%	2495	1,2435	93,13%
		POOR	7,39E-06	1,46%	1562	0,6733	91,29%
		GOOD	7,44E-06	1,54%	612	0,2696	90,25%
		Field Test	2,76E-04	24,98%	2425	0,9271	99,17%
Algorithm: Trinder	04/set/17	AWGN	7,14E-05	12,13%	676	0,3338	52,28%
		POOR	5,26E-05	8,63%	315	0,1552	51,48%
		GOOD	2,90E-05	5,09%	107	0,0516	50,98%
		Field Test	3,69E-04	34,03%	246	0,0789	83,29%
Algorithm: Trinder with ACOS	05/set/17	AWGN	3,26E-05	5,91%	1625	0,8047	84,40%
		POOR	1,21E-04	14,84%	1041	0,5035	93,76%
		GOOD	2,53E-04	27,09%	415	0,1937	79,22%
		Field Test	1,82E-04	18,49%	1509	0,6988	86,38%
Algorithm: Trinder with BEO	07/set/17	AWGN	3,26E-05	5,75%	901	0,3857	95,15%
		POOR	4,79E-05	7,71%	372	0,1690	94,42%
		GOOD	1,35E-04	16,13%	218	0,0852	83,66%
		Field Test	2,68E-04	24,53%	719	0,2283	96,44%

Chapter 7 – Summary and Future Work

This final chapter presents a summary of the developed work and also suggestions for future work in the HF communications and DRC algorithms.

7.1. Summary

The main objective of this dissertation was to design, implement and test a DRC algorithm with better performance than the existing solutions, for HF communications, using the E/R GRC-525 military radio.

The development of HF transmissions declined when the satellite communication appeared, as it allows higher data rates. However, the use of HF band offers more independency and less costs in the communications section for a nation; in Portugal, satellites are rented to the USA, making it an expensive system to use. In addition, satellites are vulnerable to physical damage, as it is supported by Earth infrastructures and, in an emergency, such as an earthquake, satellite communications can be disabled. In recent years, HF modems and adaptive techniques were developed, allowing high speed modems (until 9600 bit/s) and renewing the use of HF communications, especially in military situations with hilly terrain. These communications use the Ionosphere to reflect the sky wave, therefore it is necessary to know its composition and behaviour.

According to the HF standardisations and the adaptive techniques developed at the beginning of the millennium, two DRC algorithms were designed, implemented and simulated: Trinder and RapidM DRC algorithms. Trinder algorithm defines the data rate based on FER thresholds, and RapidM DRC algorithm updates the data rate according to BER and SNR thresholds.

A simulation system in Matlab was created to assess the original DRC algorithms and detect their vulnerabilities. After implementing the Trinder and the RapidM DRC algorithms, its main detected weakness was the data rate oscillations, which lead to many cut-off states, reducing the link availability and the average throughput and goodput.

In order to increase the performance of the original Trinder and RapidM algorithms, two new versions of each one were proposed: Avoiding Cut-Off State (ACOS) and Bit Error Optimization (BEO). When implemented on the simulation environment, these new versions showed huge link performance improvements relatively to the original versions; however, some data rate oscillations were still detected in the ACOS based versions.

After assessing all the algorithms in the simulation system, two radio stations, one in Lisbon and another in Oporto, were assembled. Each station was composed by one E/R GRC-525 military radio and a RF-1936P dipole antenna. A DRC software application, implementing all the considered DRC algorithms (original and improved versions) was developed, allowing to assess the algorithms on the field. The field propagation tests were performed within a period of 9 days, seeking similar propagation conditions during all the tests. The Ionospheric behaviour and the meteorological conditions were recorded, since these may justify eventual discrepancies on the results.

The algorithm that showed the best performance results was the RapidM DRC with BEO, increasing the goodput by 392% and the link availability by 15%, when compared to its original version. It was expected that the Trinder algorithm with BEO would present similar results, but the day of its test

(7th September 2017) coincided with the highest number of ionospheric warnings and with the worst average SNR value (3.38 dB). Nonetheless, the Trinder algorithm with BEO exceeded the performance of its original version, increasing the goodput by 189% and the link availability by 13%. The original version of Trinder algorithm presented the worst performance results among every tested algorithm.

The HF communications standards used in this dissertation were the STANAG 4539 [24] and the MIL-STD-118-110B [25].

7.2. Future Work

Despite the good results obtained, showing that the proposed solution allow a significant improvement of the DRC algorithms original versions, some issues related with HF communications and the DRC algorithms deserve to be further considered:

- Improve the user interface in the DRC application to make it more “user friendly”.
- Implementation of the STANAG 5066 in a DRC application.
- Design, implement and test an algorithm that changes the frame size according to the propagation conditions.

Appendix A – Radio E/R GRC-525 datasheet

rumo ao futuro
...nas **COMUNICAÇÕES TÁCTICAS**

Rádio Táctico Multibanda PRC-525



- Família de Rádios Tácticos Multibanda: HF, VHF, UHF
- Manpack e vasta gama de instalações veiculares
- Estações fixas e repetidores transportáveis
- Cobertura das três bandas com um único rádio em instalação veicular
- Alta segurança: COMSEC (encriptação) e TRANSEC (salto de frequência)
- Vasta gama de formas de onda para voz e dados
- Dados e ALE de 3^a geração em HF
- *Combat Net Radio* em VHF
- Formas de onda para comunicação em UHF com aeronaves
- Todas as especificações militares relevantes
- IP over the air



Rádio Táctico Multibanda PRC-525

A família de rádios digitais GRC-525 é constituída pelas versões *manpack* (PRC-525), veicular e fixa, trabalhando na banda de 1,5 a 512MHz. A sua capacidade de se adaptar a uma variada gama de situações operacionais permite utilizar o rádio como um *Combat Net Radio* em redes tácticas de voz e dados e, com equipamento adicional, como *Packet Radio*, repetidor ou PAR (Ponto de Acesso Rádio) para interligação à rede comutada ou a LANs e WANs.

Seguindo a filosofia software defined radio, o rádio é altamente configurável permitindo acrescentar novas funções e formas de onda.

Entre as características mais notáveis, destacam-se a capacidade multibanda (HF, VHF, UHF), a disponibilidade de um grande número de formas de onda e ainda uma gama de modems internos quer em HF quer em VHF/UHF.

A segurança das comunicações é outro ponto distintivo do PRC-525, ao dispor de encriptação do conteúdo da informação (COMSEC) e também salto de frequência (TRANSEC), segundo algoritmos personalizados de acordo com o cliente.



Características Técnicas

Geral

Gama de Frequências	HF/VHF: Tx: 1,5 a 108MHz Rx: 100kHz a 512MHz V/UHF: Tx: 25 a 512MHz Rx: 100kHz a 512MHz
Espaçamento do Canal:	V/UHF: 6,25; 8,33; 12,5; 25kHz
Estabilidade de Frequência	1ppm
Canais Pré-Programados	400 (10 disponíveis no comutador)
Modulações	H/V/U: A1A(CW), A3E(AM), H3E(AME), J3E(USB), LSB; F3E(FM); F1D(FSK)
Modos de Operação	SSB/FM/AM, Salto de Frequência (H/V/U); Voz e Dados em claro (FM); Voz e Dados cifrados (Salto de frequência e DFF), Controlo Remoto e GPS
Teste (BITE)	Nível de Módulo; BIT manual; Monitorização Contínua
Tensão de Alimentação	19 a 33VDC
Manpack	19 a 33VDC - MIL STD 1275
Veicular	Litio - recarregável
Baterias	Autonomia
	20H com 1:1:8, 5W, FM
Características Ambientais	
Temperatura	-40°C a +70°C -25°C a +55°C (especificações completas)
Choque e Vibração	MIL-STD - 810E
Estanquidez	1m (MIL-STD - 810E)
Dimensões e Peso (com bateria)	
L x A x P	199 x 74 x 309mm
Peso	5,8kg

Receptor

Sensibilidade (típica @ 10dB SINAD)	
HF	-117dBm
VHF-FM	-115dBm
UHF-AM	-109dBm
UHF-FM	-112dBm
Squelch	Siláxico 150Hz (NATO) RSSI 38 tons subaudíveis

Emissor

Potência de Saída: Manpack PRC-525	
HF	1mW, 0,5 a 20W PEP (em saltos de 3dB)
VHF	1mW, 0,5 a 10W (em saltos de 3dB)
UHF	1mW, 0,5 a 10W (em saltos de 3dB)
Com Amplificador Externo (instalações veiculares ou fixas)	
HF	150W ou 500W
VHF e UHF	50W

Salto Frequência

HF	SECOM H, 8,88 saltos/s
V/UHF	SECOM V, 512 saltos/s

Opções

Salto de Frequência	HAVE QUICK II; SECOS
Versão V/UHF	HF - Stanag 4285 e 4539
Transmissão de Dados	V/UHF - modem 72kbps (OFDM)
	IP over the air em HF, VHF e UHF
ALE (HF)	MIL-STD-141B; Stanag 4538

Esta publicação tem apenas um carácter informativo. A EID reserva-se o direito de alterar o desenho e as especificações do equipamento sem aviso prévio.

5090/4/0230101

Caixa Postal 535
2821-901 Charneca da Caparica · Portugal
Tel: (+351) 21 294 86 00 · Fax: (+351) 21 294 87 00
E-mail: eid@eid.pt · www.eid.pt



Appendix B – Dipole antenna RF-1936P datasheet



PORABLE CROSSED DIPOLE ANTENNA

RF-1936 (AS-2259/GR)/ RF-1938

FEATURES

- For NVIS (near vertical incidence skywave) communications
- Rapid-deployable for NVIS communications
- Lightweight and man-portable
- 5-minute installation with two people

The RF-1936/38 Series of antennas are man-portable and rapid-deployable for NVIS communications.

The NVIS communication mode is for paths from 10 to 400 km. This communication mode is particularly useful in mountainous, heavily wooded terrain, or dry sandy soil where groundwave is limited. The RF-1936 is used for general purpose NVIS communication links out to 400 km; while the RF-1938 is designed for the hard to close 10 to 200 km links.

These lightweight antenna systems are easily carried and installed by two people in five minutes (RF-1936) or 15 minutes (RF-1938). The sectional mast is a low loss coaxial feed line to feed unequal length crossed dipole radiating elements. The radiating elements are attached to guy ropes that provide mast support. The entire antenna stows within a small canvas bag. The RF-1938 has a second set of coaxial masts and guy lines which stow within a second canvas bag.



harris.com

SPECIFICATIONS FOR: RF-1936/RF-1938

SPECIFICATIONS

Dimensions	Stowed: RF-1936: 1 bag 26" long x 7" dia. RF-1938: 2 bags 26" long x 7" dia. Deployed: RF-1936 - 61 by 61 ft.
Weight	RF-1936: 15 lb. RF-1938: 27 lb.
Height	RF-1936: 15 ft. (4.6 m) RF-1938: 27.9 ft. (8.6 m)
Finish	RF-1936P-10 CARC 383 Green RF-1936P-30 Semi Gloss Green RF-1936V-10 CARC 383 Green RF-1936V-30 Semi Gloss Green RF-1938AT-10 CARC 383 Green RF-1938AT-30 Semi Gloss Green

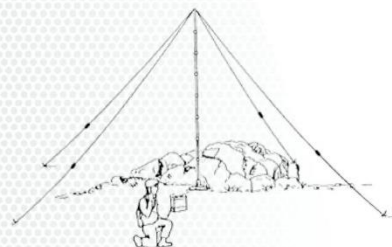
ENVIRONMENTAL

Temperature	Operating: -40° to +55° C (-40° to +131° F) Storage: -60° to +70° C (-76° to +158° F)
Wind	RF-1936: 60 mph (96 kph) with no ice

MECHANICAL

RF Connector	Side feed with wing nut
Installation Time	RF-1936: 5 min. with 2 people RF-1938: 15 min. with 2 people

TYPICAL INSTALLATION OF AN RF-1936



HARRIS

Harris Corporation
RF Communications Division
1680 University Avenue
Rochester, NY 14610, USA

585-244-5830

rf.harris.com



harris.com

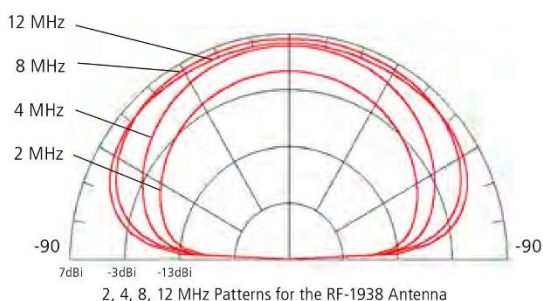
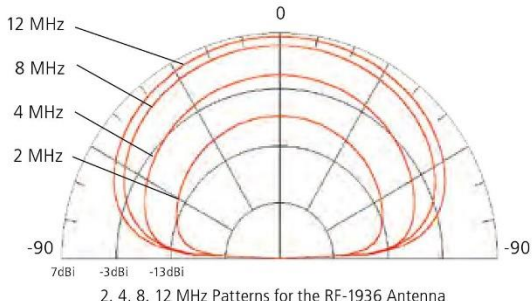
ELECTRICAL

Frequency Range	2 to 30 MHz with antenna coupler
RF Power Capacity	400 Watts
Input Impedance	Compatible with RF-5800H internal coupler and RF-382 Antenna Couplers
Radiation Pattern	Azimuth: omnidirectional Elevation: see radiation patterns below
Polarization	Horizontal for the RF-1936 or a RF-1938 Vertical if used with the monopole conversion kit option
VSWR	In accordance with RF-5800H internal coupler and RF-382 Antenna Couplers
Gain	See radiation patterns below

OPTIONS

Monopole Conversion Kit	RF-1938-AT003 (convert RF-1936/38 to top loaded monopole)
Vehicular Antenna Adapter	RF-1936-01 (included with the RF-1936V)
Mounting Plate for flat surface	RF-1936-02 (included with the RF-1936 and RF-1938AT)

RADIATION PATTERNS OVER AVERAGE GROUND



This information was approved for all publishing per the ITAR as "basic marketing information of defense articles" or as "advertising printed material" per the EAR. Specifications are subject to change without notice.

© 2014 Harris Corporation 1/14 DS-274A

Appendix C – Results from Algorithms Assessments

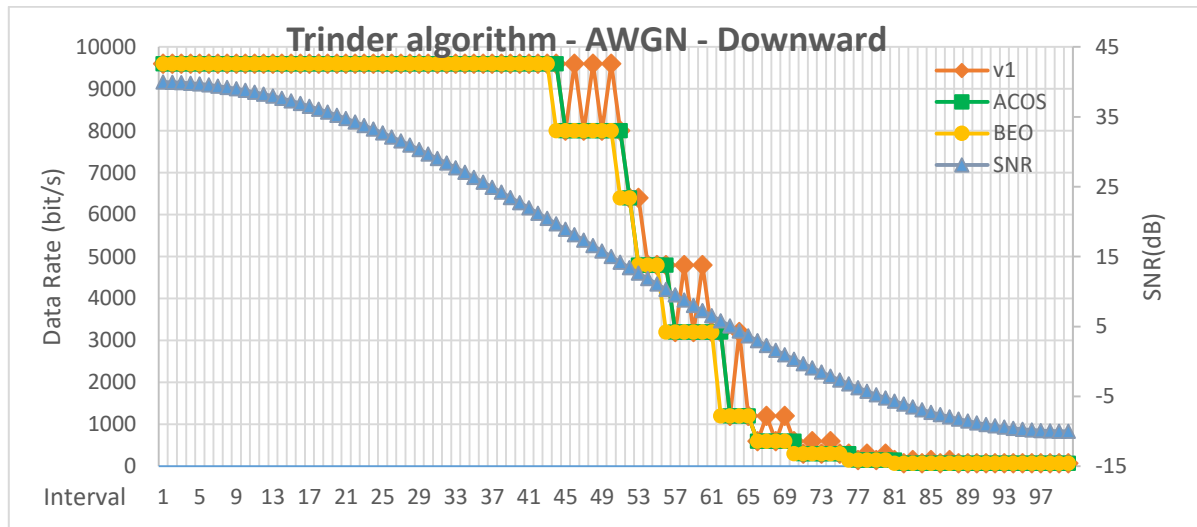


Figure C.1 – Trinder algorithm data rate adaptation for an AWGN channel using downward sinusoidal SNR variation.

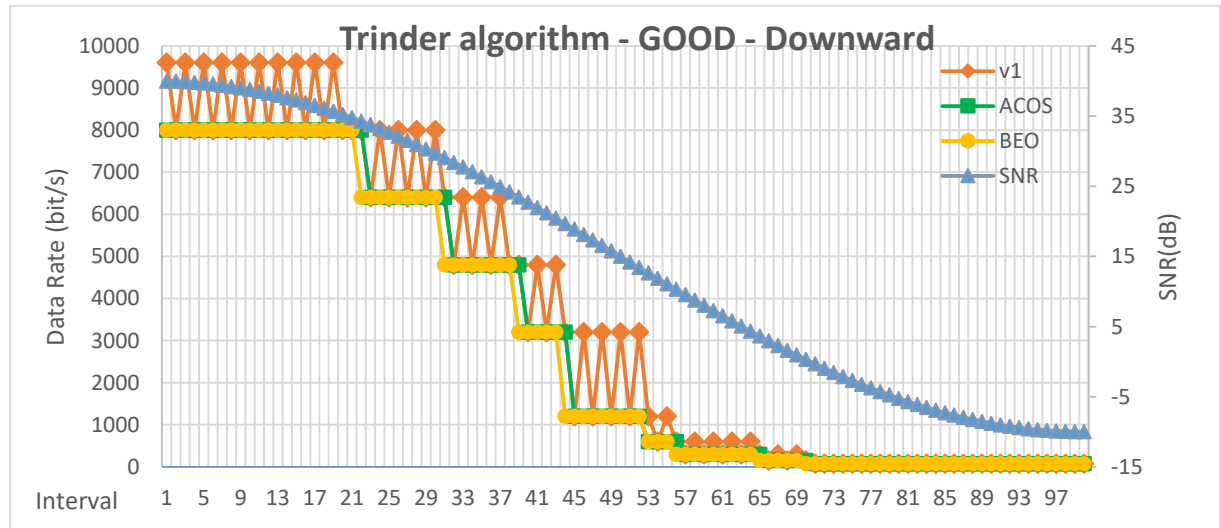


Figure C.2 – Trinder algorithm data rate adaptation for a GOOD channel using downward sinusoidal SNR variation.

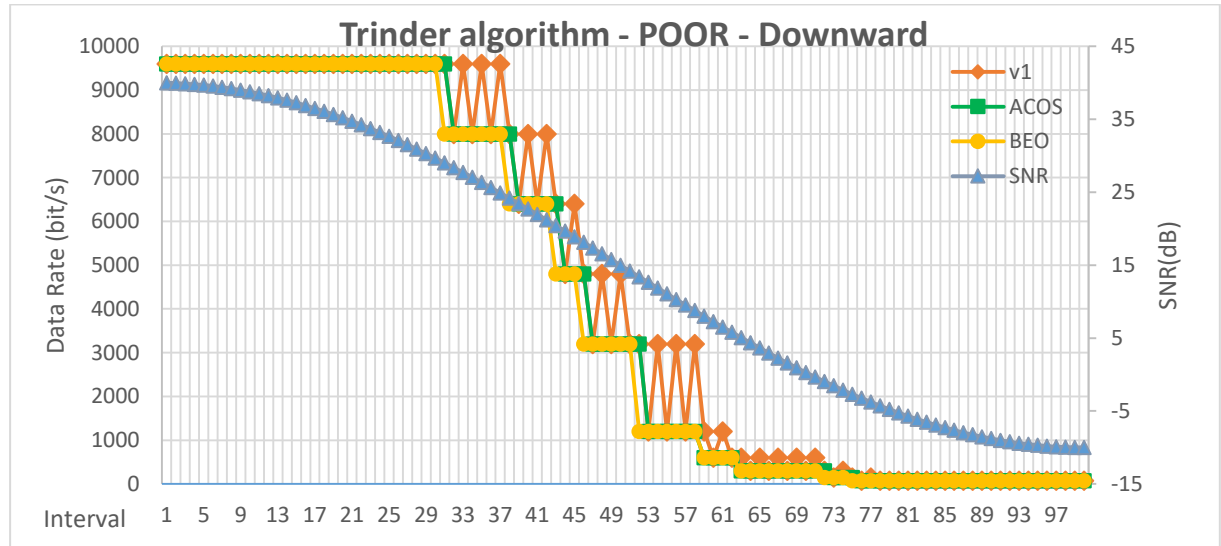


Figure C.3 - Trinder algorithm data rate adaptation for a POOR channel using downward sinusoidal SNR variation.

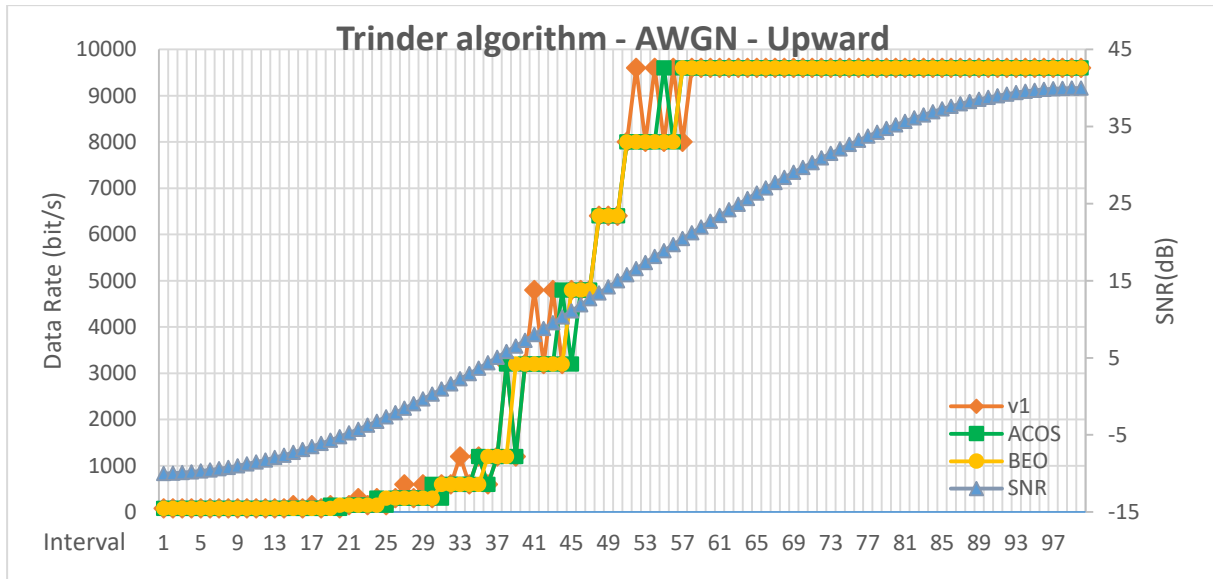


Figure C.4 – Trinder algorithm data rate adaptation for an AWGN channel using upward sinusoidal SNR variation.

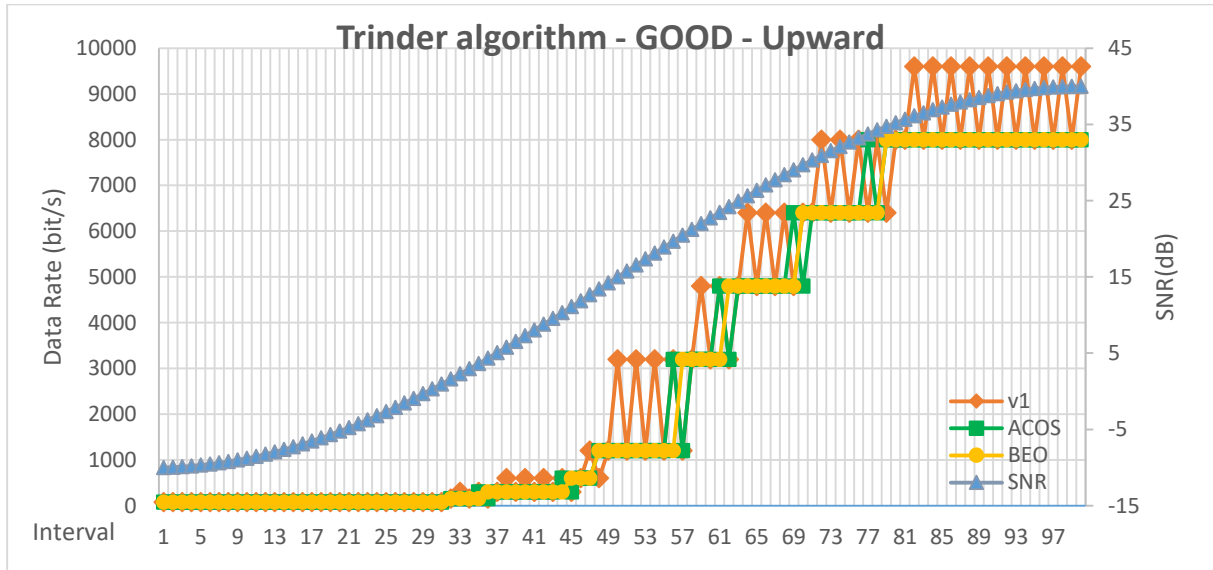


Figure C.5 – Trinder algorithm data rate adaptation for a GOOD channel using upward sinusoidal SNR variation.

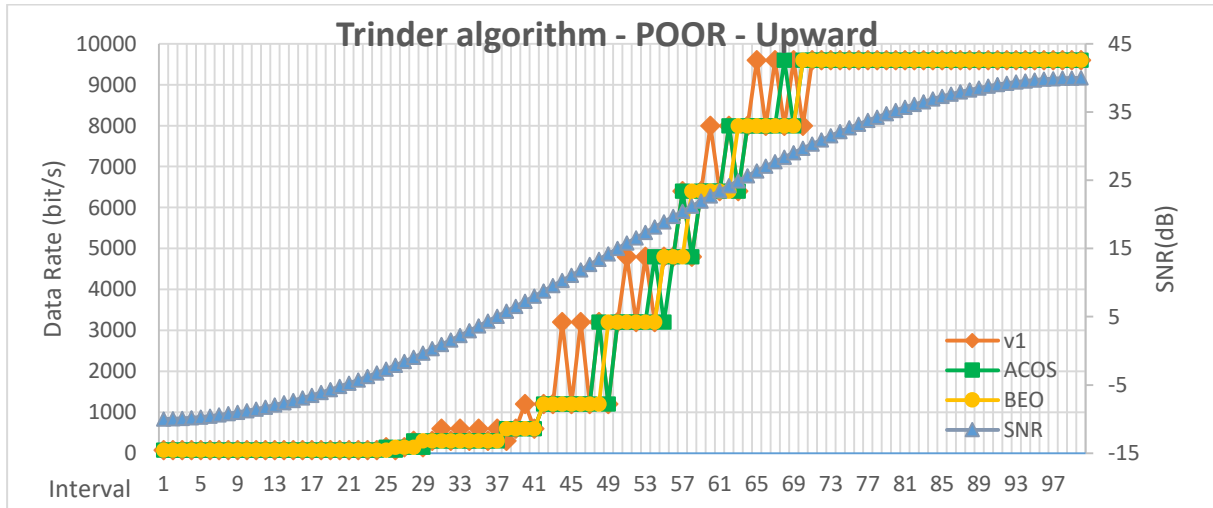


Figure C.6 – Trinder algorithm data rate adaptation for a POOR channel using upward sinusoidal SNR variation.

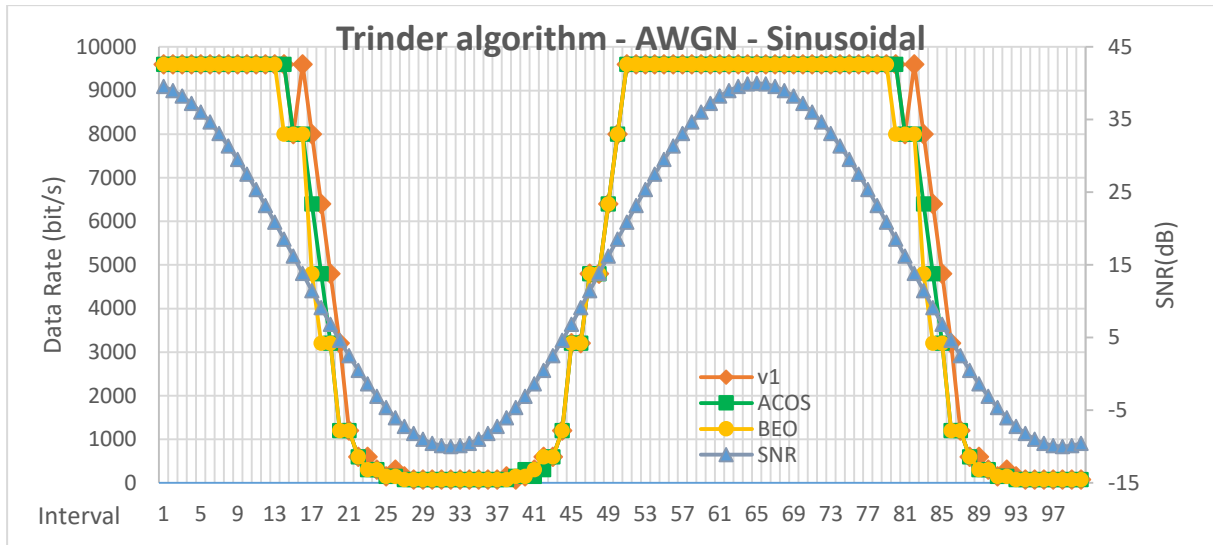


Figure C.7 – Trinder algorithm data rate adaptation for an AWGN channel using sinusoidal SNR variation.

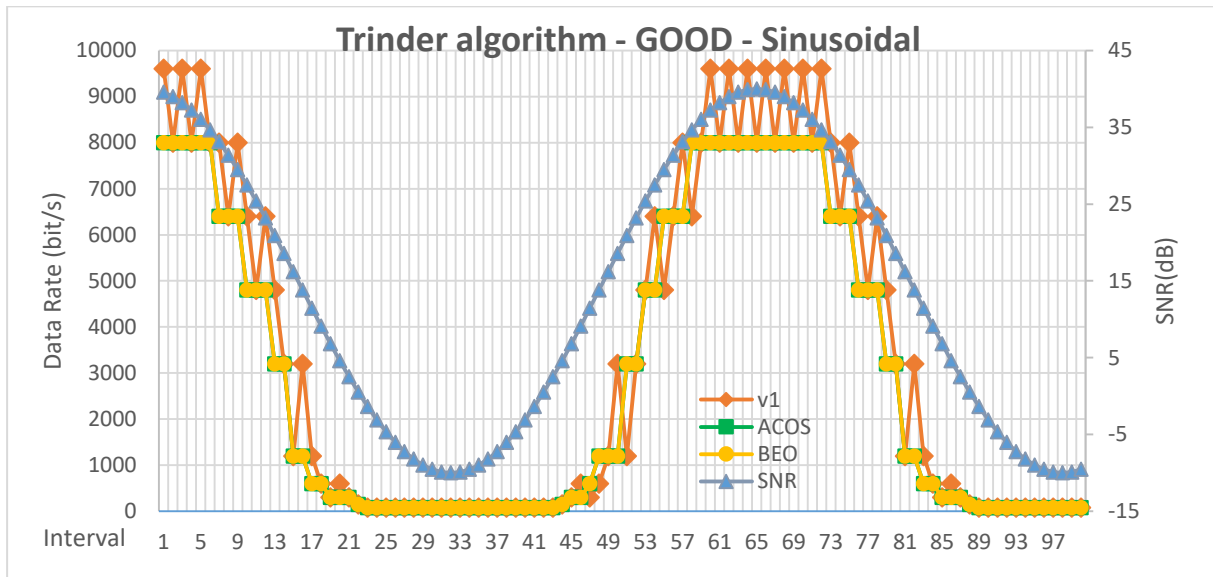


Figure C.8 – Trinder algorithm data rate adaptation for a GOOD channel using sinusoidal SNR variation.

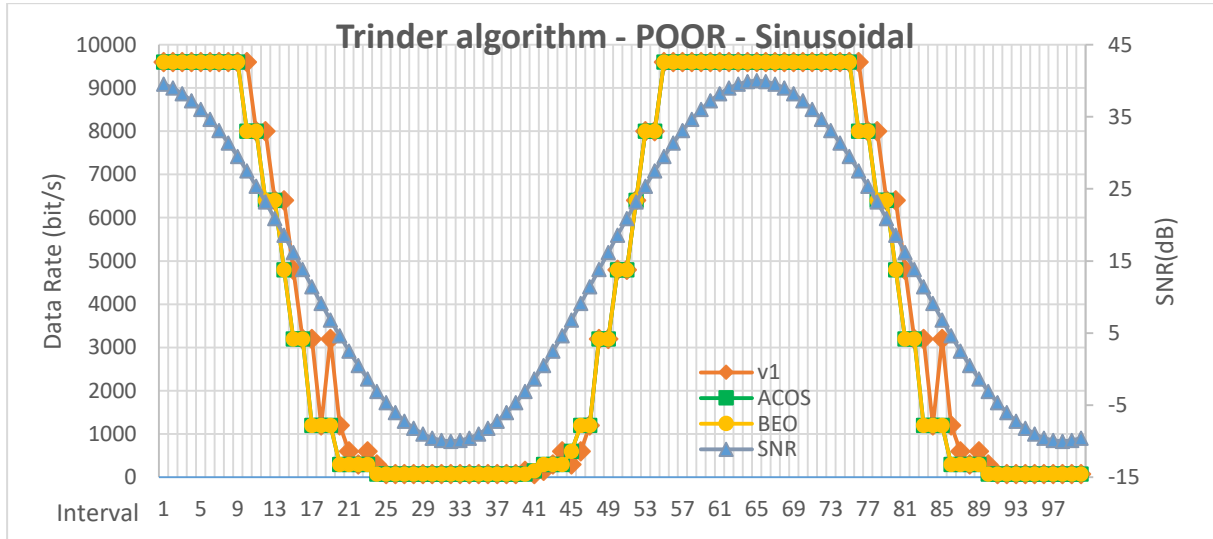


Figure C.9 – Trinder algorithm data rate adaptation for a POOR channel using sinusoidal SNR variation.

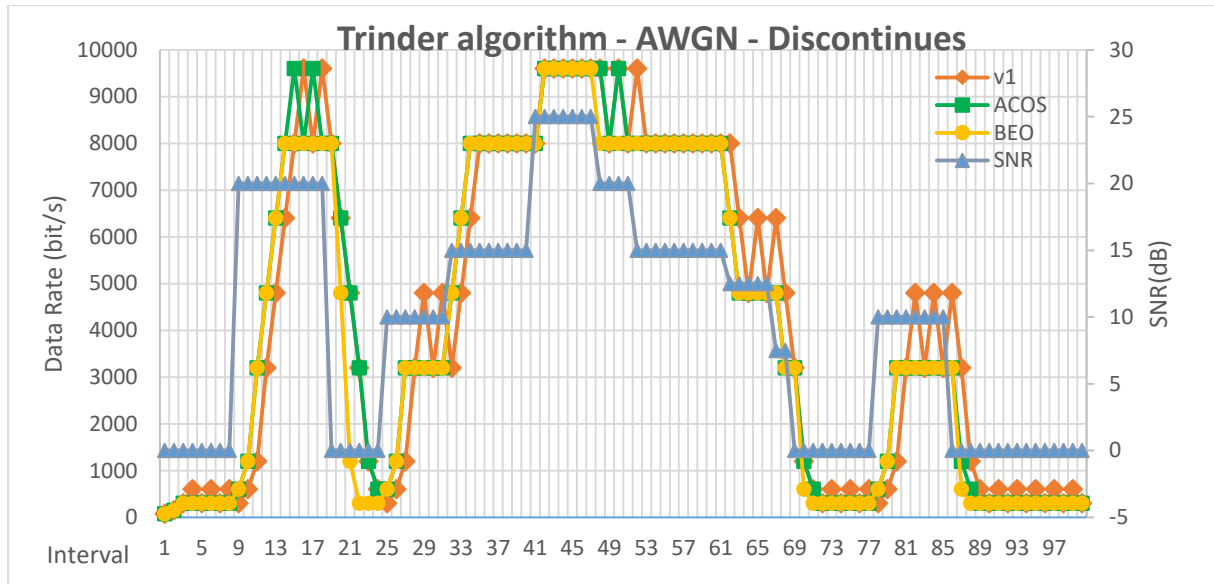


Figure C.10 – Trinder algorithm data rate adaptation for an AWGN channel using discontinues SNR variation.

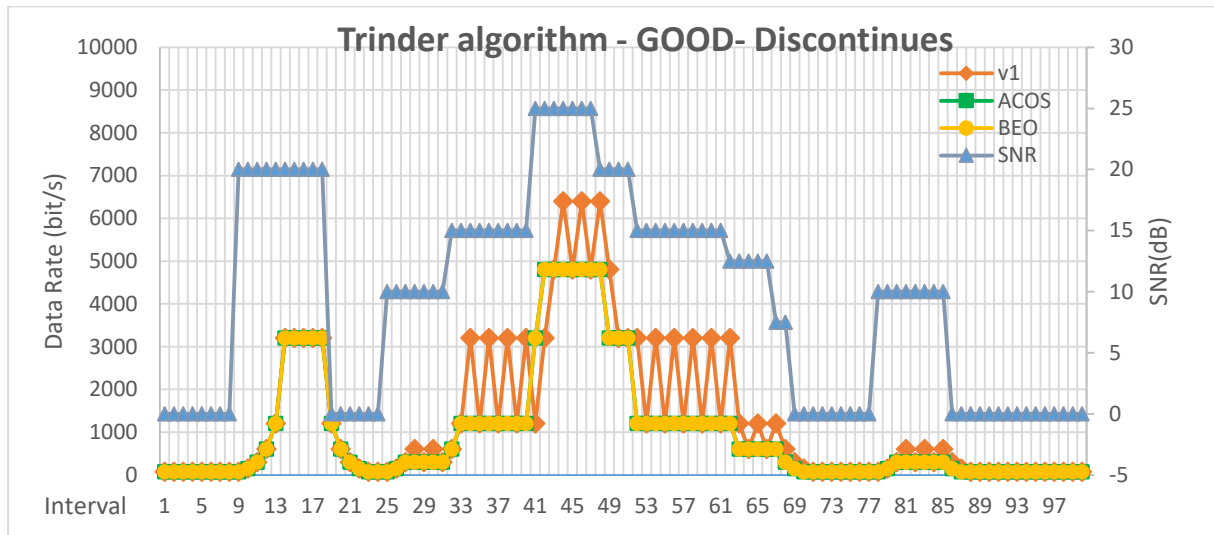


Figure C.11 – Trinder algorithm data rate adaptation for a GOOD channel using discontinues SNR variation.

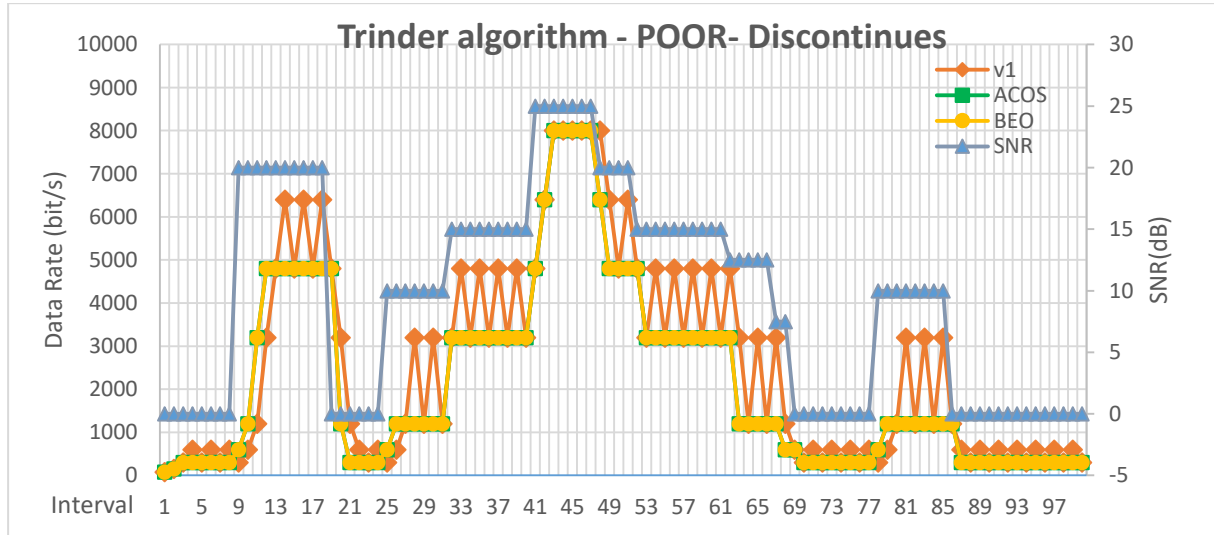


Figure C.12 – Trinder algorithm data rate adaptation for a POOR channel using discontinues SNR variation.

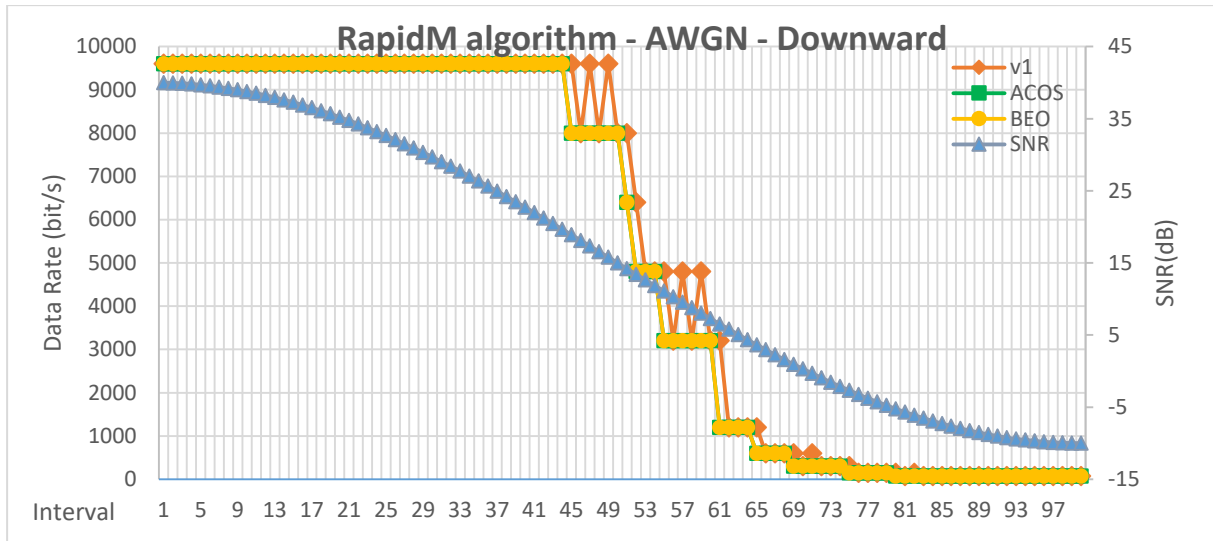


Figure C.13 – RapidM algorithm data rate adaptation for an AWGN channel using downward SNR variation.

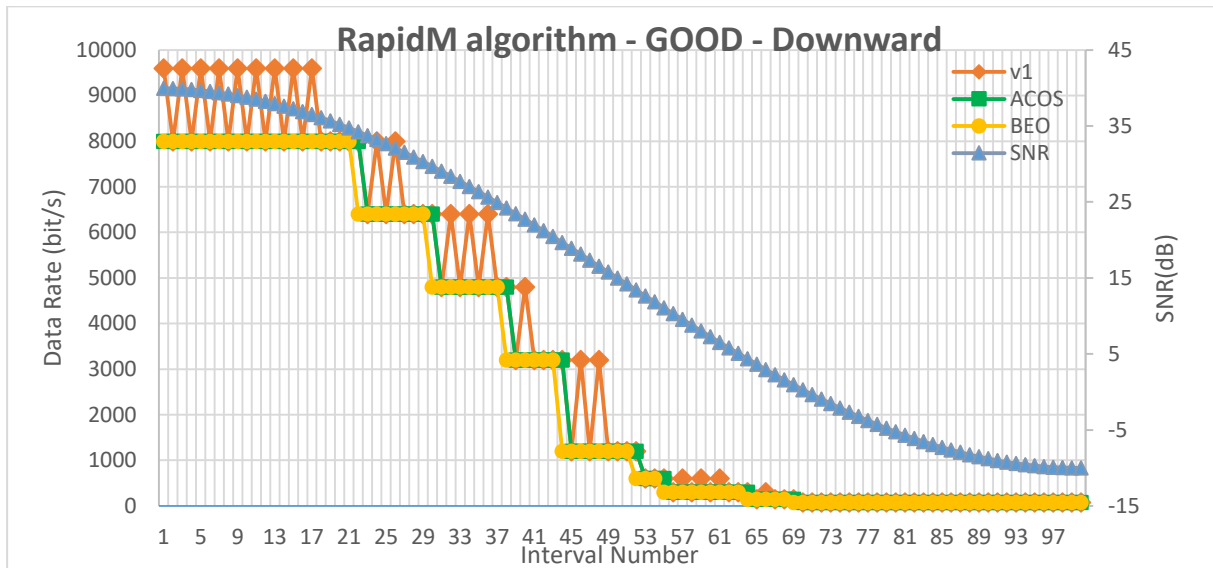


Figure C.14 – RapidM algorithm data rate adaptation for a GOOD channel using downward SNR variation.

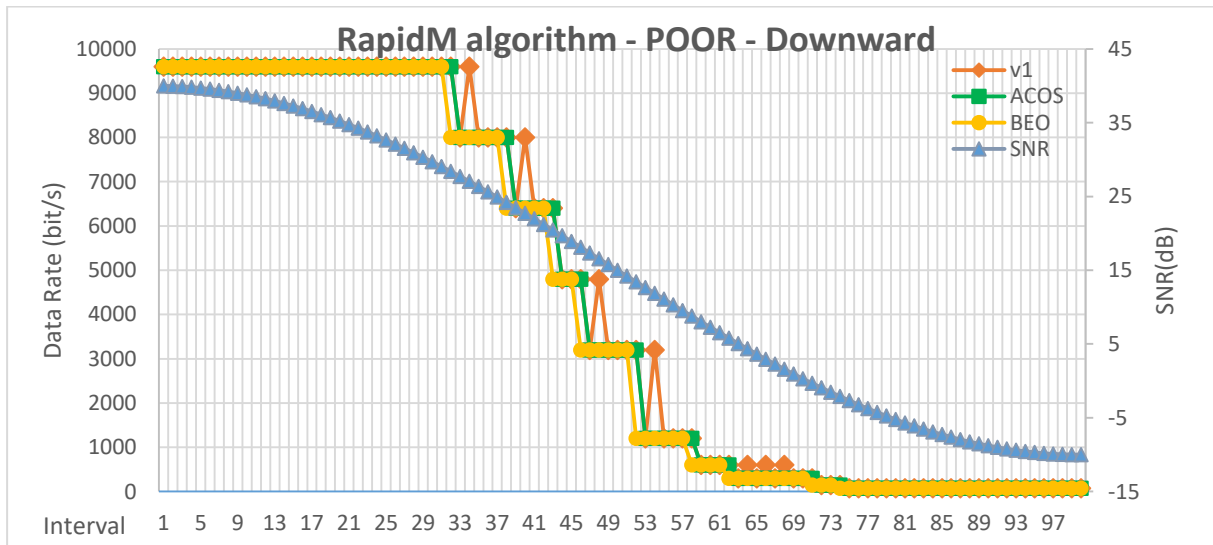


Figure C.15 – RapidM algorithm data rate adaptation for a POOR channel using downward SNR variation.

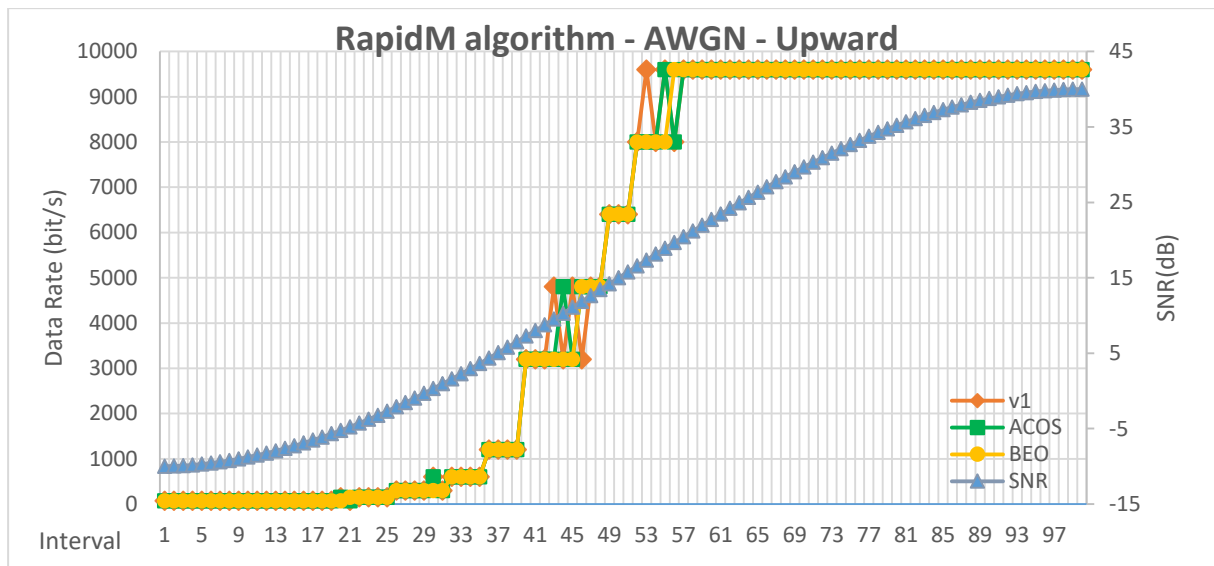


Figure C.16 – RapidM algorithm data rate adaptation for an AWGN channel using upward SNR variation.

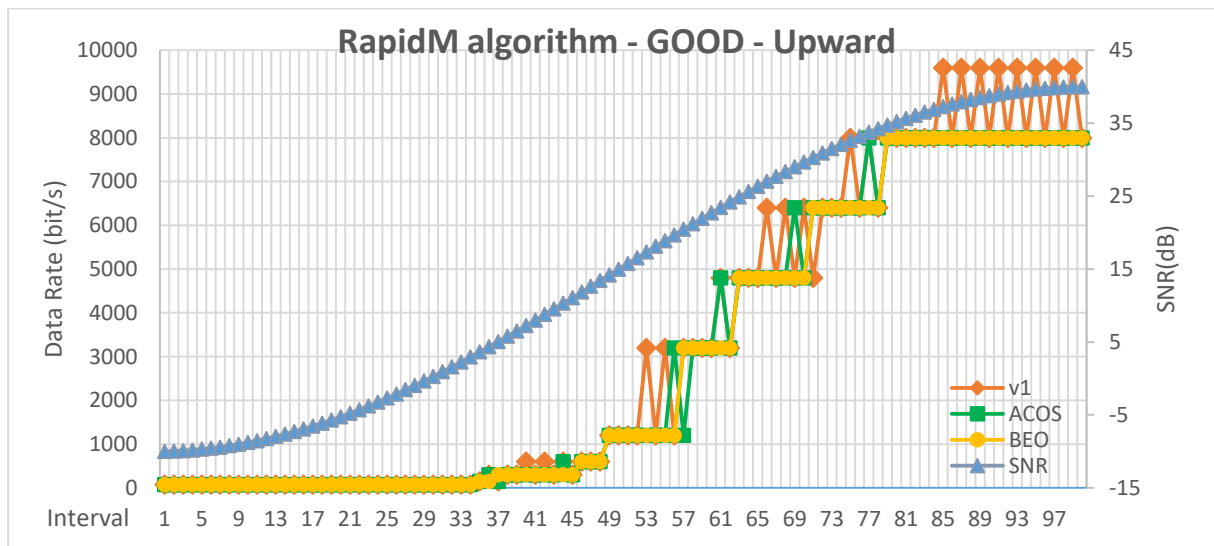


Figure C.17 – RapidM algorithm data rate adaptation for a GOOD channel using upward SNR variation.

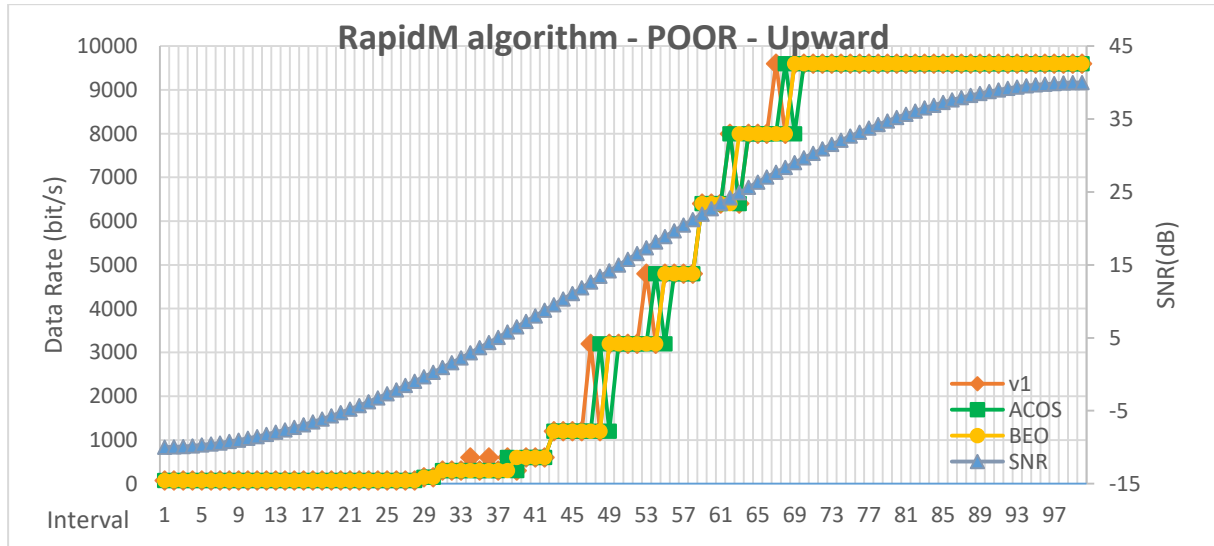


Figure C.18 – RapidM algorithm data rate adaptation for a POOR channel using upward SNR variation.

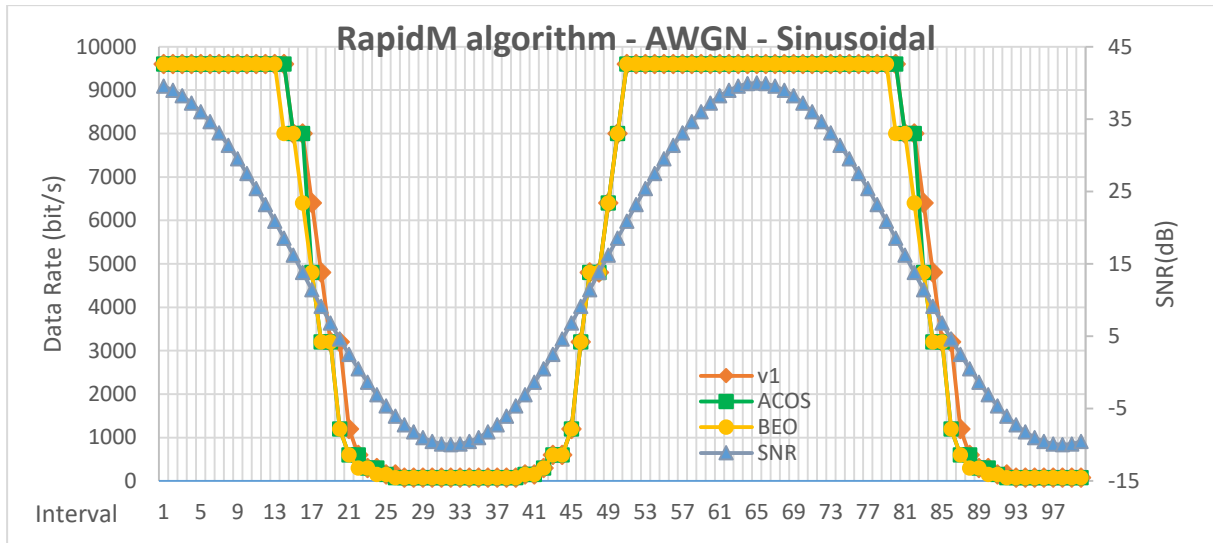


Figure C.19 – RapidM algorithm data rate adaptation for an AWGN channel using sinusoidal SNR variation.

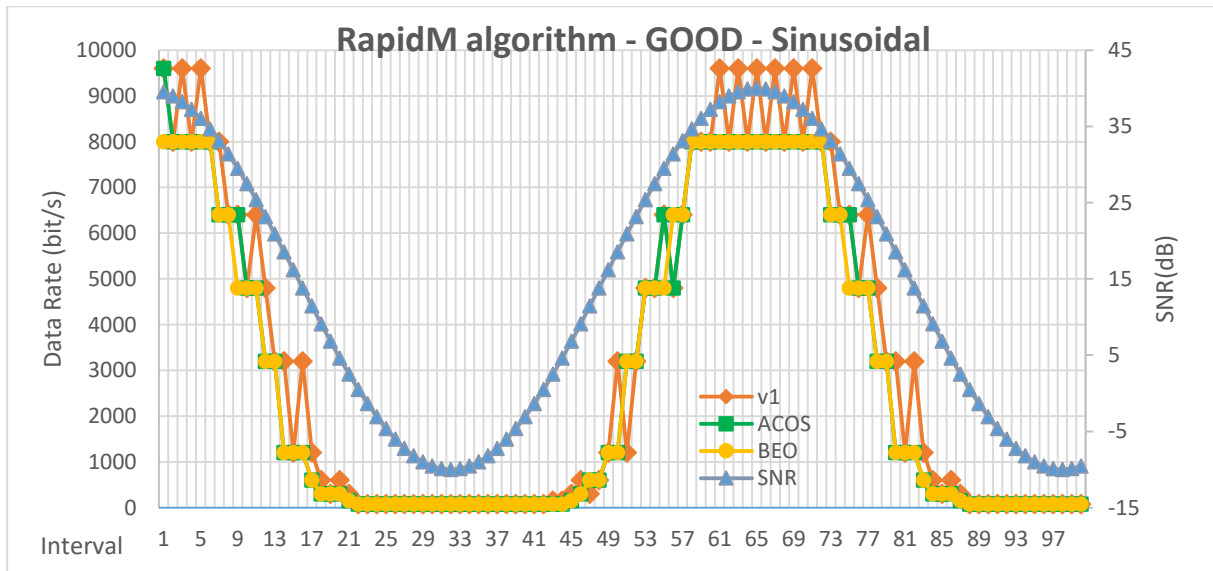


Figure C.20 – RapidM algorithm data rate adaptation for a GOOD channel using sinusoidal SNR variation.

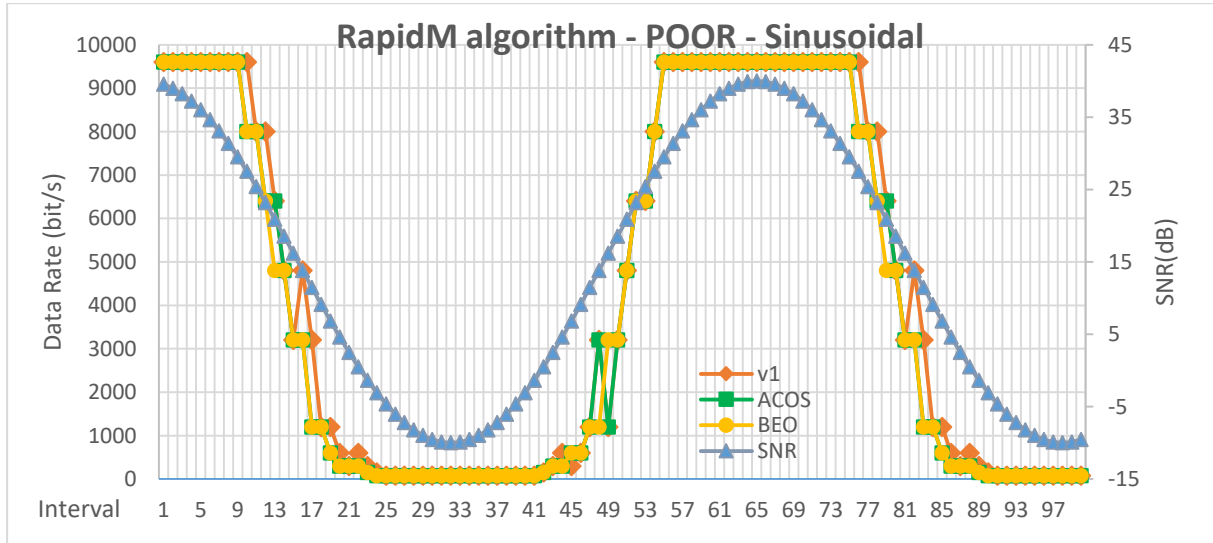


Figure C.21 – RapidM algorithm data rate adaptation for a POOR channel using sinusoidal SNR variation.

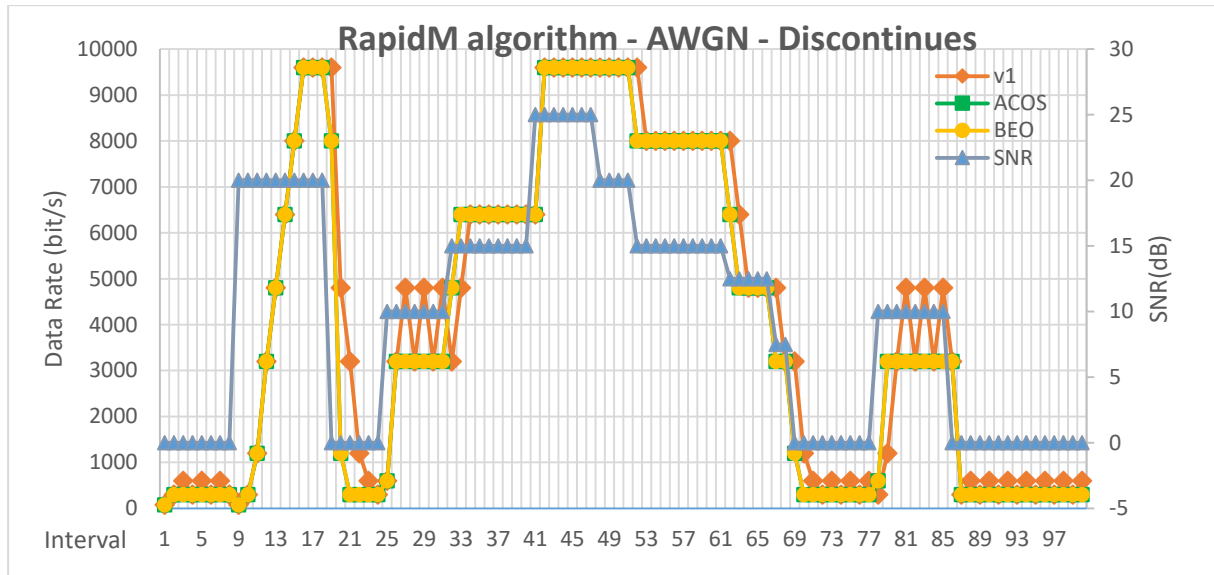


Figure C.22 – RapidM algorithm data rate adaptation for an AWGN channel using discontinues SNR variation.

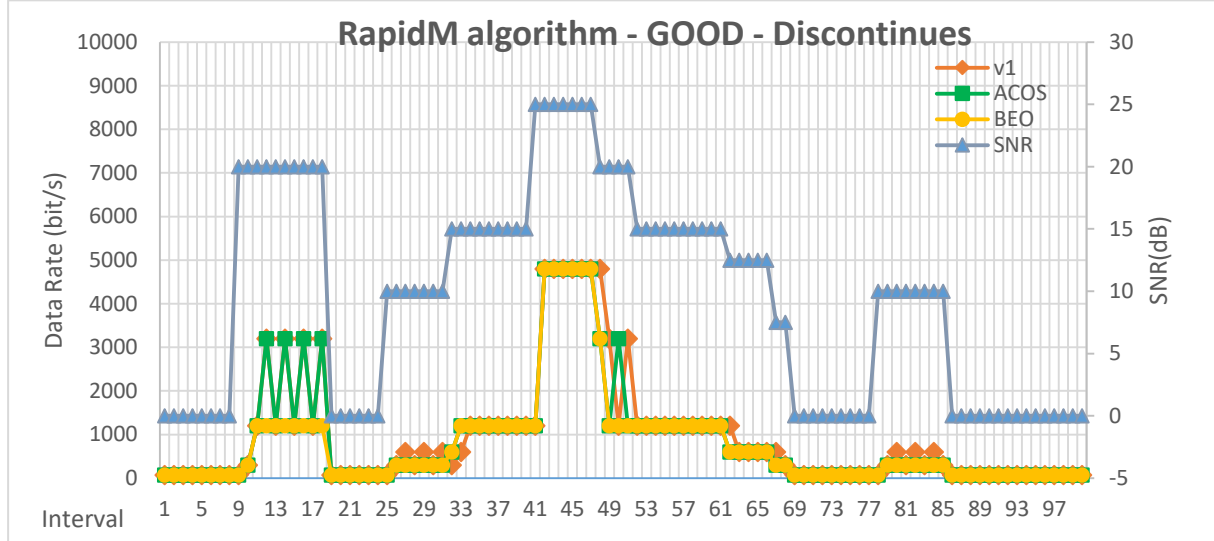


Figure C.23 – RapidM algorithm data rate adaptation for a GOOD channel using discontinues SNR variation.

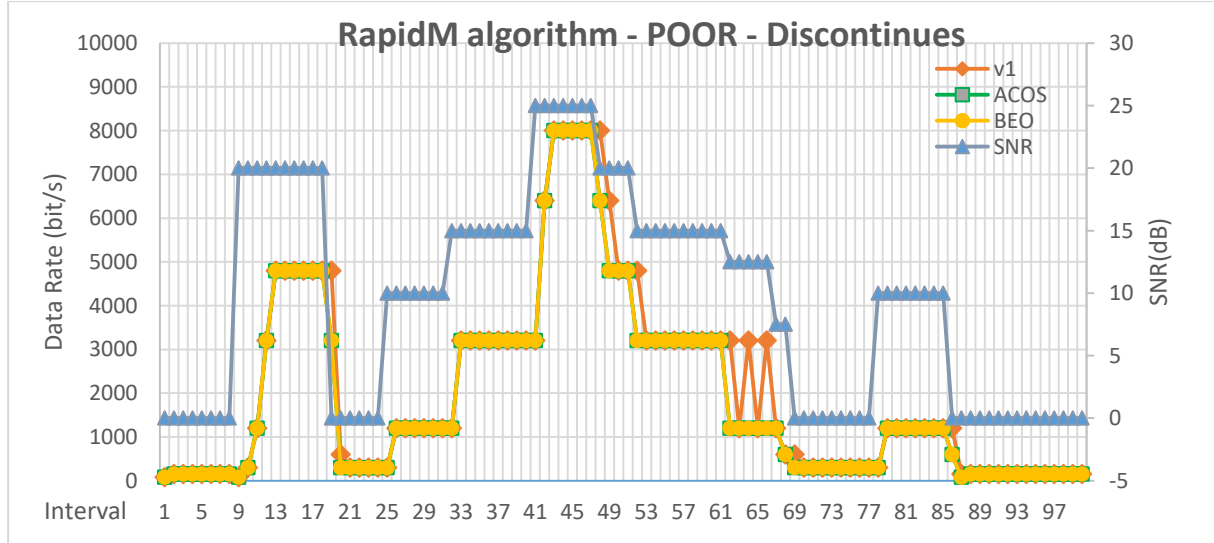


Figure C.24 – RapidM algorithm data rate adaptation for a POOR channel using discontinues SNR variation.

Appendix D – HF Communications Electrical Message

01 – 4 MHz TO 8 MHz / 8//

(Gama de frequências / Nº de frequências)

02 – PERMANENTE//

(Período de utilização das frequências)

03 – NIL//

(Distância e altura necessárias para protecção de serviço)

04 – LISBOA/POR/ 38°41'N 9°17'W//

(Local Tx [Nome do local, Código do País e coordenadas geográficas])

05 – PORTO/POR/ 41°11'N 8°38'W//

(Local Rx [Nome do local, Código do País e coordenadas geográficas])

06 – FX / 4 / 812//

(Classe Estação. / Serviço / Código da função)

07 – H240 / G8D//

(Largura de Banda / Classe TX)

08 – P /13 DBW//

(Tipo de potência / Valor em dBW [Pot. Máxima do emissor])

09 – OMNIDIRECIONAL/ VERTICAL//

(Ganho da antena /máxima direcção de radiação)

10 – J / 09-17//

(Tipo de horário de operação / hora de começo – hora de fim da operação)

11 – 4 MHZ TO 7 MHz / D / CONTÍNUA//

(Gama de sintonia de sistema, incrementos de sintonia e limitações de sintonia existentes)

12 – D//

(Tipo de operação do circuito)

13 – 29AGO17//

(Data limite para ter as frequências)

14 – A. NIL//

(Características do ar)

B. OPERACIONALIZAÇÃO DOS SISTEMAS RF-1936P-10 HARRIS. //.

(Justificações ou observações)

A finalidade é realizar testes NVIS numa distância considerável e testar uma aplicação de adaptação de débito em condições reais de propagação.

Appendix E – Assembly of the Dipole Antenna 1936P

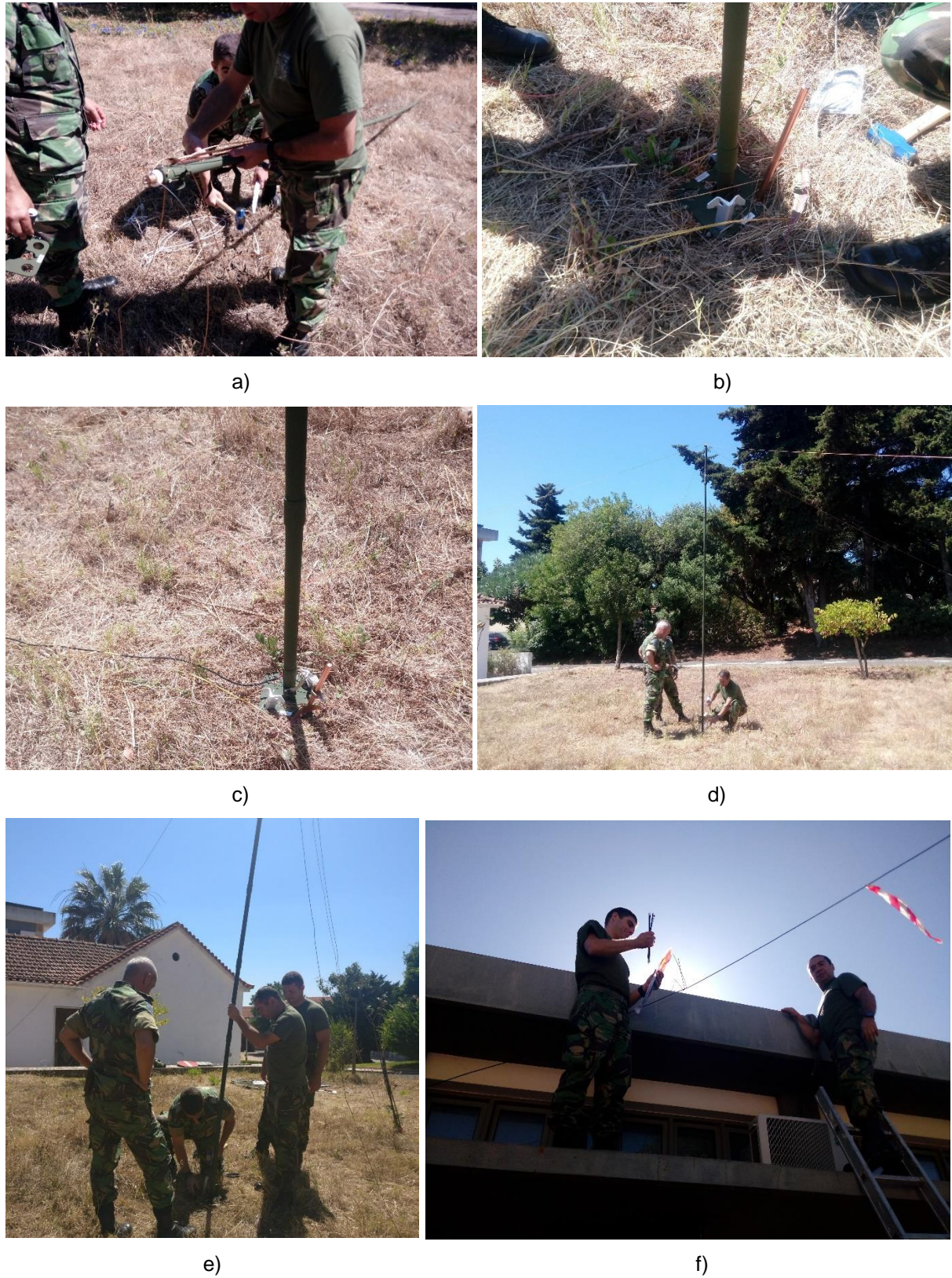


Figure E.1 – Station assembly on images: a) Unroll the dipole wires; b) Attaching the copper bar to perform the ground of the system; c) Wire that connect the radio with the antenna; d) Fixing the base of the antenna to the ground; e) Hoist the mast of the antenna; f) Stretching the coaxial cable to the radio station.

Appendix F – Results from the Field Propagation Tests

Table F.1 - Results from the Field Propagation Tests on 30th August 2017 using the DRC RapidM algorithm.

Station	Channel	Time Slot	BER	FER	SNR (dB)	Data Rate (bit/s)	Time (hh:mm:ss)	Time Interval (hh:mm:ss)	Seconds	Average Throughput (bit/s)	Average Goodput (frames/s)
ST1	4	12	0	0	11	300	11:03:02	00:10:41	641	46,47172082	0,023231216
ST1	4	12	1,00E-07	0,0002	11	600	11:13:43	00:16:34	994	144,1275835	0,072049388
ST1	4	12	1,00E-07	0,0002	10	1200	11:30:17	00:00:09	9	2,609953891	0,001302371
ST1	4	12	1,00E-06	0,001998	11	1200	11:30:26	00:00:03	3	0,8699768	0,000426379
ST1	4	12	1,00E-05	0,019801	10	1200	11:30:29	00:00:01	1	0,289705172	1,96037E-05
ST1	4	12	0,001	0,8648	11	600	11:30:30	00:00:02	2	0,289966167	0,000118713
ST1	4	12	0,0001	0,181277	12	600	11:30:32	00:05:51	351	50,89410087	0,025396233
ST1	4	12	1,00E-06	0,001998	11	600	11:36:23	00:00:11	11	1,594957467	0,000781695
ST1	4	12	1,00E-05	0,019801	10	600	11:36:34	00:00:02	2	0,289966167	0,000118713
ST1	4	12	0,0001	0,181277	11	600	11:36:36	00:07:17	437	63,36331029	0,031054624
ST1	4	12	1,00E-05	0,019801	10	600	11:43:53	00:00:04	4	0,579932334	0,000237426
ST1	4	12	0,0001	0,181277	8	600	11:43:57	00:00:01	1	0,144983084	5,93564E-05
ST1	4	12	0,0001	0,181277	7	600	11:43:58	00:00:01	1	0,144852586	9,80183E-06
ST1	4	12	0,001	0,8648	6	300	11:43:59	00:00:02	2	0	0
ST1	4	12	0,01	1	8	150	11:44:01	00:00:03	3	0,108748177	5,43632E-05
ST1	4	12	1,00E-07	0,0002	14	300	11:44:04	00:00:01	1	0,072498784	3,62421E-05
ST1	4	12	1,00E-07	0,0002	13	300	11:44:05	00:00:01	1	0,072498719	3,6177E-05
ST1	4	12	1,00E-06	0,001998	12	300	11:44:06	00:00:01	1	0,072498719	3,6177E-05
ST1	4	12	1,00E-06	0,001998	11	300	11:44:07	00:06:42	402	29,14448511	0,014543142
ST1	4	12	1,00E-06	0,001998	9	300	11:50:49	00:00:30	30	2,174942001	0,001065948
ST1	4	12	1,00E-05	0,019801	8	300	11:51:19	00:00:01	1	0,072491542	2,96782E-05
ST1	4	12	0,0001	0,181277	6	300	11:51:20	00:00:01	1	0,072426293	4,90092E-06

Station	Channel	Time Slot	BER	FER	SNR (dB)	Data Rate (bit/s)	Time (hh:mm:ss)	Time Interval (hh:mm:ss)	Seconds	Average Throughput (bit/s)	Average Goodput (frames/s)
ST1	4	12	0,001	0,8648	5	150	11:51:21	00:00:02	2	0	0
ST1	4	12	0,01	1	4	75	11:51:23	00:09:52	592	0	0
ST1	4	13	0,01	1	-4	75	12:01:15	00:00:09	9	0,163105969	6,67759E-05
ST1	4	13	0,0001	0,181277	8	75	12:01:24	00:00:01	1	0,01812468	9,04424E-06
ST1	4	13	1,00E-06	0,001998	7	75	12:01:25	00:00:02	2	0,036249396	1,81247E-05
ST1	4	13	0	0	6	150	12:01:27	00:00:01	1	0,03624936	1,80885E-05
ST1	4	13	1,00E-06	0,001998	5	150	12:01:28	00:00:01	1	0,03624936	1,80885E-05
ST1	4	13	1,00E-06	0,001998	4	150	12:01:29	00:00:01	1	0,036245771	1,48391E-05
ST1	4	13	0,0001	0,181277	3	150	12:01:30	00:00:03	3	0,108737313	4,45173E-05
ST1	4	13	0,0001	0,181277	2	150	12:01:33	00:00:44	44	0	0
ST1	2	13	0,01	1	-9	75	12:02:17	00:00:01	1	0	0
ST1	2	13	0,1	1	-8	75	12:02:18	00:00:20	20	0	0
ST1	3	13	0,01	1	-3	75	12:02:38	00:00:03	3	0	0
ST1	3	13	0,01	1	-4	75	12:02:41	00:00:02	2	0	0
ST1	3	13	0,01	1	-5	75	12:02:43	00:00:01	1	0	0
ST1	3	13	0,1	1	-6	75	12:02:44	00:00:17	17	0,308089053	0,000126132
ST1	4	13	0,0001	0,181277	1	75	12:03:01	00:00:01	1	0,018122885	7,41955E-06
ST1	4	13	0,0001	0,181277	3	75	12:03:02	00:00:01	1	0,018124517	8,8829E-06
ST1	4	13	1,00E-05	0,019801	5	75	12:03:03	00:00:01	1	0,018124698	9,06235E-06
ST1	4	13	0	0	8	150	12:03:04	00:00:01	1	0,036249033	1,77658E-05
ST1	4	13	1,00E-05	0,019801	7	150	12:03:05	00:00:03	3	0,108737313	4,45173E-05
ST1	4	13	0,0001	0,181277	6	150	12:03:08	00:01:31	91	3,298691723	0,001646052
ST1	4	13	1,00E-06	0,001998	11	150	12:04:39	00:00:02	2	0,072498784	3,62421E-05
ST1	4	13	1,00E-07	0,0002	10	300	12:04:41	00:07:19	439	31,82665128	0,015598375
ST1	4	13	1,00E-05	0,019801	8	300	12:12:00				

Availability	τ (s)										
83,88%	3471										
Average			5,08E-06	0,89%	9,501	392,64		01:08:58	4138	379,60	188,3E-3

Table F.2 – Results from the Field Propagation Tests on 31st August 2017 using the DRC RapidM algorithm with ACOS.

Station	Channel	Time Slot	BER	FER	SNR (dB)	Data Rate (bit/s)	Time (hh:mm:ss)	Time Interval (hh:mm:ss)	Seconds	Average Throughput (bit/s)	Average Goodput (frames/s)
ST1	2	12	0	0	1	75	11:18:40	00:00:04	4	0,094250714	4,71254E-05
ST1	2	12	0	0	0	150	11:18:44	00:00:11	11	0,518378891	0,000259189
ST1	3	12	0	0	-10	75	11:18:55	00:00:04	4	0,094250699	4,71253E-05
ST1	3	12	0	0	-9	75	11:18:59	00:00:02	2	0,04712535	2,35627E-05
ST1	3	12	0	0	-8	75	11:19:01	00:00:06	6	0,141376064	7,0688E-05
ST1	4	12	0	0	9	300	11:19:07	00:00:02	2	0,188501399	9,42507E-05
ST1	4	12	0	0	7	300	11:19:09	00:00:02	2	0,188499573	9,23844E-05
ST1	4	12	1,00E-05	0,019801	6	300	11:19:11	00:00:01	1	0,094249727	4,61922E-05
ST1	4	12	1,00E-05	0,019801	5	300	11:19:12	00:00:01	1	0,094249786	4,61922E-05
ST1	4	12	1,00E-05	0,019801	4	300	11:19:13	00:00:01	1	0,094241304	3,85826E-05
ST1	4	12	0,0001	0,181277	2	300	11:19:14	00:00:02	2	0,188499514	9,23844E-05
ST1	4	12	1,00E-05	0,019801	4	300	11:19:16	00:01:55	115	10,83883128	0,005419416
ST1	4	12	0	0	19	1200	11:21:11	00:00:04	4	1,508011426	0,000754006
ST1	4	12	0	0	18	3200	11:21:15	00:00:02	2	2,010681384	0,00100514
ST1	4	12	1,00E-07	0,0002	17	4800	11:21:17	00:00:08	8	12,06396982	0,005912602
ST1	4	12	1,00E-05	0,019801	14	4800	11:21:25	00:00:57	57	85,87068822	0,005810666
ST1	6	12	0,001	0,8648	8	3200	11:22:22	00:00:03	3	0	0
ST1	6	12	0,01	1	7	1200	11:22:25	00:00:01	1	0,376625676	2,54854E-05
ST1	6	12	0,001	0,8648	6	600	11:22:26	00:02:18	138	26,01319254	0,013003997
ST1	4	12	1,00E-07	0,0002	13	1200	11:24:44	00:00:41	41	15,45710053	0,007713116
ST1	4	12	1,00E-06	0,001998	11	1200	11:25:25	00:00:35	35	13,19496702	0,006466909

Station	Channel	Time Slot	BER	FER	SNR (dB)	Data Rate (bit/s)	Time (hh:mm:ss)	Time Interval (hh:mm:ss)	Seconds	Average Throughput (bit/s)	Average Goodput (frames/s)
ST1	4	12	1,00E-05	0,019801	11	1200	11:26:00	00:00:02	2	0,75400484	0,00037625
ST1	4	12	1,00E-06	0,001998	11	1200	11:26:02	00:07:37	457	172,2902749	0,086127919
ST1	4	12	1,00E-07	0,0002	14	3200	11:33:39	00:00:10	10	10,05340755	0,005025699
ST1	4	12	1,00E-07	0,0002	13	4800	11:33:49	00:00:01	1	1,507860861	0,000617322
ST1	4	12	0,0001	0,181277	11	4800	11:33:50	00:00:02	2	3,013006355	0,000203883
ST1	4	12	0,001	0,8648	9	3200	11:33:52	00:00:01	1	0	0
ST1	4	12	0,01	1	8	1200	11:33:53	00:07:53	473	178,3045052	0,072998261
ST1	4	12	0,0001	0,181277	7	1200	11:41:46	00:00:01	1	0,376625676	2,54854E-05
ST1	4	12	0,001	0,8648	6	600	11:41:47	00:00:03	3	0	0
ST1	4	12	0,01	1	5	300	11:41:50	00:00:01	1	0,094241304	3,85826E-05
ST1	4	12	0,0001	0,181277	8	300	11:41:51	00:00:01	1	0,094250635	4,70312E-05
ST1	4	12	1,00E-06	0,001998	11	300	11:41:52	00:05:57	357	33,64749898	0,016820387
ST1	4	12	1,00E-07	0,0002	9	600	11:47:49	00:00:03	3	0,565504198	0,000282696
ST1	4	12	1,00E-07	0,0002	8	1200	11:47:52	00:00:01	1	0,376998909	0,000184769
ST1	4	12	1,00E-05	0,019801	9	1200	11:47:53	00:00:01	1	0,376965215	0,00015433
ST1	4	12	0,0001	0,181277	8	1200	11:47:54	00:00:01	1	0,376625913	2,54854E-05
ST1	4	12	0,001	0,8648	7	600	11:47:55	00:00:02	2	0,376625794	2,54854E-05
ST1	4	12	0,001	0,8648	6	300	11:47:57	00:00:02	2	0,188499514	9,23844E-05
ST1	4	12	1,00E-05	0,019801	8	300	11:47:59	00:00:01	1	0,094250719	4,71159E-05
ST1	4	12	1,00E-07	0,0002	11	600	11:48:00	00:00:03	3	0,565504198	0,000282696
ST1	4	12	1,00E-07	0,0002	10	1200	11:48:03	00:09:16	556	209,5926107	0,085807681
ST1	4	12	0,0001	0,181277	9	1200	11:57:19	00:00:05	5	1,88312909	0,000127427
ST1	4	12	0,001	0,8648	8	600	11:57:24	00:00:01	1	0,188312956	1,27427E-05
ST1	4	12	0,001	0,8648	6	300	11:57:25	00:00:01	1	0,094241245	3,85826E-05
ST1	4	12	0,0001	0,181277	5	300	11:57:26	00:00:02	2	0,188312956	1,27427E-05
ST1	4	12	0,001	0,8648	4	150	11:57:28	00:00:01	1	0	0

Station	Channel	Time Slot	BER	FER	SNR (dB)	Data Rate (bit/s)	Time (hh:mm:ss)	Time Interval (hh:mm:ss)	Seconds	Average Throughput (bit/s)	Average Goodput (frames/s)
ST1	4	12	0,01	1	3	75	11:57:29	00:00:01	1	0	0
ST1	4	12	0,1	1	2	75	11:57:30	00:00:02	2	0	0
ST1	4	12	0,1	1	1	75	11:57:32	00:00:01	1	0	0
ST1	4	12	0,01	1	0	75	11:57:33	00:00:04	4	0,094156449	6,37134E-06
ST1	4	12	0,001	0,8648	-1	75	11:57:37	00:01:47	107	2,521203885	0,001258085
ST1	6	12	1,00E-06	0,001998	6	75	11:59:24	00:00:01	1	0,023562447	1,15481E-05
ST1	6	12	1,00E-05	0,019801	5	75	11:59:25	00:00:01	1	0,023560326	9,64565E-06
ST1	6	12	0,0001	0,181277	4	75	11:59:26	00:00:01	1	0,023560311	9,64564E-06
ST1	6	12	0,0001	0,181277	3	75	11:59:27	00:00:01	1	0,02353912	1,59284E-06
ST1	6	12	0,001	0,8648	2	75	11:59:28	00:00:02	2	0,047120637	1,92913E-05
ST1	6	12	0,0001	0,181277	5	75	11:59:30	00:00:06	6	0,141361926	5,78739E-05
ST1	7	12	0,0001	0,181277	3	75	11:59:36	00:00:01	1	0,023560326	9,64565E-06
ST1	7	12	0,0001	0,181277	5	75	11:59:37	00:00:01	1	0,023560311	9,64564E-06
ST1	7	12	0,0001	0,181277	4	75	11:59:38	00:00:02	2	0,047078224	3,18567E-06
ST1	7	12	0,001	0,8648	3	75	11:59:40	00:00:02	2	0	0
ST1	7	12	0,01	1	2	75	11:59:42	00:00:01	1	0	0
ST1	7	12	0,01	1	1	75	11:59:43	00:00:02	2	0	0
ST1	7	12	0,1	1	0	75	11:59:45	00:00:05	5	0	0
ST1	7	12	0,1	1	-1	75	11:59:50	00:00:09	9	0,212042874	8,68108E-05
ST1	8	12	0,0001	0,181277	4	75	11:59:59	00:00:03	3	0,070680963	2,89369E-05
ST1	8	12	0,0001	0,181277	3	75	12:00:02	00:00:02	2	0,047078239	3,18567E-06
ST1	8	12	0,001	0,8648	2	75	12:00:04	00:00:04	4	0	0
ST1	8	12	0,01	1	1	75	12:00:08	00:00:30	30	0,706873235	0,000346442
ST1	4	13	1,00E-05	0,019801	7	75	12:00:38	00:00:01	1	0,023560311	9,64564E-06
ST1	4	13	0,0001	0,181277	5	75	12:00:39	00:00:02	2	0,047120652	1,92913E-05
ST1	4	13	0,0001	0,181277	4	75	12:00:41	00:00:01	1	0,023560311	9,64564E-06

Station	Channel	Time Slot	BER	FER	SNR (dB)	Data Rate (bit/s)	Time (hh:mm:ss)	Time Interval (hh:mm:ss)	Seconds	Average Throughput (bit/s)	Average Goodput (frames/s)
ST1	4	13	0,0001	0,181277	3	75	12:00:42	00:00:01	1	0,02353912	1,59284E-06
ST1	4	13	0,001	0,8648	1	75	12:00:43	00:00:02	2	0,047078224	3,18567E-06
ST1	4	13	0,001	0,8648	0	75	12:00:45	00:01:20	80	0	0
ST1	4	13	0,01	1	-1	75	12:02:05	00:00:02	2	0	0
ST1	4	13	0,1	1	-2	75	12:02:07	00:00:01	1	0	0
ST1	4	13	0,1	1	-1	75	12:02:08	00:00:02	2	0	0
ST1	4	13	0,1	1	-2	75	12:02:10	00:00:01	1	0	0
ST1	4	13	0,1	1	-1	75	12:02:11	00:00:01	1	0	0
ST1	4	13	0,01	1	0	75	12:02:12	00:00:01	1	0,023560326	9,64565E-06
ST1	4	13	0,0001	0,181277	5	75	12:02:13	00:00:01	1	0,023560311	9,64564E-06
ST1	4	13	0,0001	0,181277	4	75	12:02:14	00:00:02	2	0,047078224	3,18567E-06
ST1	4	13	0,001	0,8648	3	75	12:02:16	00:00:03	3	0	0
ST1	4	13	0,01	1	2	75	12:02:19	00:00:09	9	0,212063884	0,00010582
ST1	6	13	1,00E-06	0,001998	11	300	12:02:28	00:00:01	1	0,094250719	4,71159E-05
ST1	6	13	1,00E-07	0,0002	14	600	12:02:29	00:00:03	3	0,56550408	0,000282696
ST1	6	13	1,00E-07	0,0002	13	1200	12:02:32	00:00:02	2	0,754005077	0,00037625
ST1	6	13	1,00E-06	0,001998	12	1200	12:02:34	00:00:06	6	2,2619944	0,001108613
ST1	7	13	1,00E-05	0,019801	8	1200	12:02:40	00:00:02	2	0,753930194	0,000308661
ST1	7	13	0,0001	0,181277	7	1200	12:02:42	00:00:01	1	0,376625676	2,54854E-05
ST1	7	13	0,001	0,8648	6	600	12:02:43	00:00:01	1	0,188499573	9,23844E-05
ST1	7	13	1,00E-05	0,019801	9	600	12:02:44	00:00:03	3	0,565503689	0,000282187
ST1	7	13	1,00E-06	0,001998	8	600	12:02:47	00:00:02	2	0,377002759	0,000188464
ST1	7	13	1,00E-07	0,0002	11	1200	12:02:49	00:00:13	13	0	0
ST1	8	13	0,01	1	3	600	12:03:02	00:00:01	1	0,188312956	1,27427E-05
ST1	8	13	0,001	0,8648	4	300	12:03:03	00:00:01	1	0,094241304	3,85826E-05
ST1	8	13	0,0001	0,181277	5	300	12:03:04	00:00:04	4	0,376625794	2,54854E-05

Station	Channel	Time Slot	BER	FER	SNR (dB)	Data Rate (bit/s)	Time (hh:mm:ss)	Time Interval (hh:mm:ss)	Seconds	Average Throughput (bit/s)	Average Goodput (frames/s)
ST1	8	13	0,001	0,8648	4	150	12:03:08	00:00:03	3	0,141361926	5,78739E-05
ST1	8	13	0,0001	0,181277	3	150	12:03:11	00:00:31	31	1,460739854	0,00059803
ST1	4	13	0,0001	0,181277	3	150	12:03:42	00:00:01	1	0,047124893	2,30961E-05
ST1	4	13	1,00E-05	0,019801	8	150	12:03:43	00:00:01	1	0,047125364	2,35627E-05
ST1	4	13	0	0	12	300	12:03:44	00:00:03	3	0,282752127	0,000141376
ST1	4	13	0	0	15	600	12:03:47	00:07:41	461	86,89914299	0,043440887
ST1	4	13	1,00E-07	0,0002	14	1200	12:11:28	00:00:09	9	3,393025191	0,001696173
ST1	4	13	1,00E-07	0,0002	13	3200	12:11:37	00:00:01	1	1,005330423	0,000492717
ST1	4	13	1,00E-05	0,019801	11	3200	12:11:38	00:00:01	1	1,005331055	0,000492717
ST1	4	13	1,00E-05	0,019801	10	3200	12:11:39	00:00:01	1	1,005240574	0,000411548
ST1	4	13	0,0001	0,181277	8	3200	12:11:40	00:00:01	1	1,004335136	6,7961E-05
ST1	4	13	0,001	0,8648	7	1200	12:11:41	00:00:02	2	0,754005077	0,00037625
ST1	4	13	1,00E-06	0,001998	8	1200	12:11:43				
Availability	τ (s)										
95,95%	3054										
Average			6,69E-05	9,26%	9,328	904,44		00:53:03	3183	892,22	369,0E-3

Table F.3 – Results from the Field Propagation Tests on 1st September 2017 using the DRC RapidM algorithm with BEO.

Station	Channel	Time Slot	BER	FER	SNR (dB)	Data Rate (bit/s)	Time (hh:mm:ss)	Time Interval (hh:mm:ss)	Seconds	Average Throughput (bit/s)	Average Goodput (frames/s)
ST1	4	10	0	0	-3	75	09:43:09	00:00:01	1	0,02300614	1,15031E-05
ST1	4	10	0	0	-2	150	09:43:10	00:00:02	2	0,092024532	4,60123E-05
ST1	4	10	0	0	1	300	09:43:12	00:00:02	2	0,184049065	9,20245E-05
ST1	4	10	0	0	0	300	09:43:14	00:00:01	1	0,092024561	4,60123E-05

Station	Channel	Time Slot	BER	FER	SNR (dB)	Data Rate (bit/s)	Time (hh:mm:ss)	Time Interval (hh:mm:ss)	Seconds	Average Throughput (bit/s)	Average Goodput (frames/s)
ST1	4	10	0	0	-1	300	09:43:15	00:00:01	1	0,092024561	4,60123E-05
ST1	4	10	0	0	0	300	09:43:16	00:00:02	2	0,184049065	9,20245E-05
ST1	4	10	0	0	-1	300	09:43:18	00:00:03	3	0,27607335	0,000137761
ST1	4	10	1,00E-06	0,001998	8	1200	09:43:21	00:00:50	50	18,38650297	0,001244171
ST1	2	10	0,001	0,8648	-7	150	09:44:11	00:00:05	5	0,230038339	9,41782E-05
ST1	2	10	0,0001	0,181277	-3	150	09:44:16	00:00:07	7	0,321763821	2,1773E-05
ST1	3	10	0,001	0,8648	-7	75	09:44:23	00:00:02	2	0,045966254	3,11043E-06
ST1	3	10	0,001	0,8648	-6	75	09:44:25	00:00:02	2	0,045966254	3,11043E-06
ST1	3	10	0,001	0,8648	-7	75	09:44:27	00:00:02	2	0	0
ST1	3	10	0,01	1	-8	75	09:44:29	00:03:21	201	4,619608892	0,000312598
ST1	3	10	0,001	0,8648	-5	75	09:47:50	00:00:06	6	0	0
ST1	3	10	0,01	1	-6	75	09:47:56	00:00:02	2	0	0
ST1	3	10	0,1	1	-5	75	09:47:58	00:00:05	5	0,115030661	5,75038E-05
ST1	3	10	1,00E-07	0,0002	8	300	09:48:03	00:00:11	11	1,012269843	0,000506034
ST1	7	10	1,00E-07	0,0002	11	600	09:48:14	00:00:01	1	0,184048989	9,20061E-05
ST1	7	10	1,00E-07	0,0002	14	1200	09:48:15	00:00:01	1	0,368098209	0,000184012
ST1	7	10	1,00E-07	0,0002	15	3200	09:48:16	00:00:02	2	1,963188063	0,000979634
ST1	7	10	1,00E-06	0,001998	14	3200	09:48:18	00:10:07	607	595,822263	0,292014987
ST1	7	10	1,00E-05	0,019801	12	3200	09:58:25	00:02:04	124	121,7176698	0,0607373
ST1	7	10	1,00E-06	0,001998	14	3200	10:00:29	00:00:01	1	0,981584888	0,000481079
ST1	7	10	1,00E-05	0,019801	14	3200	10:00:30	00:00:01	1	0,981585506	0,000481079
ST1	7	10	1,00E-05	0,019801	13	3200	10:00:31	00:00:01	1	0,981496545	0,000401827
ST1	7	10	0,0001	0,181277	11	3200	10:00:32	00:00:01	1	0,981497162	0,000401827
ST1	7	10	0,0001	0,181277	10	3200	10:00:33	00:00:01	1	0,980613726	6,63558E-05
ST1	7	11	0,001	0,8648	8	1200	10:00:34	00:00:06	6	2,208566693	0,001082428
ST1	7	11	1,00E-05	0,019801	7	1200	10:00:40	00:00:03	3	1,104293401	0,000551044

Station	Channel	Time Slot	BER	FER	SNR (dB)	Data Rate (bit/s)	Time (hh:mm:ss)	Time Interval (hh:mm:ss)	Seconds	Average Throughput (bit/s)	Average Goodput (frames/s)
ST1	7	11	1,00E-06	0,001998	11	1200	10:00:43	00:00:47	47	17,29888355	0,007082201
ST1	2	11	0,0001	0,181277	-4	150	10:01:30	00:00:01	1	0,046011792	2,25506E-05
ST1	2	11	1,00E-05	0,019801	-1	150	10:01:31	00:00:01	1	0,046011821	2,25506E-05
ST1	2	11	1,00E-05	0,019801	-2	150	10:01:32	00:00:03	3	0,138035433	6,76517E-05
ST1	2	11	1,00E-05	0,019801	-3	150	10:01:35	00:00:03	3	0,138023009	5,65069E-05
ST1	2	11	0,0001	0,181277	-4	150	10:01:38	00:00:13	13	0	0
ST1	3	11	0,01	1	-10	75	10:01:51	00:00:04	4	0	0
ST1	3	11	0,01	1	-8	75	10:01:55	00:00:08	8	0,184049079	9,20245E-05
ST1	4	11	0	0	14	300	10:02:03	00:00:01	1	0,092024504	4,60123E-05
ST1	4	11	0	0	17	600	10:02:04	00:00:04	4	0,736196302	0,000368025
ST1	4	11	1,00E-07	0,0002	16	1200	10:02:08	00:00:01	1	0,368097977	0,000184012
ST1	4	11	1,00E-07	0,0002	15	3200	10:02:09	00:00:01	1	0,981595223	0,0004907
ST1	4	11	1,00E-07	0,0002	14	4800	10:02:10	00:09:57	597	879,0096147	0,430806294
ST1	4	11	1,00E-05	0,019801	13	4800	10:12:07	00:00:11	11	16,18012278	0,001094871
ST1	4	11	0,001	0,8648	12	3200	10:12:18	00:00:03	3	2,9447559	0,001443237
ST1	4	11	1,00E-05	0,019801	11	3200	10:12:21	00:09:43	583	571,6976686	0,038685426
ST1	4	11	0,001	0,8648	9	1200	10:22:04	00:00:05	5	1,840306716	0,000753426
ST1	4	11	0,0001	0,181277	8	1200	10:22:09	00:00:04	4	1,472378027	0,000721619
ST1	4	11	1,00E-05	0,019801	11	1200	10:22:13	00:00:05	5	1,84047236	0,000902023
ST1	4	11	1,00E-05	0,019801	10	1200	10:22:18	00:00:30	30	11,04184053	0,004520554
ST1	7	11	0,0001	0,181277	10	1200	10:22:48	00:00:05	5	1,840306716	0,000753426
ST1	7	11	0,0001	0,181277	8	1200	10:22:53	00:00:43	43	15,82663803	0,006479461
ST1	2	11	0,0001	0,181277	-5	150	10:23:36	00:00:05	5	0,230038339	9,41782E-05
ST1	2	11	0,0001	0,181277	-6	150	10:23:41	00:00:41	41	1,886501188	0,000941367
ST1	4	11	1,00E-06	0,001998	9	600	10:24:22	00:00:02	2	0,368097762	0,000183681
ST1	4	11	1,00E-06	0,001998	8	600	10:24:24	00:12:56	776	142,8206576	0,069997003

Station	Channel	Time Slot	BER	FER	SNR (dB)	Data Rate (bit/s)	Time (hh:mm:ss)	Time Interval (hh:mm:ss)	Seconds	Average Throughput (bit/s)	Average Goodput (frames/s)
ST1	4	11	1,00E-05	0,019801	6	600	10:37:20	00:00:01	1	0,184047282	9,02023E-05
ST1	4	11	1,00E-05	0,019801	5	600	10:37:21	00:00:01	1	0,184030718	7,53426E-05
ST1	4	11	0,0001	0,181277	4	600	10:37:22	00:00:03	3	0,5521467	0,000275522
ST1	4	11	1,00E-06	0,001998	8	600	10:37:25	00:00:01	1	0,184048989	9,20061E-05
ST1	4	11	1,00E-07	0,0002	11	1200	10:37:26	00:00:02	2	0,736188898	0,000360809
ST1	4	11	1,00E-05	0,019801	9	1200	10:37:28	00:00:01	1	0,368094565	0,000180405
ST1	4	11	1,00E-05	0,019801	8	1200	10:37:29				
Availability	τ (s)										
99,17%	3233										
Average			2,76E-04	24,98%	9,548	2426,79		00:54:20	3260	2425,23	927,1E-3

Table F.4 – Results from the Field Propagation Tests on 4th September 2017 using the Trinder algorithm.

Station	Channel	Time Slot	BER	FER	SNR (dB)	Data Rate (bit/s)	Time (hh:mm:ss)	Time Interval (hh:mm:ss)	Seconds	Average Throughput (bit/s)	Average Goodput (frames/s)
ST1	6	15	0	0	5	150	14:42:41	00:00:10	10	0,444312816	0,000222156
ST1	7	15	0	0	2	300	14:42:51	00:00:01	1	0,088862524	4,44313E-05
ST1	7	15	0	0	1	600	14:42:52	00:00:02	2	0,35509487	2,40284E-05
ST1	7	15	0,001	0,8648	0	300	14:42:54	00:00:01	1	0,088853638	3,63769E-05
ST1	7	15	0,0001	0,181277	-1	600	14:42:55	00:00:02	2	0,355094758	2,40284E-05
ST1	7	15	0,001	0,8648	0	300	14:42:57	00:00:01	1	0,088861691	4,35515E-05
ST1	7	15	1,00E-05	0,019801	2	600	14:42:58	00:08:33	513	91,16386846	0,03732269
ST1	7	15	0,0001	0,181277	1	1200	14:51:31	00:00:08	8	2,840758288	0,000192227
ST1	6	15	0,001	0,8648	4	600	14:51:39	00:00:01	1	0,177547435	1,20142E-05
ST1	6	15	0,001	0,8648	3	300	14:51:40	00:00:01	1	0	0

Station	Channel	Time Slot	BER	FER	SNR (dB)	Data Rate (bit/s)	Time (hh:mm:ss)	Time Interval (hh:mm:ss)	Seconds	Average Throughput (bit/s)	Average Goodput (frames/s)
ST1	6	15	0,01	1	1	150	14:51:41	00:00:03	2,999999	0,13316052	9,01066E-06
ST1	6	15	0,001	0,8648	0	75	14:51:44	00:00:02	2	0,044426847	1,81884E-05
ST1	6	15	0,0001	0,181277	-1	150	14:51:46	00:10:00	600	26,65874112	0,013302752
ST1	6	16	1,00E-06	0,001998	13	300	15:01:46	00:00:34	34	3,021323973	0,001507645
ST1	6	16	1,00E-06	0,001998	11	600	15:02:20	00:00:07	7	1,243951377	0,000509276
ST1	6	16	0,0001	0,181277	9	1200	15:02:27	00:00:01	1	0,35509487	2,40284E-05
ST1	6	16	0,001	0,8648	7	600	15:02:28	00:00:01	1	0	0
ST1	6	16	0,01	1	6	300	15:02:29	00:00:01	1	0	0
ST1	6	16	0,1	1	5	150	15:02:30	00:00:02	2	0	0
ST1	6	16	0,1	1	4	75	15:02:32	00:00:01	1	0	0
ST1	6	16	0,01	1	3	75	15:02:33	00:10:01	601	13,33824793	0,000902568
ST1	6	16	0,001	0,8648	3	75	15:12:34	00:03:21	201	4,465298945	0,002188462
ST1	6	16	1,00E-05	0,019801	8	150	15:15:55	00:00:24	24	1,066244074	0,000436523
ST1	6	16	0,0001	0,181277	6	300	15:16:19	00:00:01	1	0,088773717	6,00711E-06
ST1	6	16	0,001	0,8648	5	150	15:16:20	00:09:18	558	0	0
ST1	6	16	0,01	1	4	75	15:25:38	00:00:44	44	0,977487179	0,000487768
ST1	4	16	1,00E-06	0,001998	11	150	15:26:22	00:00:01	1	0,044430818	2,17757E-05
ST1	4	16	1,00E-05	0,019801	10	300	15:26:23	00:00:01	1	0,088853694	3,63769E-05
ST1	4	16	0,0001	0,181277	9	600	15:26:24	00:05:49	349	61,96404026	0,00419296
ST1	4	16	0,001	0,8648	8	300	15:32:13	00:00:07	7	0,621975745	0,000254638
ST1	6	16	0,0001	0,181277	8	600	15:32:20	00:00:07	7	1,242831709	8,40995E-05
ST1	6	16	0,001	0,8648	9	300	15:32:27	00:06:30	390	34,65605154	0,016985076
ST1	6	16	1,00E-05	0,019801	11	600	15:38:57				
Availability	τ (s)										
83,29%	2812										
Average			3,69E-04	34,03%	3,971	270,96		00:56:16	3376	245,61	78,9E-3

Table F.5 – Results from the Field Propagation Tests on 5th September 2017 using the Trinder algorithm with ACOS.

Station	Channel	Time Slot	BER	FER	SNR (dB)	Data Rate (bit/s)	Time (hh:mm:ss)	Time Interval (hh:mm:ss)	Seconds	Average Throughput (bit/s)	Average Goodput (frames/s)
ST1	4	13	0	0	8	300	12:06:40	00:00:09	9	1,138268577	0,00055787
ST1	4	13	1,00E-05	0,019801	8	600	12:06:49	00:03:51	231	58,43111887	0,028637336
ST1	4	13	1,00E-05	0,019801	7	1200	12:10:40	00:00:02	2	1,011703123	0,000414194
ST1	4	13	0,0001	0,181277	6	3200	12:10:42	00:00:02	2	2,69544751	0,000182395
ST1	4	13	0,001	0,8648	5	1200	12:10:44	00:00:02	2	1,011703123	0,000414194
ST1	4	13	0,0001	0,181277	4	1200	12:10:46	00:00:02	2	1,010792499	6,83979E-05
ST1	4	13	0,001	0,8648	3	600	12:10:48	00:00:05	5	1,263490703	8,54974E-05
ST1	4	13	0,001	0,8648	2	300	12:10:53	00:00:01	1	0,12646293	5,17742E-05
ST1	4	13	0,0001	0,181277	1	600	12:10:54	00:00:01	1	0,252925701	0,000103548
ST1	4	13	0,0001	0,181277	0	600	12:10:55	00:04:09	249	62,92183821	0,004257772
ST1	4	13	0,001	0,8648	1	300	12:15:04	00:00:03	3	0,379422859	0,000185957
ST1	4	13	1,00E-05	0,019801	2	600	12:15:07	00:05:21	321	81,18918202	0,033239032
ST1	4	13	0,0001	0,181277	0	600	12:20:28	00:00:01	1	0,252698204	1,70995E-05
ST1	4	13	0,001	0,8648	-1	300	12:20:29	00:00:03	3	0,379388711	0,000155323
ST1	4	13	0,0001	0,181277	-2	300	12:20:32	00:00:01	1	0,126349102	8,54974E-06
ST1	4	13	0,001	0,8648	-3	150	12:20:33	00:00:01	1	0	0
ST1	4	13	0,01	1	-4	75	12:20:34	00:00:02	2	0,063237137	3,09928E-05
ST1	4	13	1,00E-05	0,019801	-5	150	12:20:36	00:01:27	87	5,501631338	0,002696373
ST1	4	13	1,00E-05	0,019801	0	300	12:22:03	00:00:02	2	0,252925781	0,000103548
ST1	4	13	0,0001	0,181277	1	600	12:22:05	00:00:01	1	0,252698204	1,70995E-05
ST1	4	13	0,001	0,8648	2	300	12:22:06	00:00:02	2	0,252925781	0,000103548
ST1	4	13	0,0001	0,181277	1	600	12:22:08	00:00:04	4	1,010792658	6,83979E-05
ST1	4	13	0,001	0,8648	0	300	12:22:12	00:00:03	3	0	0
ST1	4	13	0,01	1	-1	150	12:22:15	00:00:11	11	0,695614783	0,000347113

Station	Channel	Time Slot	BER	FER	SNR (dB)	Data Rate (bit/s)	Time (hh:mm:ss)	Time Interval (hh:mm:ss)	Seconds	Average Throughput (bit/s)	Average Goodput (frames/s)
ST1	6	13	1,00E-06	0,001998	7	300	12:22:26	00:00:01	1	0,126475451	6,31114E-05
ST1	6	13	1,00E-06	0,001998	6	600	12:22:27	00:00:02	2	0,505851561	0,000207097
ST1	6	13	0,0001	0,181277	5	1200	12:22:29	00:00:03	3	1,517554843	0,00062129
ST1	6	13	0,0001	0,181277	8	3200	12:22:32	00:00:06	6	0	0
ST1	7	13	0,01	1	2	1200	12:22:38	00:00:04	4	0	0
ST1	7	13	0,01	1	1	600	12:22:42	00:00:02	2	0	0
ST1	7	13	0,01	1	-1	300	12:22:44	00:00:01	1	0,126349023	8,54974E-06
ST1	7	13	0,001	0,8648	-2	150	12:22:45	00:00:03	3	0,189694355	7,76613E-05
ST1	7	13	0,0001	0,181277	-3	300	12:22:48	00:00:01	1	0	0
ST1	7	13	0,1	1	-4	150	12:22:49	00:01:32	92	0	0
ST1	7	13	0,01	1	-5	75	12:24:21	00:00:02	2	0,063174531	4,27487E-06
ST1	7	13	0,001	0,8648	-6	75	12:24:23	00:00:09	9	0,284541533	0,000116492
ST1	7	13	0,0001	0,181277	-3	150	12:24:32	00:00:28	28	1,770655879	0,00088356
ST1	8	13	1,00E-06	0,001998	4	300	12:25:00	00:00:01	1	0,126474313	6,19856E-05
ST1	8	13	1,00E-05	0,019801	5	600	12:25:01	00:00:02	2	0,505897092	0,000247942
ST1	8	13	1,00E-05	0,019801	8	1200	12:25:03	00:01:30	90	0	0
ST1	4	13	0,01	1	-1	600	12:26:33	00:00:02	2	0,505396249	3,4199E-05
ST1	4	13	0,001	0,8648	-2	300	12:26:35	00:00:01	1	0,126349102	8,54974E-06
ST1	4	13	0,001	0,8648	-3	150	12:26:36	00:00:05	5	0,315872676	2,13744E-05
ST1	4	13	0,001	0,8648	-2	75	12:26:41	00:00:03	3	0,094855715	4,64892E-05
ST1	4	13	1,00E-05	0,019801	-1	150	12:26:44	00:00:12	12	0,758853191	0,000379351
ST1	6	13	1,00E-07	0,0002	8	300	12:26:56	00:00:01	1	0,126475565	6,32251E-05
ST1	6	13	1,00E-07	0,0002	7	600	12:26:57	00:00:01	1	0,252950743	0,000126223
ST1	6	13	1,00E-06	0,001998	8	1200	12:26:58	00:00:04	4	2,023588688	0,000991769
ST1	6	13	1,00E-05	0,019801	7	3200	12:27:02	00:00:06	6	0	0
ST1	7	13	0,1	1	-3	1200	12:27:08	00:00:02	2	0	0

Station	Channel	Time Slot	BER	FER	SNR (dB)	Data Rate (bit/s)	Time (hh:mm:ss)	Time Interval (hh:mm:ss)	Seconds	Average Throughput (bit/s)	Average Goodput (frames/s)
ST1	7	13	0,1	1	-4	600	12:27:10	00:00:02	2	0	0
ST1	7	13	0,1	1	-5	300	12:27:12	00:00:19	19	2,403033015	0,001199117
ST1	8	13	1,00E-06	0,001998	7	600	12:27:31	00:00:01	1	0,252948626	0,000123971
ST1	8	13	1,00E-05	0,019801	6	1200	12:27:32	00:00:01	1	0,50539609	3,4199E-05
ST1	8	13	0,001	0,8648	4	600	12:27:33	00:00:01	1	0,252698204	1,70995E-05
ST1	8	13	0,001	0,8648	3	300	12:27:34	00:00:01	1	0,126349102	8,54974E-06
ST1	8	13	0,001	0,8648	2	150	12:27:35	00:00:03	2,999999	0,18971139	9,29783E-05
ST1	8	13	1,00E-05	0,019801	1	300	12:27:38	00:00:34	34	4,300164385	0,002145788
ST1	6	13	1,00E-06	0,001998	6	600	12:28:12	00:00:01	1	0,252948467	0,000123971
ST1	6	13	1,00E-05	0,019801	5	1200	12:28:13	00:01:24	84	0	0
ST1	4	13	0,01	1	-1	600	12:29:37	00:00:01	1	0	0
ST1	4	13	0,01	1	-2	300	12:29:38	00:00:02	2	0,252698125	1,70995E-05
ST1	4	13	0,001	0,8648	-3	150	12:29:40	00:00:01	1	0,063174551	4,27487E-06
ST1	4	13	0,001	0,8648	-4	75	12:29:41	00:00:02	2	0,063231445	2,58871E-05
ST1	4	13	0,0001	0,181277	-5	150	12:29:43	00:00:03	3	0,189694355	7,76613E-05
ST1	4	13	0,0001	0,181277	-1	300	12:29:46	00:00:03	3	0,379422859	0,000185957
ST1	4	13	1,00E-05	0,019801	0	300	12:29:49	00:00:11	11	1,391217124	0,000681841
ST1	6	13	1,00E-05	0,019801	4	600	12:30:00	00:00:01	1	0,252925701	0,000103548
ST1	6	13	0,0001	0,181277	3	600	12:30:01	00:00:01	1	0,25292586	0,000103548
ST1	6	13	0,0001	0,181277	2	600	12:30:02	00:00:01	1	0,252698204	1,70995E-05
ST1	6	13	0,001	0,8648	1	300	12:30:03	00:00:01	1	0,126462851	5,17742E-05
ST1	6	13	0,0001	0,181277	0	300	12:30:04	00:00:07	7	0	0
ST1	7	13	0,01	1	-4	150	12:30:11	00:00:01	1	0,063174511	4,27487E-06
ST1	7	13	0,001	0,8648	-3	75	12:30:12	00:00:02	2	0,063231445	2,58871E-05
ST1	7	13	0,0001	0,181277	-1	150	12:30:14	00:00:05	5,000001	0,315872715	2,13744E-05
ST1	7	13	0,001	0,8648	-2	75	12:30:19	00:00:05	5	0,158078623	6,47177E-05

Station	Channel	Time Slot	BER	FER	SNR (dB)	Data Rate (bit/s)	Time (hh:mm:ss)	Time Interval (hh:mm:ss)	Seconds	Average Throughput (bit/s)	Average Goodput (frames/s)
ST1	7	13	0,0001	0,181277	-1	150	12:30:24	00:00:08	8	0,505897132	0,000247942
ST1	6	13	1,00E-05	0,019801	1	300	12:30:32	00:00:02	2	0,252925781	0,000103548
ST1	6	13	0,0001	0,181277	0	300	12:30:34	00:01:34	94	11,88858263	0,005826644
ST1	4	13	1,00E-05	0,019801	0	300	12:32:08	00:00:03	3	0,379047227	2,56492E-05
ST1	4	13	0,001	0,8648	-2	150	12:32:11	00:00:09	9	0,56913998	0,00028457
ST1	6	13	0	0	9	300	12:32:20	00:00:01	1	0,126475498	6,32377E-05
ST1	6	13	0	0	12	600	12:32:21	00:00:02	2	0,505902101	0,0002529
ST1	6	13	1,00E-07	0,0002	11	1200	12:32:23	00:00:02	2	1,01180452	0,000505801
ST1	6	13	1,00E-07	0,0002	10	3200	12:32:25	00:00:02	2	2,698117826	0,001322359
ST1	6	13	1,00E-05	0,019801	9	3200	12:32:27	00:00:01	1	1,347723755	9,11973E-05
ST1	6	13	0,001	0,8648	8	1200	12:32:28	00:00:01	1	0,505896933	0,000247942
ST1	6	13	1,00E-05	0,019801	7	3200	12:32:29	00:00:01	1	1,347723755	9,11973E-05
ST1	6	13	0,001	0,8648	6	1200	12:32:30	00:00:03	3	1,517554843	0,00062129
ST1	6	13	0,0001	0,181277	5	1200	12:32:33	00:00:10	10	0	0
ST1	7	13	0,01	1	-1	600	12:32:43	00:00:01	1	0	0
ST1	7	13	0,01	1	-2	300	12:32:44	00:00:02	2	0,252698125	1,70995E-05
ST1	7	13	0,001	0,8648	-3	75	12:32:46	00:00:02	2	0,063231445	2,58871E-05
ST1	7	13	0,0001	0,181277	-4	150	12:32:48	00:00:07	7	0,442660016	0,00021695
ST1	8	13	1,00E-05	0,019801	1	300	12:32:55	00:00:01	1	0,126462851	5,17742E-05
ST1	8	13	0,0001	0,181277	0	300	12:32:56	00:00:02	2	0,252698125	1,70995E-05
ST1	8	13	0,001	0,8648	-1	150	12:32:58	00:00:02	2	0,126349102	8,54974E-06
ST1	8	13	0,001	0,8648	-2	75	12:33:00	00:00:01	1	0,031618843	1,57778E-05
ST1	8	13	1,00E-06	0,001998	0	150	12:33:01	00:00:03	3	0,189694355	7,76613E-05
ST1	8	13	0,0001	0,181277	-1	300	12:33:04	00:00:05	5	0,631745351	4,27487E-05
ST1	8	13	0,001	0,8648	-2	150	12:33:09	00:00:27	27	1,707402826	0,000836805
ST1	6	13	1,00E-05	0,019801	3	300	12:33:36	00:00:01	1	0,126474313	6,19856E-05

Station	Channel	Time Slot	BER	FER	SNR (dB)	Data Rate (bit/s)	Time (hh:mm:ss)	Time Interval (hh:mm:ss)	Seconds	Average Throughput (bit/s)	Average Goodput (frames/s)
ST1	6	13	1,00E-05	0,019801	2	600	12:33:37	00:00:01	1	0,252698204	1,70995E-05
ST1	6	13	0,001	0,8648	1	300	12:33:38	00:00:01	1	0,126349023	8,54974E-06
ST1	6	13	0,001	0,8648	0	150	12:33:39	00:00:01	1	0,063174551	4,27487E-06
ST1	6	13	0,001	0,8648	-1	75	12:33:40	00:00:01	1	0,031618558	1,54964E-05
ST1	6	13	1,00E-05	0,019801	-2	150	12:33:41	00:00:02	2	0,126349102	8,54974E-06
ST1	6	13	0,001	0,8648	-3	75	12:33:43	00:00:04	4	0,126474273	6,19856E-05
ST1	6	13	1,00E-05	0,019801	-4	150	12:33:47	00:01:24	84	5,311441831	0,002174516
ST1	4	13	0,0001	0,181277	-2	300	12:35:11	00:00:01	1	0,126349102	8,54974E-06
ST1	4	13	0,001	0,8648	-3	150	12:35:12	00:00:02	2	0	0
ST1	4	13	0,01	1	-4	75	12:35:14	00:00:01	1	0,031587276	2,13744E-06
ST1	4	13	0,001	0,8648	-5	75	12:35:15	00:00:06	6	0,189694335	7,76613E-05
ST1	4	13	0,0001	0,181277	-3	150	12:35:21	00:00:01	1	0,063237156	3,09928E-05
ST1	4	13	1,00E-05	0,019801	0	300	12:35:22	00:00:12	12	1,517706534	0,000758853
ST1	6	13	0	0	11	600	12:35:34	00:00:02	2	0,505901805	0,000252446
ST1	6	13	1,00E-06	0,001998	10	1200	12:35:36	00:00:01	1	0,505896933	0,000247942
ST1	6	13	1,00E-05	0,019801	9	3200	12:35:37	00:00:03	3	4,047177164	0,001983538
ST1	6	13	1,00E-05	0,019801	14	4800	12:35:40	00:00:07	7	0	0
ST1	7	13	0,1	1	-5	3200	12:35:47	00:00:01	1	0	0
ST1	7	13	0,1	1	-3	1200	12:35:48	00:00:01	1	0	0
ST1	7	13	0,1	1	1	600	12:35:49	00:00:02	2	0,505396249	3,4199E-05
ST1	7	13	0,001	0,8648	3	300	12:35:51	00:00:02	2	0,252925781	0,000103548
ST1	7	13	0,0001	0,181277	4	600	12:35:53	00:00:05	5,000001	1,26474297	0,000619856
ST1	7	13	1,00E-05	0,019801	8	1200	12:35:58	00:00:11	11	5,564923269	0,002781905
ST1	8	13	1,00E-07	0,0002	14	3200	12:36:09	00:00:01	1	1,349059337	0,00066118
ST1	8	13	1,00E-05	0,019801	15	4800	12:36:10	00:10:02	602	1218,200297	0,597045068
ST1	8	13	1,00E-05	0,019801	14	6400	12:46:12				

Availability	τ (s)										
86,38%	2049										
Average			1,82E-04	18,49%	4,980	1645,87		00:39:32	2372	1508,52	698,8E-3

Table F.6 – Results from the Field Propagation Tests on 7th September 2017 using the Trinder algorithm with BEO.

Station	Channel	Time Slot	BER	FER	SNR (dB)	Data Rate (bit/s)	Time (hh:mm:ss)	Time Interval (hh:mm:ss)	Seconds	Average Throughput (bit/s)	Average Goodput (frames/s)
ST1	6	15	0	0	-1	75	14:42:32	00:00:02	2	0,055066075	2,7533E-05
ST1	6	15	0	0	0	150	14:42:34	00:00:01	1	0,055066087	2,75275E-05
ST1	6	15	1,00E-07	0,0002	1	300	14:42:35	00:04:03	243	26,76208773	0,013354322
ST1	6	15	1,00E-06	0,001998	1	600	14:46:38	00:03:21	201	44,2687004	0,018123704
ST1	6	15	0,0001	0,181277	0	300	14:49:59	00:00:06	6	0,66078636	0,000323854
ST1	6	15	1,00E-05	0,019801	-1	300	14:50:05	00:00:01	1	0,110121171	4,50839E-05
ST1	6	15	0,0001	0,181277	-3	150	14:50:06	00:00:05	5	0,275055061	1,86123E-05
ST1	6	15	0,001	0,8648	-4	75	14:50:11	00:00:01	1	0,027532771	1,34939E-05
ST1	6	15	1,00E-05	0,019801	-5	150	14:50:12	00:00:56	56	3,083700434	0,00154185
ST1	4	15	0	0	9	300	14:51:08	00:00:01	1	0,110132104	5,5055E-05
ST1	4	15	1,00E-07	0,0002	7	600	14:51:09	00:00:01	1	0,220264148	0,000109912
ST1	4	15	1,00E-06	0,001998	5	1200	14:51:10	00:00:03	3	1,321453776	0,000541006
ST1	4	15	0,0001	0,181277	3	600	14:51:13	00:01:21	81	17,83962557	0,007303582
ST1	4	15	0,0001	0,181277	1	300	14:52:34	00:00:01	1	0,110131014	5,39757E-05
ST1	4	15	1,00E-05	0,019801	0	300	14:52:35	00:00:01	1	0,110121171	4,50839E-05
ST1	4	15	0,0001	0,181277	-2	150	14:52:36	00:00:21	21	0	0
ST1	6	15	0,01	1	-6	75	14:52:57	00:00:06	6	0,165181722	6,76258E-05
ST1	6	15	0,0001	0,181277	-5	75	14:53:03	00:00:07	7	0,192731078	9,61731E-05
ST1	7	15	1,00E-06	0,001998	0	150	14:53:10	00:00:02	2	0,110132074	5,49561E-05
ST1	7	15	1,00E-06	0,001998	1	300	14:53:12	00:00:01	1	0,110131014	5,39757E-05

Station	Channel	Time Slot	BER	FER	SNR (dB)	Data Rate (bit/s)	Time (hh:mm:ss)	Time Interval (hh:mm:ss)	Seconds	Average Throughput (bit/s)	Average Goodput (frames/s)
ST1	7	15	1,00E-05	0,019801	2	600	14:53:13	00:00:02	2	0,440524332	0,000215903
ST1	7	15	1,00E-05	0,019801	3	600	14:53:15	00:00:03	2,999999	0,660792168	0,000329736
ST1	7	15	1,00E-06	0,001998	4	600	14:53:18	00:14:15	855	188,325803	0,093974858
ST1	7	16	1,00E-06	0,001998	5	1200	15:07:33	00:00:10	10	4,405242213	0,002159028
ST1	6	16	1,00E-05	0,019801	8	3200	15:07:43	00:00:01	1	1,173567819	7,94126E-05
ST1	6	16	0,001	0,8648	6	1200	15:07:44	00:00:01	1	0,440484684	0,000180335
ST1	6	16	0,0001	0,181277	4	600	15:07:45	00:00:01	1	0,220242342	9,01677E-05
ST1	6	16	0,0001	0,181277	2	300	15:07:46	00:00:01	1	0,110131014	5,39757E-05
ST1	6	16	1,00E-05	0,019801	4	600	15:07:47	00:00:01	1	0,220262166	0,000107951
ST1	6	16	1,00E-05	0,019801	6	1200	15:07:48	00:08:42	522	229,7259912	0,015545013
ST1	6	16	0,001	0,8648	-2	600	15:16:30	00:00:14	14	3,080616769	0,000208458
ST1	6	16	0,001	0,8648	-3	300	15:16:44	00:01:12	72	0	0
ST1	3	16	0,1	1	-10	150	15:17:56	00:00:12	12	0,660792933	0,000330396
ST1	4	16	0	0	7	300	15:18:08	00:00:01	1	0,110132173	5,50551E-05
ST1	4	16	1,00E-07	0,0002	6	600	15:18:09	00:00:01	1	0,220262166	0,000107951
ST1	4	16	1,00E-05	0,019801	5	1200	15:18:10	00:00:03	3	1,321453776	0,000541006
ST1	4	16	0,0001	0,181277	4	600	15:18:13	00:00:02	2	0,440524194	0,000215903
ST1	4	16	1,00E-05	0,019801	3	600	15:18:15	00:00:02	2	0,440528158	0,000219824
ST1	4	16	1,00E-06	0,001998	8	1200	15:18:17	00:05:02	302	133,0383173	0,065202637
ST1	4	16	1,00E-05	0,019801	6	1200	15:23:19	00:01:50	110	48,4096916	0,003275769
ST1	4	16	0,001	0,8648	0	600	15:25:09	00:00:12	12	2,64052856	0,000178678
ST1	6	16	0,001	0,8648	-1	300	15:25:21	00:00:03	3	0,330066087	2,23348E-05
ST1	6	16	0,001	0,8648	-2	150	15:25:24	00:01:33	93	5,121094183	0,00250987
ST1	4	16	1,00E-05	0,019801	-1	300	15:26:57	00:00:01	1	0,110131014	5,39757E-05
ST1	4	16	1,00E-05	0,019801	-2	300	15:26:58	00:00:01	1	0,110121171	4,50839E-05
ST1	4	16	0,0001	0,181277	-3	150	15:26:59	00:00:01	1	0,055011026	3,72247E-06

Station	Channel	Time Slot	BER	FER	SNR (dB)	Data Rate (bit/s)	Time (hh:mm:ss)	Time Interval (hh:mm:ss)	Seconds	Average Throughput (bit/s)	Average Goodput (frames/s)
ST1	4	16	0,001	0,8648	-4	75	15:27:00	00:00:01	1	0,027505496	1,86123E-06
ST1	4	16	0,001	0,8648	-5	75	15:27:01	00:00:02	2	0	0
ST1	4	16	0,01	1	-6	75	15:27:03	00:00:02	2	0	0
ST1	4	16	0,1	1	-7	75	15:27:05	00:00:16	16	0,440524228	0,000215903
ST1	6	16	1,00E-05	0,019801	-2	150	15:27:21	00:00:01	1	0,055065507	2,69878E-05
ST1	6	16	1,00E-05	0,019801	-3	150	15:27:22	00:00:01	1	0,055060586	2,25419E-05
ST1	6	16	0,0001	0,181277	-4	75	15:27:23	00:00:15	15	0,412991457	0,000202409
ST1	7	16	1,00E-05	0,019801	-3	150	15:27:38	00:00:02	2	0,110121171	4,50839E-05
ST1	7	16	0,0001	0,181277	-5	75	15:27:40	00:00:16	16	0,440528633	0,000220264
ST1	8	16	0	0	9	150	15:27:56				
Availability	τ (s)										
96,44%	2627										
Average			2,68E-04	24,53%	3,383	728,432		00:45:24	2724	718,94	228,3E-3

Appendix G – Ionospheric Conditions for the Test Days

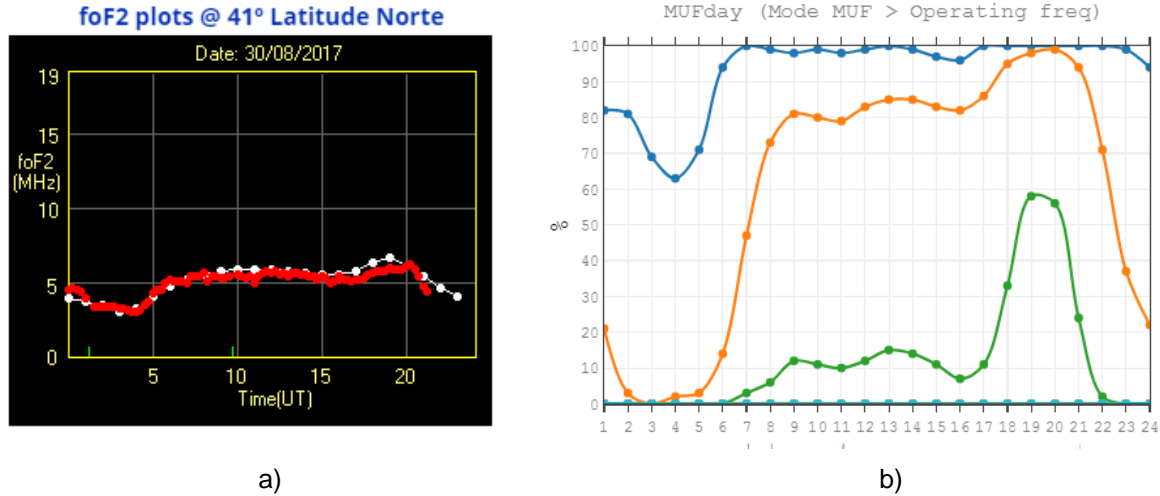


Figure G.1 – Ionospheric conditions for the 30th August 2017: a) foF2 real measure in red colour, and foF2 predicted value in white colour during the day; b) MUF values during the day.

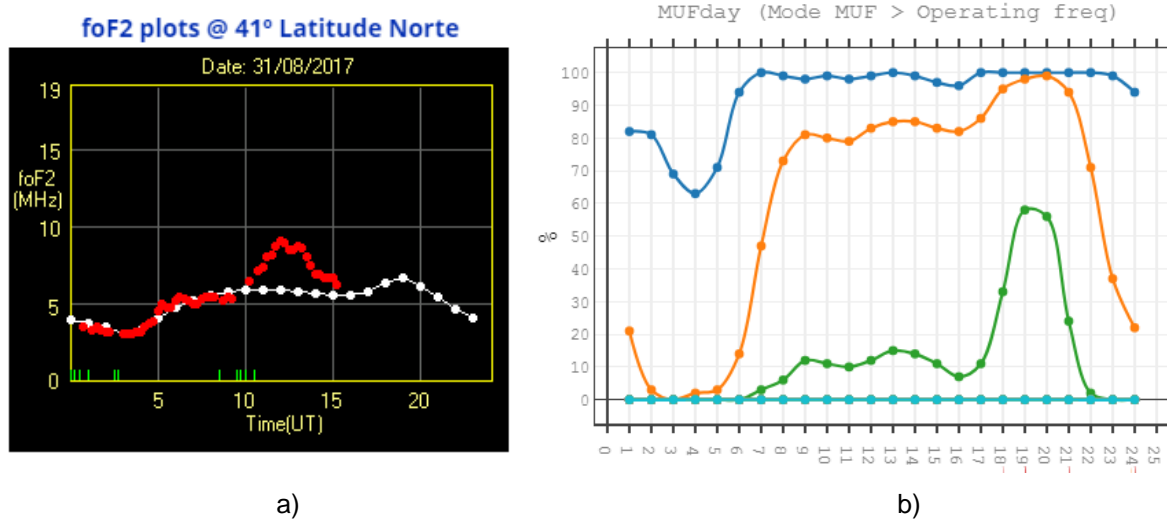


Figure G.2 – Ionospheric conditions for the 31st August 2017: a) foF2 real measure in red colour, and foF2 predicted value in white colour during the day; b) MUF values during the day.

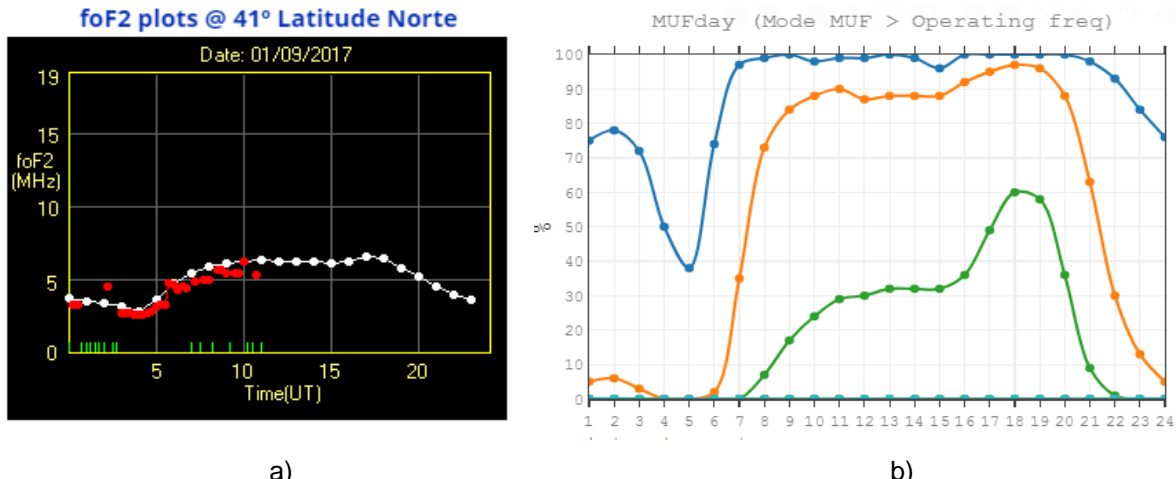


Figure G.3 – Ionospheric conditions for the 1st September 2017: a) foF2 real measure in red colour, and foF2 predicted value in white colour during the day; b) MUF values during the day.

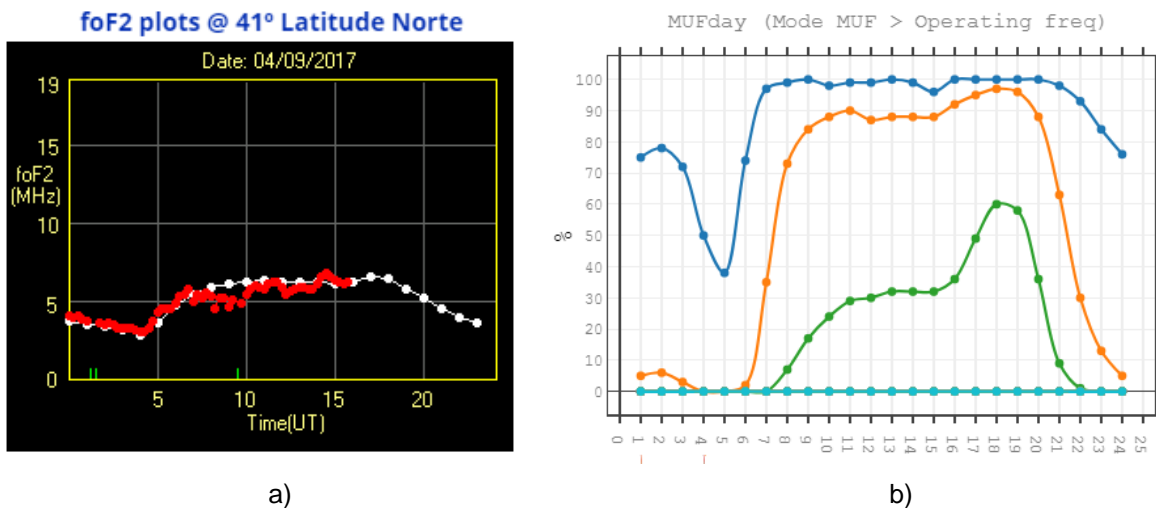


Figure G.4 – Ionospheric conditions for the 4th September 2017: a) foF2 real measure in red colour, and foF2 predicted value in white colour during the day; b) MUF values during the day.

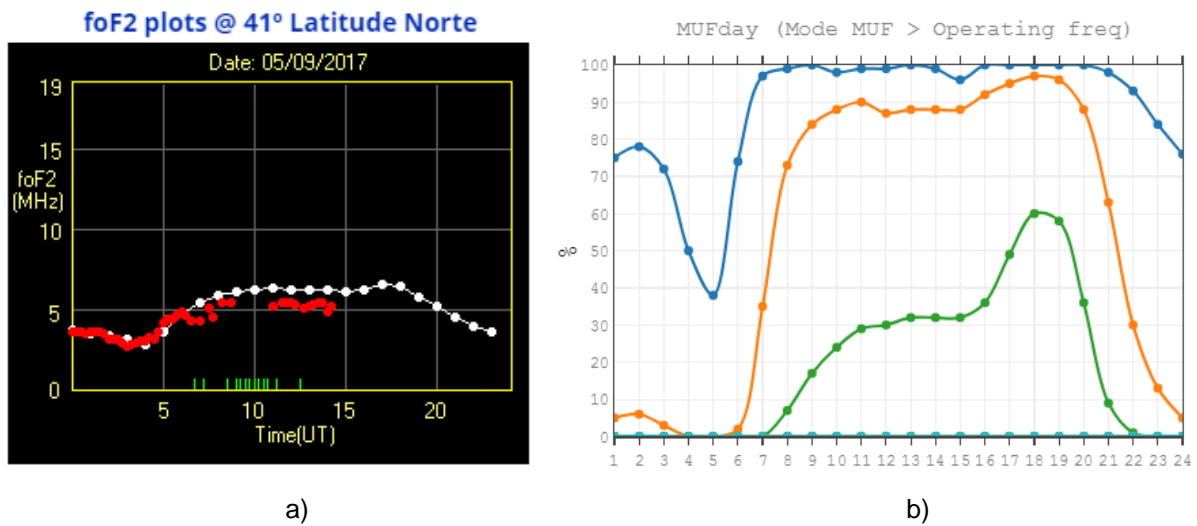


Figure G.5 – Ionospheric conditions for the 5th September 2017: a) foF2 real measure in red colour, and foF2 predicted value in white colour during the day; b) MUF values during the day.

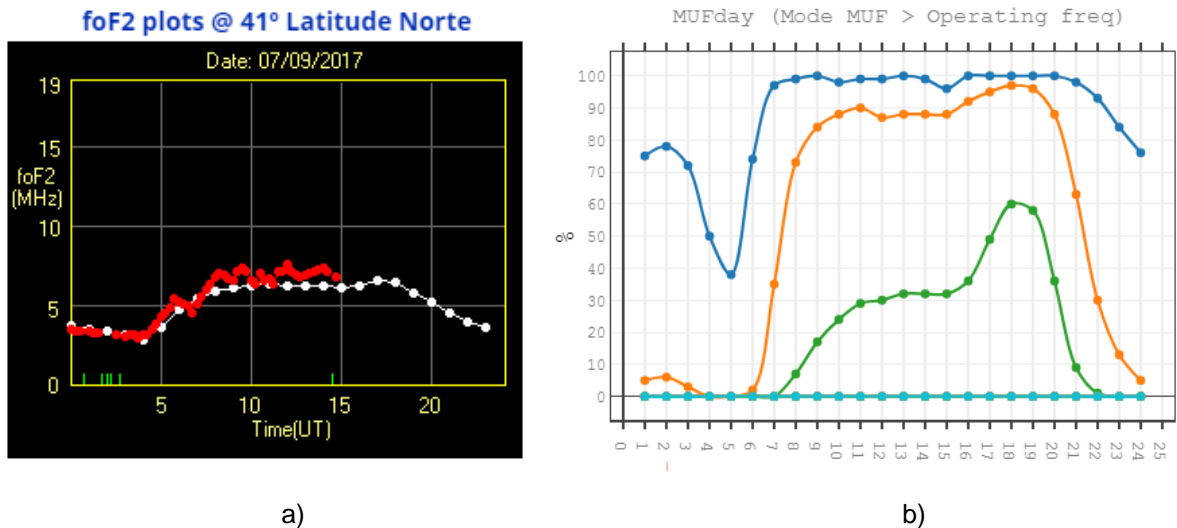


Figure G.6 – Ionospheric conditions for the 7th September 2017: a) foF2 real measure in red colour, and foF2 predicted value in white colour during the day; b) MUF values during the day.

Bibliography

- [1] S. Sarac, F. Kara and C. Vural, "Real-Time Implementation of STANAG 4539 High-Speed HF Model," *International Journal of Social, Behavioural, Educational, Economic, Business, and Industrial Engineering*, vol. 6, pp. 1289-1294, 2012.
- [2] Empresa de Investigação e Desenvolvimento de Electrónica, S.A., *Rádio Táctico HF/VHF/UHF TR-525, Manual de Operação e Manutenção Nível I*, Ed. 4 ed.
- [3] S. Schulze and G. P. Hancke, *Design and Implementation of a STANAG 5066 Data Rate Change Algorithm for High Data Rate Autobaud Waveforms*, Lynnwood Road, Pretoria, 0002, South Africa: Department of Electrical, Electronic and Computer Engineering, University of Pretoria , 2005.
- [4] Wikipédia, "Link Quality Analysis," 15 August 2012. [Online]. Available: https://en.wikipedia.org/wiki/Link_quality_analysis. [Accessed 8 November 2016].
- [5] Wikipedia, "Automatic Link Establishment," 16 November 2016. [Online]. Available: https://en.wikipedia.org/wiki/Automatic_link_establishment. [Accessed 19 November 2016].
- [6] S. Trinder and A. Gillespie, "Optimisation of the STANAG 5066 ARQ Protocol to Support High Data Rate HF Communication," in *Proceedings of IEEE Military Communications Conference (MILCOM) 2001*, Washington, DC, October 2001.
- [7] E. E. Johnson, E. Koski, W. N. Furman, M. Jorgenson and J. Nieto, *Third-Generation and Wideband HF Radio Communications*, 685 Canton Street Norwood MA 02062: Artech House, 2013.
- [8] "Science Pole," [Online]. Available: <http://sciencepole.com/radio-spectrum/#>. [Accessed 8 October 2016].
- [9] K. Davies, *Ionospheric Radio*, Peter Peregrinus Ltd, 1990.
- [10] Wikipédia, "Ionosphere," 5 December 2016. [Online]. Available: <https://en.wikipedia.org/wiki/Ionosphere>. [Accessed 21 December 2016].
- [11] D. Bilitza, *International Reference Ionosphere*, Radio Science , 2001.
- [12] J. K. Hargreaves, *The Solar-Terrestrial Environment*, Cambridge University Press, 1995.
- [13] Wikipedia, "Ionosphere Layers," 11 November 2015. [Online]. Available: http://wiki.robotz.com/index.php/Ionosphere_Layers. [Accessed 27 December 2016].
- [14] J. J. Carr, *Practical Antenna Handbook*, 4º ed., McGraw-Hill, 2001.
- [15] T. R. Rocha, *Comunicações Tácticas e de Emergência por propagação por efeito NVIS*, Instituto Superior Técnico; Academia Militar, 2013.
- [16] C. P. Grifo, *Relatório de Avaliação do Emprego Operacional do E/R GRC-525 na banda HF*, Calçada da Ajuda 134, 1349-053 Lisboa: Direcção de Comunicações e Sistemas de Informação, Exército Português, Ministério da Defesa Nacional, 2014.

- [17] AMSAT-CT, “Associação Observatório AeroEspacial Amadores de Satélite - CT,” [Online]. Available: http://www.amsat-ct.pt/?page_id=1221. [Accessed 17 July 2017].
- [18] R. Matyszkiel, P. Kaniewski and B. Grochowina, *Selected issues of modern HF communications*, 05-130 Zegrze Pld, Warszawska 22 A str., Poland: Military Communication Institute, 2013.
- [19] Raynet HF Team, “Propagation: What is NVIS?,” 2016. [Online]. Available: <http://raynet-hf.net/propagation/>. [Accessed 21 December 2016].
- [20] Wikipedia, “Critical Frequency,” 6 August 2016. [Online]. Available: https://en.wikipedia.org/wiki/Critical_frequency. [Accessed 13 November 2016].
- [21] T. A. Ceita, *Estudo Comparativo entre duas Antenas para Comunicação com Efeito NVIS*, Lisboa: Instituto Superior Técnico, Academia Militar, 2014.
- [22] International Telecommunication Union, *Handbook Frequency-Adaptive Communication Systems and Networks in the MF/HF bands*, Place des Nations CH-1211 Geneva 20, Switzerland, 2002.
- [23] B. Crystal, “HF Link,” 2007. [Online]. Available: <http://hflink.com/alehamradio/>. [Accessed 27 December 2016].
- [24] STANAG 4539, *Technical Standards for Non-Hopping HF Communications Waveforms*, NATO, 2000.
- [25] MIL-STD-188-110B, *Interoperability and Performance Standards for Data Modems*, Department of Defense United States of America, 2000 .
- [26] M. Jorgenson and K. Moreland, *HF Serial-Tone Waveform Design*, 307 Carling Ave., Ottawa, Canada, K2H 8S2: Communications Research Centre , 1999 .
- [27] Rapid Mobile (Pty) Lda., “RapidM,” 2016. [Online]. Available: <http://www.rapidm.com/standard.shtml>. [Accessed 4 December 2016].
- [28] International Telecommunication Union, *Draft Modification of Recommendation ITU-R F.763-4: Data transmission over HF circuits using phase shift keying or quadrature amplitude modulation*, 2004.
- [29] M. Carlsen, *Adaptive Coding and Modulation Techniques for HF Communication*, Trondheim, Norway: Norwegian University of Science and Technology , 2009.
- [30] S. Trinder and D. Brown, *Algorithms for the Adaption of Data Rate using STANAG 5066*, London, United Kingdom: IEE Colloquium on Frequency Selection and Management Techniques, 1999.
- [31] J. Nieto, *An investigation of Throughput Performance for STANAG 5066 High Data Rate HF Waveforms*, Anaheim, CA: Proceedings of IEEE MILCOM 2002, 2002.
- [32] C. Salema, *Feixes Hertzianos*, 3^a ed., Av. Rovisco Pais, Lisbon, Portugal: Instituto Superior Técnico Press, 2011.
- [33] Rohde & Schwarz, *GB2 Platform Protocol -M3TR / Series 4100 - Common Part*, Munich, Germany: 2GE5, 2008.
- [34] Space Weather Prediction Center - National Oceanic and Atmospheric Administration , “Geomagnetic Storms,” [Online]. Available: <http://www.swpc.noaa.gov/phenomena/geomagnetic-storms>. [Accessed 29 August 2017].

- [35] Korean Space Weather Center , “Solar flares and HF communication fadeouts,” National Radio Research Agency, 2011. [Online]. Available: http://spaceweather.rra.go.kr/effect/english/03_02_02. [Accessed 29 August 2017].
- [36] J. Perkiölä, J. Watson and J. Juopperi, “VOACAP Online,” Voice of America Coverage Analysis Program, 2010-2017. [Online]. Available: <http://www.voacap.com/p2p/index.html>. [Accessed 2017 August 2017].
- [37] Tutorials Point (I) Pvt. Ltd., C# Programming: Object-Oriented Programming, 3rd Floor, Jyoti Celestia, Madhapur, Hyderabad, Telangana 500081, India: Tutorials Point - Simply Easy Learning, 2014.
- [38] Impala Multimedia, “Impala News,” [Online]. Available: <http://www.impala.pt/>. [Accessed 29 August 2017].